LIQUID BIOPSY TO PREDICT TUMOR PROGRESSION IN UVEAL MELANOMA

Prisca Bustamante Alvarez

Department of Pathology

McGill University

Montreal, Quebec, Canada

April 2022

A thesis submitted to McGill University in partial fulfillment of the requirements for the degree of Doctor of Philosophy

Table of contents

LIST OF TABLES ..... **VIII**

LIST OF FIGURES ..... **IX**

LIST OF ABBREVIATIONS ..... **X**

ABSTRACT ..... **II**

RÉSUMÉ ..... **IV**

ACKNOWLEDGMENTS ..... **VI**

CONTRIBUTIONS TO ORIGINAL KNOWLEDGE ..... **VIII**

CONTRIBUTION OF AUTHORS ..... **XII**

INTRODUCTION **1**

CHAPTER 1: LITERATURE REVIEW **4**

1. LIQUID BIOPSY 4

1.1. Cell-free DNA and circulating tumor DNA 4

1.2. Methods to detect ctDNA 6

1.3. Experimental techniques for ctDNA analysis 9

1.4. ctDNA-based liquid biopsy applications 12

1.4.1. ctDNA as an early diagnostic and screening maker 12

1.4.2. ctDNA to monitor tumor dynamics and treatment 14

1.4.2.1. ctDNA to evaluate tumor burden 15

1.4.2.2. ctDNA to monitor treatment response 15

2. UVEAL MELANOMA 17

2.1. Introduction 17
2.2. Molecular signaling 19
2.3. Metastatic disease 20
2.4. Prognostic indicators of poor prognosis in uveal melanoma 21
2.4.1. Clinical and histopathological factors 21
2.4.2. Genetic indicators 23
2.5. Current and prospective treatments for primary and metastatic uveal melanoma 28
2.5.1. Current treatments 28
2.5.2. Prospective treatments 29
3. ctDNA in Uveal melanoma 31
PREAMBLE TO CHAPTER 2 36
CHAPTER 2: CIRCULATING TUMOR DNA TRACKING THROUGH DRIVER MUTATIONS AS A LIQUID BIOPSY-BASED BIOMARKER FOR UVEAL MELANOMA 38
Abstract 39
Background 41
Material and Methods 43
Cell lines and culture conditions 43
Animal model 44
Patient recruitment and categorization 45
Blood specimen collection and sample preparation 45
Aqueous humor collection from rabbits 46
DNA isolation 46

Analysis of mutated DNA fragments 47
Data analysis 48
RESULTS 48
Validation of wild type and mutant cfDNA detection in conditioned medium of human UM cell line cultures 48
Blood mutated ctDNA levels correlated with tumor development and progression in a UM animal model 49
UM-derived cfDNA detected in the aqueous humor correlated with tumor size and progression 51
Mutant GNA11/Q cfDNA was detected in patient blood biopsy and correlated with the degree of lesion malignancy 52
FIGURES 55
TABLES 60
DISCUSSION 64
CONCLUSION 68
LIST OF ABBREVIATIONS 68
DECLARATIONS 69
PREAMBLE TO CHAPTER 3 70
CHAPTER 3: THE KINETICS AND FRAGMENTATION OF CELL-FREE DNA FROM CANCER CELLS ARE INFLUENCED BY ANTICANCER TREATMENTS 72
ABSTRACT 73
BACKGROUND 75
METHODS 77

Cell lines culture conditions 77
Cell exposure to cytotoxic treatments 77
Cell cycle analysis 78
Cell death analyses 79
Senescence analysis 79
DNA isolation and quantification 80
Measurement of cfDNA by ddPCR 80
Fragment size profiling 80
Data analysis 81
RESULTS 83
Cancer cell emission of mutant cfDNA correlates with cell viability 83
All cytotoxic treatments resulted in larger cfDNA fragment 86
FIGURES 88
DISCUSSION 96
ACKNOWLEDGMENTS 100
AUTHOR CONTRIBUTIONS 100
CONFLICTS OF INTEREST 100
PREAMBLE TO CHAPTER 4 101
CHAPTER 4: CTDNA AS A BIOMARKER OF TREATMENT RESPONSE FOR POTENTIAL NEW THERAPIES IN UM 103
ABSTRACT 103
BACKGROUND 104
METHODS 106

Cell culture 106
Drug Treatments 107
Cell viability assay 107
Cell-free DNA detection 108
Cell death assay 108
Data analysis 108
RESULTS 109
Potential anticancer drugs induce the release of cell-free DNA into the culture media 109
DISCUSSION 115
CONCLUSIONS 116
CHAPTER 5: GENERAL DISCUSSION 117
5.1 SUMMARY 117
5.2 DISCUSSION 120
5.2.1 What is the origin of cfDNA? 120
5.2.2 Clinical utility of ctDNA 122
5.2.4 Models to study ctDNA 125
5.2.5 Factors that influence ctDNA analysis 127
5.3 LIMITATIONS 129
5.4 DIRECTIONS FOR FUTURE STUDIES 130
5.4.1 Steps to the clinic 133
5.5 CONCLUSION 135
REFERENCES 136
APPENDIX 164

A.1 SUPPLEMENTARY MATERIAL -CHAPTER 2 164

A.1.1 Supplementary Figures 164

A.1.2 Supplementary Tables 168

A.2 SUPPLEMENTARY MATERIAL -CHAPTER 3 169

List of Tables

TABLE 1 SUMMARY OF EXPERIMENTAL TECHNIQUES FOR CTDNA ANALYSIS 11

TABLE 2 SUMMARY OF STUDIES ON CLINICAL RELEVANCE OF CTDNA IN UM 34

TABLE 3. DDPCR PRIMERS AND PROBES INFORMATION FOR THIS STUDY 60

TABLE 4 SUMMARY OF PATIENT CHARACTERISTICS 61

TABLE 5 UM PATIENTS CHARACTERISTICS 62

TABLE 6 CHARACTERISTICS OF PATIENTS WITH NEVI 63

TABLE 7 DDPCR PRIMER AND PROBES SEQUENCES 82

List of Figures

FIGURE 1. 1: SCHEMATIC REPRESENTATION OF CTDNA AS A LIQUID BIOPSY FOR CANCER. 9
FIGURE 1. 2: ANATOMY OF THE HUMAN EYE. 17

FIGURE 2. 1: WILDTYPE AND MUTANT CFDNA WERE ACCURATELY DETECTED IN HUMAN UM CELL LINE CONDITIONED MEDIUM. 55
FIGURE 2. 2: A HUMAN UM RABBIT MODEL WAS USED TO VALIDATE THE DETECTION OF MUTATED CTDNA IN LIQUID BIOPSIES. 56
FIGURE 2. 3: MUTATED CTDNA PLASMA AND AQUEOUS HUMOR LEVELS MIRRORED THE PATTERN OF INTRAOCULAR DISEASE BEHAVIOR IN RABBITS. 57
FIGURE 2. 4: THE LEVELS OF MUTATED CTDNA IN UM PATIENTS AND PATIENTS WITH UVEAL NEVI CORRELATED WITH THE STAGE OF DISEASE PROGRESSION AND WITH THE PRESENCE OF RISK FACTORS FOR MALIGNANT TRANSFORMATION, RESPECTIVELY 59

FIGURE 3. 1 : THE LEVELS OF CANCER CELL-RELEASED MUTANT CFDNA CORRELATED WITH THE NUMBER OF VIABLE CELLS. 88
FIGURE 3. 2:APO2L/TRIAL INDUCED CANCER CELL APOPTOSIS AND A SUBSTANTIALLY INCREASE IN CFDNA LEVEL. 89
FIGURE 3. 3: VALPROIC ACID-INDUCED CANCER CELL ACCUMULATION AT THE G1 PHASE OF CELL CYCLE AND IS ASSOCIATED WITH CFDNA RELEASE. 90
FIGURE 3. 4: GAMMA IRRADIATION DECREASED INDUCED CELL DEATH AND SENESCENCE ON CANCER CELLS. 92
FIGURE 3. 5: APOPTOSIS IS THE MAIN CONTRIBUTOR OF CFDNA RELEASE. 94
FIGURE 3. 6: CANCER CELLS EXPOSURE TO CYTOTOXIC INSULTS RELEASED CFDNA WITH DIFFERENT SIZES. 95

FIGURE 4. 1: MF TREATMENT INDUCES THE RELEASE OF CFDNA INTO THE MEDIA SUPERNATANT. 111
FIGURE 4. 2: CELL VITALITY DECREASED AFTER DRUG TREATMENT. 112

List of Abbreviations

AH: aqueous humor

AJCC: American Joint Committee on Cancer

AKT : Serine/threonine-specific protein kinase

ANOVA: Analysis of variance

APO: APO2L/TRIAL

ARF6: ADP-ribosylation factor 6

ASXL1: ASXL Transcriptional Regulator 1

ATCC: American Type Culture Collection

BAP1: BRCA-1 associated protein 1

BEAMing: beads, emulsion, amplification, and magnetics

bi-PAP: bidirectional pyrophosphorolysisactivated polymerization

Bp: Base pairs

cAMP: cyclic adenosine monophosphate

CAPP-Seq: cancer personalized profiling by deep sequencing

CCK8: Cell counting kit 8

CDK: cyclin-dependent kinase

CEA: carcinoembryonic antigen

cfDNA: cell-free DNA

CM: cutaneous melanoma

CNV: copy number of variations

CRC: colorectal cancer

CTCs: circulating tumor cells

ctDNA: circulating tumor DNA

CYSLTR2: cysteinyl leukotriene receptor 2

DAG: diacylglycerol

ddPCR: droplet digital Polymerase Chain Reaction

DNA: Deoxyribonucleic acid

DNMT3A: DNA Methyltransferase 3 Alpha

EDTA: ethylenediaminetetraacetic acid

EIF1AX: Eukaryotic translation initiator factor 1A X-linked

EVs: extracellular vesicles

F: fluid

FA: percentage of fractional abundance

FDA: The United States Food and Drug Administration

FITC: Fluorescein isothiocyanate

FU: follow-up time

G:Growth

GENAIR: Genetic Susceptibility to Air Pollution and Environmental Tobacco Smoking

GNA11: G protein subunit alpha 11.

GNA11: guanine nucleotide-binding protein G subunit alpha 11

GNAQ: G protein subunit alpha Q

GNAQ: guanine nucleotide-binding protein G subunit alpha

GTP: Guanosine triphosphate

Gy: Gray

IP3: inositol triphosphate

IR: irradiation

LOH: loss of heterozygosity

LUMPO: Liverpool Uveal Melanoma Prognosticator Online

MAPK: mitogen-activated protein kinase

MEK : Mitogen-activated protein kinase

MF: mifepristone

MM: milometer

MRD: Minimal residual disease

mTOR: mammalian target of rapamycin

NCM: normal choroidal melanocytes

ng: nanogram

NGS: next-generation sequencing

NSCLS: non-small cell lung cancer

OP: orange pigment

OS: overall survival

PAP: pyrophosphorolysis-activated polymerization

PBS: Phosphate-buffered saline

PCR: polymerase chain reaction

PDX: patient-derived xenograft

PFS: progression-free survival

PGE2: prostaglandin E2

PI: propidium iodide

PI3K: phosphoinositide 3-kinase

PIP2: Phosphatidylinositol 4,5-bisphosphate

PKC: protein kinase C

PKCi: protein kinase C inhibition

PLCB4: phospholipase C beta 4

PP: peripapillary

PRAME: preferentially expressed antigen in melanoma

qPCR: real-time Polymerase Chain Reaction

RAC1: Rac family small GTPase

RFI: recurrence-free interval

RNA: Ribonucleic acid

RO: roscovitine

RPMI: Roswell Park Memorial Institute

Rx: Treatment

Safe-Seqs: safe-sequencing system

SCNA: somatic copy number alteration

SF3B1: splicing factor 3b subunit 1

SNV: single nucleotide variation

SRSF2: serine and arginine rich splicing factor 2

TAmSeq: tagged-amplicon deep sequencing

TCGA: The Cancer Genome Atlas

TEC-SEQ: targeted error correction sequencing

TET2: Tet Methylcytosine Dioxygenase 2

TNM: Tumor-Node-Metastasis

UM: uveal melanoma

VA: valproic acid

WES: whole-exome sequencing

WGS: whole-genome sequencing

WT: Wild type

YAP: Yes-associated protein

β-AR: beta-adrenoceptor

Abstract

Liquid biopsy has emerged as a minimally invasive approach to detect and monitor cancer progression, recurrence, and response to treatment. Tumor cells release fragments of circulating tumor (ct) DNA that can be isolated from a liquid biopsy. ctDNA is released from all tumor cells and reflects an integrative genetic profile of all tumor subclones. ctDNA analysis is especially useful when a tissue biopsy is not possible due to tumor localization. Uveal melanoma (UM) is the most common intraocular tumor in adults, occurring in the posterior segment of the eye, and it is associated with a high risk of metastasis. It can arise *de novo* or from a malignant transformation from a nevus. In this thesis, ctDNA was evaluated as a biomarker of UM to monitor tumor development and disease course. We established a novel assay to detect and quantify mutant alleles of UM-specific early mutations in ctDNA using a liquid biopsy. Our hypothesis is that ctDNA can be detectable using driver mutations, and fluctuations of its levels indicate tumor formation. Using preclinical models, we also investigated the etiology and kinetics of ctDNA release under cytotoxic and stress conditions, in order to gain insight into the mechanisms underlying cell-free (cf) DNA release in human cancer cells.

Using a combination of *in vitro* cell culture systems, a human UM xenograft animal model, and a clinical study, we demonstrated both the feasibility and clinical utility of using UM initiating mutations to detect and quantify ctDNA. Using human UM cancer cell lines, we showed the potential of culture systems to detect cfDNA released by cancer cells. We found a strong correlation between blood-based ctDNA levels and tumor development and progression in a rabbit xenografted model. We then conducted a clinical study in primary UM and nevus patients, and healthy individuals. ctDNA levels were detected in all UM patients, whereas it was only detected

in nevus patients at risk for malignant transformation, demonstrating the clinical utility of this biomarker assay to detect cancer development.

Finally, to gain a better understanding of the etiology and kinetics of ctDNA, we performed robust analyses on ctDNA emission and fragmentation in response to clinically relevant cytotoxic agents and cellular stress. We demonstrated that ctDNA release and fragment length were altered under cytotoxic conditions, further demonstrating the relevance of ctDNA emission in cell culture systems as a biomarker of drug response.

Taken together, this thesis provides comprehensive data demonstrating that ctDNA through a liquid biopsy is a powerful tool to detect and monitor cancer in a minimally invasive, sensitive, and specific approach.

Résumé

La biopsie liquide est une approche peu invasive pour détecter et surveiller la progression du cancer, sa récurrence, et sa réponse au traitement. Les cellules tumorales libèrent des fragments d'ADN tumoral circulant (tc) qui peuvent être isolés à partir d'une biopsie liquide. L'ADNct est libéré de toutes les cellules tumorales et reflète un profil génétique intégratif de tous les sous-clones tumoraux. L'analyse de l'ADNct est particulièrement utile lorsqu'une biopsie tissulaire n'est pas possible en raison de la localisation de la tumeur. Le mélanome de l'uvée (MU) est la tumeur intraoculaire la plus fréquente chez les adultes et il est associé à un risque élevé de métastases. Cette tumeur survient dans le segment postérieur de l'œil, soit *de novo* ou à la suite d'une transformation maligne à partir d'un naevus. Dans cette thèse, nous évaluons l'ADNtc en tant que biomarqueur du MU pour surveiller le développement tumoral et l'évolution de la maladie. Nous avons établi un nouveau test pour détecter et quantifier les allèles associées à des mutations précoces spécifiques au MU dans l'ADNtc à l'aide d'une biopsie liquide. Nous émettons l'hypothèse que l'ADNtc peut être détectée à l'aide de mutations conductrices, et que les fluctuations de ses niveaux indiquent la formation de tumeurs. À l'aide de modèles précliniques, nous avons également étudié l'étiologie et la cinétique de la libération de l'ADNtc dans des conditions cytotoxiques et de stress cellulaire, afin de mieux comprendre les mécanismes sous-jacents à la libération d'ADN acellulaire dans les cellules cancéreuses humaines.

En utilisant une combinaison de systèmes de culture cellulaire *in vitro*, un modèle animal de xénogreffe de cellules MU humaines, et une étude clinique, nous avons démontré à la fois la faisabilité et l'utilité clinique de l'utilisation de mutations initiatrices UM pour détecter et quantifier l'ADNct. En utilisant des lignées de cellules cancéreuses UM humaines, nous avons démontré le potentiel des systèmes de culture pour détecter l'ADN acellulaire libéré par les cellules

cancéreuses. Nous avons ensuite trouvé une forte corrélation entre les taux sanguins d'ADNct et le développement et la progression de la tumeur dans un modèle xénogreffé de lapin. Nous avons aussi mené une étude clinique chez des patients atteints de MU primaire et de naevus, et chez des individus en bonne santé. Les niveaux d'ADNct ont été détectés chez tous les patients UM, alors qu'ils n'ont été détectés que chez les patients atteints de naevus à risque de transformation maligne; démontrant l'utilité clinique de ce dosage de biomarqueurs pour détecter le développement du cancer.

Finalement, pour mieux comprendre l'étiologie et la cinétique de la libération de l'ADNtc, nous avons effectué des analyses robustes sur l'émission et la fragmentation de l'ADNtc en réponse à des agents cytotoxiques cliniquement pertinents et au stress cellulaire. Nous avons démontré que la libération de l'ADNtc et la longueur des fragments étaient modifiées dans des conditions cytotoxiques, démontrant d'avantage la pertinence de l'émission de l'ADNtc dans les systèmes de culture cellulaire en tant que biomarqueur de la réponse aux médicaments.

Dans son ensemble, cette thèse fournit des données exhaustives démontrant que l'ADNtc obtenue par biopsie liquide est un outil puissant pour détecter et surveiller le cancer via une approche peu invasive, sensible et spécifique.

Acknowledgments

The best of this journey has been the company. I have been tremendously lucky for being surrounded by extraordinary people without whom this work could not have been done.

I cannot express my gratuity enough to my wonderful supervisor and mentor Dr Julia Burnier, for granting me the opportunity to be here. It has been a very extraordinary experience to embark on this liquid biopsy journey along with her. Since I met Dr. Burnier, working with her has been a great honour. I will always be thankful for all her support, guidance, encouragement, and help to discover the potential that I even did not know I had.

I am very grateful to my committee, Drs Jonathan Cools-Lartigue and Peter Metrakos for their support, suggestions, and comments throughout my doctoral studies.

I am very thankful for MITACS and CONACYT (#739468) financial support.

I would also like to thank the Department of Pathology wholeheartedly, especially Dr. Edith Zorychta and Hua Ling, for their exceptional support and involvement.

I offer my heartfelt appreciation to my lab colleagues: past and present members of Dr. Julia Burnier's laboratory. I cannot imagine how I would have endured these last years without the support of this incredible team.

Thank you so much to our collaborators: Drs Sonia Callejo, Jacqueline Coblentz, and Miguel Burnier. Their collaboration was highly instrumental to this work.

Also, infinite thank you to all current and past members of the Ocular Pathology & Translational Research Laboratory. A special thanks to Tiffany Porraccio, Sabrina Bergeron, Christina Mastromonaco, Ana Dias, Denise Miyamoto, Alicia Goyeneche, and last but not least, Mohamed Abdouh for their support, friendship, and enthusiasm.

Many thanks to my friends from all over the world and those who have made Montreal feel like home.

Thank you to my mom, Rosa, and my brother, Louis, for their enduring support and love. And the most special thank you from the bottom of my heart is for my life partner, my husband, Rodrigo Lopez. There are not enough words to describe his love and support.

Contributions to original knowledge

In conformity with the "Guideline for Thesis Preparation" policy reported at McGill University, this doctoral thesis is manuscript-based, presenting as a collection of four original research articles and a review, all written by me with the collaboration of co-authors.

Chapter 1 reviews liquid biopsy, including different studies, applications, and methodologies. It also contains an introduction about uveal melanoma [1] and the link between liquid biopsy and uveal melanoma. Portions of the introduction are adapted from a review article on uveal melanoma. This comprehensive review article focuses on the pathogenesis of uveal melanoma, particularly focusing on the communication between UM cells and the liver microenvironment, where the majority of UM metastasis occurs.

Manuscript 1: Bustamante, P., Piquet, L., Landreville, S. & Burnier, J. V. Uveal melanoma pathobiology: Metastasis to the liver. *Semin Cancer Biol* 71, 65-85, doi:10.1016/j.semcancer.2020.05.003 (2021).

Chapter 2 is based on a published manuscript [2] showing the feasibility of using UM mutations (*GNAQ, GNA11, PLCB4, CYSLTR2*) to detect ctDNA. I first assessed fragmented DNA extracted from supernatant from human UM cell lines by ddPCR. Subsequently, ctDNA levels and tumor formation and progression were correlated using blood isolated from fifteen rabbits xenografted with UM cells. No detectable ctDNA levels were found at the time of cell inoculation. In contrast, ctDNA levels in rabbit plasma were detected as early as four weeks post-inoculation (preceding clinical detection of the tumors). Moreover, eye fluid (aqueous humor) was evaluated as a source of ctDNA. While no detectable levels of ctDNA were found at the time of cell inoculation, ctDNA from AH was detected when tumors were formed. ctDNA levels derived from

rabbit blood and AH correlated with tumor formation and progression. Finally, to validate our methodology in a clinical setting. ctDNA levels in patient blood were assessed in a clinical study conducted at the McGill Academic Eye Centre. ctDNA was isolated from patient blood from primary UM participants, patients with a nevus (eye pigmented lesion), and healthy individuals; and then analyzed by ddPCR using UM mutations. ctDNA levels were detected in all UM patients. In the choroidal nevus cohort, levels of ctDNA were detected in 44% of cases and correlated with the presence of risk factors for malignant transformation into choroidal melanoma. Overall, ctDNA is a powerful clinical biomarker of UM, and can provide clinically relevant information on malignant tumors from benign nevi and UM disease.

Manuscript 2: Bustamante, P. *et al.* Circulating tumor DNA tracking through driver mutations as a liquid biopsy-based biomarker for uveal melanoma. *J Exp Clin Cancer Res* 40, 196, doi:10.1186/s13046-021-01984-w (2021).

Chapter 3: To gain a better understanding of ctDNA, we utilized our *in vitro* model to evaluate the effects of cellular stress and death on DNA emission to determine how kinetics influence ctDNA levels. Human cancer cells were subjected to various agents, specifically valproic acid to inhibit cell growth, APO2L (apoptosis-inducing ligand) to induce apoptosis, roscovitine (a CDK inhibitor, which induces cell cycle arrest and initiates apoptosis), irradiation (to induce senescence), and heat (to induce necrosis). All treatments caused increased emission of mutant cfDNA compared to control conditions, with apoptotic cell death leading to the highest levels of cfDNA. Treatments also influence the fragmentation of cfDNA, with different fragment lengths associated with cell death mechanisms. This data adds to the growing body of literature

demonstrating the importance of understanding cfDNA kinetics in order to effectively interpret liquid biopsy-based ctDNA data in the clinic.

Manuscript 3: Bustamante et al, 2022. The kinetics and fragmentation of cell-free DNA from cancer cells are influenced by anticancer treatments. Submitted to Scientific Reports.

Chapter 4 is based on two published manuscripts that demonstrate the utility of ctDNA to monitor drug response, showing that cell death is associated with increased release of cfDNA into the culture media [3, 4]. This chapter shows the dose-dependent cfDNA release from melanoma cells following two different treatments with potential anticancer drugs, a beta-blocker or mifepristone, both proposed as adjuvant therapy, suggesting ctDNA can monitor their treatment response. Our data demonstrated that ctDNA was released in a dose-dependent manner from melanoma cells following an anticancer treatment. These findings highlighted cfDNA biomarker role for treatment response.

Manuscript 4: Bustamante Alvarez, P. *et al.* Anticancer effects of mifepristone on human uveal melanoma cells. *Cancer Cell International* **21**, 607, doi:10.1186/s12935-021-02306-y (2021).

Manuscript 5: Bustamante *et* al. Beta-blockers exert potent anti-tumor effects in cutaneous and uveal melanoma. *Cancer Med* **8**, 7265-7277, doi:10.1002/cam4.2594 (2019).

These studies outlined in this thesis collectively investigated whether fragments of DNA circulating in the fluids inform cancer cell biology. In particular, by using *in vitro* cultures, I extensively studied ctDNA release under cytotoxic conditions, which include mechanistically

relevant drugs and potential anticancer treatments. Using a consistent methodology in UM preclinical model and a clinical study, this thesis validated the use of ctDNA as a first-ever blood-based biomarker of UM development and disease progression.

The ideas of this dissertation were supported by the following grants and awards:

2021 MITACS Award for Outstanding Innovation- PhD

2021 Zu-hua Gao Graduate Award Department of Pathology. McGill University

2021 Scholarship Competition Entrepreneurship in Oncology

2020 Travel award. Post-Graduate Students' Society- McGill University

2020 Travel award. Department of Pathology. McGill University

2019-2021 MITACS accelerate

2019-2022. Scholarship for doctoral studies by The National Council of Science and Technology of Mexico (CONACYT)

2019 Best Poster award Pathology Finlayson Research Day

2019 GREAT Travel award. Department of Pathology. McGill University

2019 Travel award The Association for Research in Vision and Ophthalmology

2018 Grad Excellence Award in Medicine. McGill University

Contribution of Authors

I am the first author of all manuscripts included in this thesis. My PhD supervisor, Dr Julia Valdemarin Burnier, appears as a senior author on all manuscripts as a reflection of her involvement in supervision, study design, data analysis, funding and manuscription preparation. Contributions of the student and co-authors are explicitly stated below.

1. Chapter 1: The literature view was written by me. Some portions regarding uveal melanoma (section 2) are adapted from the review "Uveal melanoma pathobiology: Metastasis to the liver" published in Seminars in Cancer Biology, where I am first author [1]. (Manuscript 1).

2. Chapter 2 (Manuscript 2): I carried out all experiments for the cell culture, animal model, and analysis of human samples, consented patients, and partially oversaw ethics approval. TT optimized GNA11 ddPCR conditions, supported cfDNA, and plasma isolation, and consented some of the patients. JC saw patients, performed cell inoculation, conducted fundoscopy, and ultrasound examination through the animal model, and supported clinical samples analysis. CM oversaw ethics review and approval, consented patients and coordinated animal study. MA supported data analysis, discussion, and graph generation. CF and RPP performed cell inoculation, conducted fundoscopy and ultrasound examination through the animal model, and supported clinical samples analysis. NB and CLD took blood from patients. RASA supported cfDNA isolation from aqueous humor derived from some animals. EY organized fundoscopy and ultrasound data. MNB and SAC are the attending ophthalmologists, JVB designed the study, provided the funding, supervised staff and students, and analyzed data. All authors helped to draft the manuscript.

3. Chapter 3 (Manuscript 3): I carried out all experiments. MA supported data analysis and discussion, and graph generation. TT supported study designing and data analysis. JVB

designed the study, provided the funding, and supervised staff and students.

4. Chapter 4 (Manuscripts 4 and 5): This chapter reflects selected data from two manuscripts: “Beta-blockers exert potent anti-tumor effects in cutaneous and uveal melanoma” and “Anticancer effects of mifepristone on human uveal melanoma cells” published in Cancer Medicine and Cancer Cell International, respectively, by me as the first author. All of the experiments on ctDNA quantification shown in this thesis were performed by me. A.L. and A.G. supported some cytotoxicity analysis. JVB designed the study, support data interpretation, provided the funding, and supervised staff and students.

Introduction

Precision oncology is the molecular profiling of a tumor with the ultimate goal to provide an accurate diagnosis and treatment of cancer patients [5]. To characterize tumor genomes in detail, this profiling can be done with a biopsy followed by histology and/or next-generation sequencing (NGS). NGS can uncover numerous types of gene alterations, including point mutations, as well as insertions and deletions of bases, by determining the nucleotide sequence of DNA or RNA. Since the 2000s, NGS has informed about genetic alterations in patients, leading to actionable findings in clinical settings, such as modifying treatment based on identified alterations [5]. Moreover, immunohistochemistry on tissue is often used to profile a tumor through specific antibodies [6]. Therefore, access to a tumor specimen for NGS or histology is paramount. However, tumor tissue is not always available depending on a patient's tumor localization and/or conditions, and cannot be repeatedly performed over time, such as during and after treatment. Tissue biopsies require specialized equipment and a medical team, limiting their utility in remote regions [7]. Notably, procedural complications have been reported in a range from 1.6% to 17.1% of cases in a total of 57 clinical trials [7]. Moreover, serial tissue biopsies to perform NGS or histology analyses might be impossible to perform due to a tumor's localization and/or invasiveness. Finally, a single snapshot from a tumor is not representative of spatial and temporal tumor heterogeneity [8]. Tumor heterogeneity refers to the diversity in bulk tumor cells that harbor different genetic and epigenetic characteristics across and within tumor sites or in subclones over time [9]. Altogether, the challenge to obtain tumor material repeatedly and the lack of information about humor heterogeneity are challenges associated with tissue biopsy as a tool to monitor tumor burden and progression [8, 10].

To address this need, liquid biopsy has emerged as an alternative method to sample bodily fluids, mainly blood, but also urine, saliva, ascites, spectrum, aqueous humor, and pleural fluid [11, 12]. Since these fluids are easy to access, they are collected in a non- or minimally invasive manner. In oncology, liquid biopsy refers to sampling and analyzing circulating tumor cells (CTCs) and their components [11-14]. These components can specifically include circulating tumor (ct) nucleic acids, extracellular vesicles (EVs) such as exosomes [15] and tumor-educated platelets [16]. In particular, circulating nucleic acids encompass RNA (including small RNAs and mRNA) and DNA [17]. Performing a liquid biopsy is especially useful when a tissue biopsy is not possible due to tumor localization, low amount of tissue, or the vulnerable condition of a patient [8].

Uveal melanoma (UM) is the most common intraocular tumor in adults and arises from melanocytes in the pigmented uveal (iris, ciliary body, and choroidal) tissue of the eye, mainly from the choroid (posterior part of the eye) [1]. This tumor occasionally arises from a pre-existing choroidal nevus, a benign pigmented lesion [18]. Unlike most solid malignancies, the diagnosis of UM is made through imaging, with intraocular biopsies done for prognostication. Although UM is a rare type of cancer, with an incidence of 6-7 cases per million, it is associated with a high mortality rate: about 50% of UM patients succumb to metastasis, mainly of the liver [1].

The spread of tumor cells from the eye to distal organs occurs through hematogenous dissemination. It has been shown that before any clinical sign of spread, cancer cells can already begin the process of micrometastasis [19]. By using blood as an analyte, some studies have reported the presence of micrometastasis 2.9 years prior to primary tumor diagnosis [19, 20]. In addition, a study that evaluated 30 primary UM cases, detected circulating tumor cells in 87.5% of

the cases regardless of their treatment [21]. Therefore, using blood as a liquid biopsy may provide clinically useful information about disease progression [22].

To distinguish circulating DNA fragments derived from tumor cells (ctDNA) from those derived from all cells (cell-free DNA, cfDNA), fragments can be tracked through tumor-specific molecular alterations, such as hotspot somatic mutations [12]. UM is characterized by a mutually exclusive hotspot mutation in either *GNAQ* or *GNA11*, making up 57% and 41% of cases, respectively [23, 24]. The remaining proportion of UM tumors is reported to have a mutation in either *PLCB4* [25] or *CYSLTR2 [26]*. Therefore, virtually all UM cases have a mutation in one of these four genes.

This dissertation hypothesizes that initiating UM mutations can be used to detect ctDNA, and that their levels reflect disease burden. Moreover, while it is known that ctDNA is a product of apoptosis, necrosis, and cellular secretions [27]; the exact mechanism responsible for ctDNA release is unclear. To overcome this gap, this work also hypothesizes that ctDNA emission is altered by cytotoxic and stress conditions and its levels indicate drug response. To address these hypotheses, this dissertation aims to:

1. Evaluate ctDNA as a biomarker of disease course in UM and evaluate ctDNA kinetics to predict prognosis and disease progression in real-time (Chapter 2).
2. Determine the release pattern of ctDNA upon cytotoxic agents to understand the mechanisms underlying DNA released by tumor cells during anti-cancer treatment (Chapter 3).
3. Assess the release pattern of ctDNA upon potential UM adjuvant therapies to identify a biomarker of treatment response (Chapter 4).

Chapter 1: Literature review

1. Liquid biopsy

Liquid biopsy has gained much attention in precision oncology as a tool of diagnosis and treatment monitoring [28]. In this section, I will include a comprehensive review of the relevant literature on liquid biopsy with a focus on ctDNA. After introducing ctDNA applications and methodologies, I will then review UM. Finally, I will include a summary of the clinical relevance of ctDNA in UM.

1.1. Cell-free DNA and circulating tumor DNA

Cell-free (cf) DNA is a mix of fragments of non-encapsulated DNA [17, 29]. These fragments are mainly double-stranded (ds) DNA [30] but may also encompass single-stranded (ss) [31], mitochondrial DNA [32], and small extrachromosomal circular DNA[33]. While cfDNA is predominantly released by hematopoietic cells in physiological conditions [34-37], cfDNA has been also observed in cancer [17], acute trauma [38], cerebral infarction [39], transplantation [40], sepsis [41], and pregnancy [42]. Indeed, fetal DNA sequences in maternal blood have led to various purposes in prenatal medicine, such as sex determination, screening for aneuploidies (e.g. trisomy 21 aka Down Syndrome), and monogenic disorders [42].

cfDNA has been detected mainly in blood but also in other bodily fluids, for instance, urine [43], saliva [44], pleural fluid [45], and cerebrospinal fluid [46]. In the bloodstream, the half-life of cfDNA ranges from 15 minutes to 2.5 hours [47], and the range of time may depend on cfDNA clearance, a process that is not fully understood. Some studies have suggested that cfDNA is cleared from the circulation via nuclease action and renal excretion into the urine [27]. In particular, cfDNA is partially removed by plasma nucleases [48], mainly DNase I. Then, macrophages in the liver, spleen, and kidney take up and degrade cfDNA, and it is finally

eliminated by DNase activity and renal excretion processes [49]. This short half-life of cfDNA is particularly important in pathological conditions in which cfDNA may have a role as a real-time biomarker.

In both physiological and pathological conditions. cfDNA encompasses small fragments from ~70 base pairs(bp) to large fragments that measure >10,000 bp [50-54]. The majority of fragments are ~166 bp [55]. This size correlates with the length of DNA wrapped around a nucleosome (147 bp), plus an extra stretch of DNA (20bp) to link two nucleosome cores [56]. This pattern of cfDNA size is probably a result of apoptotic inter-nucleosomal DNA cleavage coordinated by the caspases-activated DNase and Dnase II during dying cells or phagocytosis respectively [57]. The size of cfDNA, thus, provides clues for its release mechanism. While ~166 bp fragments corresponding to apoptotic cells, 10,000 bp fragments likely originate from necrotic cells.

The release of cfDNA mainly occurs during cellular turnover, such as during apoptosis [35, 58, 59], necrosis [35, 53, 59], and senescence [60]. In addition, active secretion, autophagy, pyroptosis, and NETosis have also been shown to contribute to its release [61]. In healthy individuals, cfDNA concentration in blood ranges from 0-100 ng/ml, with apoptotic leukocytes the main source. In contrast, elevated levels of cfDNA, up to >1000 ng/ml, are detected in cancer patients, which may be a result of tumor cell-derived DNA. Tumor-derived cfDNA is referred to as circulating tumor (ct) DNA. ctDNA has gained wide interest as a real-time liquid biopsy-based biomarker [29, 59]. Various studies in oncology have reported that its levels correspond to tumor burden [47] and tumor cell metabolism which inform about tumor behavior or aggressiveness [62]. It is therefore important to distinguish ctDNA and normal cfDNA. This distinction is possible because ctDNA contains genomic alterations specific to the tumor cells [35] (**Figure 1.1**).

1.2. Methods to detect ctDNA

ctDNA represents a portion of cfDNA from all cells in the body, but must be identified through tumor-specific characteristics to distinguish from cfDNA originating from normal cells. The most commonly used method to differentiate ctDNA within total cfDNA is through genetic alterations that are present in cancer or precancerous cells but that are absent in normal cells.

Somatic mutations and genomic alterations

Tumor-specific alterations used to detect ctDNA include single nucleotide variants, insertions and deletions, and chromosomal abnormalities such as copy number variations and translocations. For example, mutations in tumor suppressor gene (e.g., *TP53*) and oncogenes (e.g., *BRAF* and *KRAS*) can be used to detect the ctDNA fraction in tumors that express these signatures. These mutations, therefore, allow us to discriminate ctDNA from normal circulating cfDNA.

Somatic mutations have been widely used to analyze ctDNA in cancer patients. Interestingly, the first FDA approved liquid biopsy-based test, called Cobas EGRG mutation test v2, focuses on detecting various deletions, substitutions, or mutations in exon 18, 19, 20, and 21 of the epidermal growth factor receptor (EGFR) gene in patients with non-small lung cancer (NSCLC) when tissue biopsy is unavailable [63]. Another widely used example of a mutation to detect ctDNA is *KRAS*. *KRAS* mutations are frequently expressed in various cancer types, such as colorectal[64] and pancreatic cancer [65]. Detection of ctDNA via a *KRAS* mutation has been used to monitor tumor progression [66] and treatment response [67]. For example, a study conducted in 150 colorectal (CRC) patients showed that *KRAS* mutated ctDNA correlates with clinicopathologic factors, suggesting that *KRAS*-mutant ctDNA is an independent risk factor for recurrence [68].

In addition to somatic mutations, ctDNA can be also detected by loss of heterozygosity (LOH)[69], microsatellite instability [70], and the integrity of non-coding genomic DNA repeat sequencing [71]. However, their clinical utility is still under investigation [17].

Epigenetic events

Given that epigenetic alterations, such as methylation, are relevant in tumorigenesis and progression, methylation profiling has been used as a marker to analyze ctDNA. One example is the detection of methylated Septin 9 DNA which is associated with CRC occurrence. This detection enabled the development of the Epi proColon 2.0 test, a blood-based FDA-approved test for the early diagnosis of CRC that allows screening suspected patients, whose diagnosis will then be confirmed by colonoscopy and sigmoidoscopy. Although lower endoscopy is still needed, this test has shown to be highly sensitive as a CRC screening approach [72].

Fragment size

cfDNA encompasses a mix of non-encapsulated DNA with fragments mostly ranging from 140-220 bp, with a peak at 166 bp [52] and a few fragments of several kilobases [50]. The analysis of fragment size has also been proposed as a prognostic factor, an emerging field called fragmentomics [73]. Importantly, the fragment size differs between cfDNA from normal cells and cfDNA derived from tumor cells (ctDNA) [74-77]. In particular, some reports have stated cfDNA fragments derived from patients with hepatocellular carcinoma [78], melanoma [79], and localized prostate cancer [80] are shorter compared to cfDNA isolated from healthy individuals. Furthermore, shorter fragments have been correlated with poor prognosis in renal cell carcinoma [81] and advance pancreatic cancer [74]. In addition, fragmentation pattern of ctDNA correlates with tumor size, with metastatic colorectal patients showing higher fragmentation than non-cancerous samples[82]. Interestingly, tissue-specific differences in nucleosome wrapping result in

different fragment size. Therefore, cfDNA fragmentation pattern may inform on what tissue the fragments are coming from. For example, cfDNA size derived from hematopoietic cells is different from fragments derived from other tissue of origin [79]. Overall, ctDNA size seems to reflect emission procession and inform on the tissue of origin [79].

Concentration

The concentration of total ctDNA yield of plasma has been proposed to differentiate between healthy and cancer patients [83, 84]. While healthy patients have normal cfDNA levels between 0 to 77 ng/ml [85], with an average of 6 ng/ml [84, 86], cancer patients have documented a range from 0-5 [80] to >1,000 ng/ml [17, 85]. Moreover, ctDNA levels differ between primary and metastatic patients as well according to tumor localization [87]. Higher levels of ctDNA have been found associated with more advanced diseases, likely reflecting disease burden [12]. The total amount of ctDNA shed into the blood by tumor cells varies from 0.01- up to 40% of the total cfDNA[47, 59, 87-89] according to tumor burden, cancer stage, and response to treatment [90]. Given that ctDNA levels may represent 0.01% of the total cfDNA fraction, highly sensitive technologies are needed for its analysis in the bloodstream of cancer patients[87].

Various experimental approaches have paved a better understanding of ctDNA biology and its clinical utility [29]. Next, I will focus on some methods and experimental techniques to analyze ctDNA.

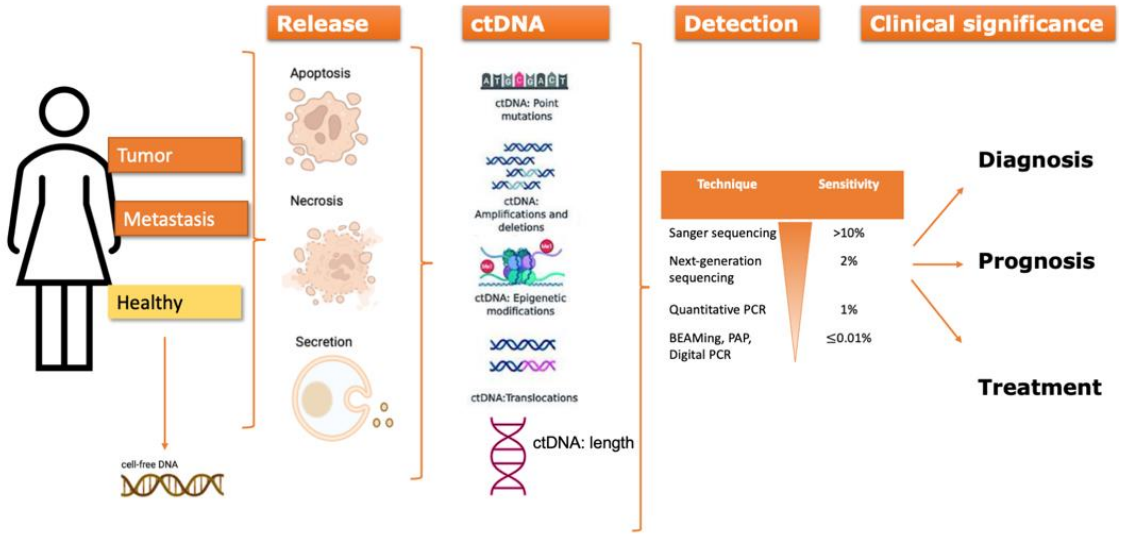

Figure 1. 1: Schematic representation of ctDNA as a liquid biopsy for cancer.

cfDNA is released by dying or dead cells and secretions in normal and pathological conditions. Tumor-specific DNA (ctDNA) can be evaluated by different techniques, which inform about cancer diagnosis, prognosis, and treatment response. Adapted from Diaz *et* al. 2014 [12], Heitzer *et* al. 2015 [13], and Pessoa *et* al, 2022[91].

1.3. Experimental techniques for ctDNA analysis

Current technologies have enabled us to advance ctDNA analysis. The most used methodologies (**Table 1**) have been divided into i) targeted approaches to detect specific gene mutations or structural chromosome rearrangements in specific genome region, and ii) untargeted approaches to find *de novo* ctDNA mutations and somatic copy number variations (CNVs) [90, 92].

Targeted methods are high sensitivity, such as digital droplet (dd), qualitative-real time (qPCR), and BEAMing (i.e. beads-emulsion-amplification-magnetics) polymerase chain reaction (PCR) that target DNA sequencing to a single or limited panel of tumor-specific mutations.

BEAMing is a sensitive technique that combines PCR with flow cytometry to detect known mutations [93]. Another highly sensitive method to detect rare mutations is ddPCR. ddPCR allows absolute quantification of wildtype and mutant alleles separately at an endpoint. ddPCR detects very low levels of ctDNA. Particularly, by partitioning the reaction in twenty thousand individual droplets per well, and then amplifying and fluorescence reading, ddPCR has up to 0.001% sensitivity [94]. Sensitivity is defined as the ability to detect tumor DNA in a mixture of tumor and normal DNA [12]. In other words, this technique can detect up to 3 positive events out of 300,000 screened [95]. Although both techniques rely on knowledge of the mutational profile and only detect specific genomic sequences, they are fast, cheap, and highly sensitive [93].

Moreover, NGS encompasses targeted and untargeted approaches. Targeted methods-NGS can simultaneously detect numerous specific mutations in ctDNA. These methods include the safe-sequencing system (Safe-Seqs), cancer personalized profiling by deep sequencing (CAPP-Seq), and tagged-amplicon deep sequencing (TAmSeq). On the other hand, untargeted approaches such as whole-genome sequencing (WGS) and whole-exome sequencing (WES) allow for assessment of genomic alterations across the genome or exome, respectively [96]. NGS-based methods are useful when there is no or limited information on the mutations profile of the tumor. For example, in cases where tumor biopsies are missing. Therefore, no information about the primary tumor is available or when mutations are scattered through almost the entire domain of the gene, such as in *TP53*. Although errors introduced during the NGS library construction can be mitigated by using molecular barcoding, this technique usually offers a relatively lower (0.1%) sensitivity [28] and often requires a high input sample volume

Altogether various methodologies can be used to detect and analyze ctDNA from liquid biopsies, selecting the appropriate technique to study ctDNA depends on tumor burden, disease

stage, prior knowledge of tumor-specific alterations, the amount anticipated of sample, and cost. The ability to accurately detect ctDNA has led to multiple clinical applications [12].

Table 1 Summary of experimental techniques for ctDNA analysis

Methods		Approach	Advantage	Limitation	Sensitivity	Ref
Targeted ctDNA	NGS-based technologies	safe-sequencing system (Safe-Seqs), cancer personalized profiling by deep sequencing (CAPP-Seq), and tagged-amplicon deep sequencing (TAmSeq)	Provides a comprehensive view of genomic regions. Detect somatic mutations in a predefined gene panel.	Need an assay customized. Less comprehensive than untargeted approaches.	<0.01%-2%	[97]
	PCR-based technologies	Quantitative-real time polymerase chain reaction (PCR)	Amplifies mutant DNA molecules. Easy and low cost	Less sensitive compared to other PCR-based methods.	1%	[98]
		digital droplet (dd), qualitative-real time (q), and BEAMing (i.e. beads-emulsion-amplification-magnetics)	Counts mutant molecules via partitioning of DNA molecules. High sensitivity	A prior knowledge of a tumor-specific mutation. Test a small number of genomic positions.	0.01%	[99-101]
Untargeted ctDNA	NGS-based technologies	whole-genome sequencing (WGS) and whole-exome sequencing (WES)	Analysis of entire genome and copy number alterations.	Low sensitivity Expensive	>5%	[102]

1.4. ctDNA-based liquid biopsy applications

While the term liquid biopsy has gained interest recently [11], the presence of fragmented material in blood under non-physiological conditions dates back to 1948 when it was first described by Mandel and Métais [103]. Following this, Leon *et* al. in 1977 demonstrated a greater level of ctDNA in the serum of metastatic cancer patients compared to nonmetastatic patients[104]. This study also observed an association between fluctuations of ctDNA levels in blood and treatment response, suggesting the utility of free DNA in blood to evaluate treatment response [104]. Later, Stroun *et* al. reported ctDNA in plasma in ten of 37 cancer patients, whereas no blood-derived DNA was seen in healthy individuals [30]. In 1994, by amplifying *KRAS* gene with polymerase chain reaction in three pancreatic adenocarcinoma patients, Sorenson *et* al. reported the occurrence of mutated sequences in tumor tissue and plasma simultaneously [105]. In the same year, Vasioukhin *et* al. showed the presence of a point mutation in the *NRAS* gene in DNA isolated from plasma, blood cells, and bone marrow of ten patients suffering from acute myelogenous leukaemia or myelodysplastic syndrome [106]. Both studies reflect the clinical utility of circulating DNA in blood, suggesting that blood could be an alternative material to monitor disease. It was not until the advancement in the quantitative polymerase chain reaction, the advent of next-generation sequencing, and the cancer genome project, that seminal studies solidified the concept that ctDNA could play a major role in cancer research [107].

1.4.1. ctDNA as an early diagnostic and screening maker

Given that an early cancer diagnosis might allow earlier intervention and thus better outcome [108], ctDNA has gained attention as a biomarker in early-stage cancer detection and in screening. However, this application is limited by the low fraction, about 0.01%-1% of ctDNA to

cfDNA in early-stage diseases [109], the presence of relevant mutations to monitor, and the sensitivity of current detection methods [12]. Another limitation is the documented accumulation of age-related mutations in blood and skin from noncancerous individuals [110, 111]. For example, somatic mutations (*DNMT3A*, *TET2*, and *ASXL1*) were detected in 219 of 2300 individuals from 70 to 79 years old, 37 of 317 subjects from 80-89 years old, and 19 of 103 persons 90-108 years of age [112]. *TP53* has been also detected in 11% of 225 healthy individuals [113]. The presence of such mutated DNA may arise due to clonal hematopoiesis in normal cells, a process in which somatic mutations in hematopoietic stem cells may lead to clonal expansion of mutations in blood cells [114]. Although these mutations from hematopoietic cells can be detected in the elderly population, they have been associated with a low risk of cancer [115].

Despite limitations in the collection, detection, and analysis of ctDNA, a few studies have reported the potential of ctDNA in early-stage cancers, mainly in cancers with common hot-spot mutations in which high sensitivity techniques (**Table 1**) can be performed [113]. In particular, one study showed that 47% of patients in stage I of colorectal, gastroesophageal, pancreatic, and breast cancer had detected levels of ctDNA [87]. Similarly, ctDNA was detected in 35.7% of early-stage small-cell lung cancer [113]. ctDNA has also been found in patients with early-stage breast cancer before and after surgery [109] and who were receiving a neoadjuvant therapy [116].

In addition, the GENAIR study, which investigated the effect of air population and environmental tobacco smoke on human health in a European cohort, found *TP53* and *KRAS2* mutations in healthy individuals on average 14.3 and 20.8 months before cancer diagnosis, respectively [117]. In that study, *KRAS* mutations were associated with bladder cancer susceptibility [117].

Subsequent studies have also shown the role of ctDNA as an early biomarker. To detect early-stage tumors noninvasively, an ultrasensitive method, named targeted error correction sequencing (TEC-SEQ), was developed. Using TEC-Seq, ctDNA was analyzed in 44 healthy individuals in order to detect genome alterations found in breast, colorectal, lung, and ovarian cancer prior to knowledge of any disease. This method identified genomic modifications associated with clonal hematopoiesis in 16% of the participants but no tumor-specific alterations. The authors claimed, by contrast, that using the same approach, some tumor-specific alterations were found in about 50% of 200 cancer patients, suggesting that ctDNA might be useful in early-stage tumor detection [118]. More recently, a non-invasive blood test, called PanSeer, evaluated methylation signatures on ctDNA from 605 healthy participants, of which 191 were diagnosed with stomach, esophageal, colorectal, lung, or liver cancer within four years of the first blood analysis. This study concluded that ctDNA might be a non-invasive way to detect cancer up to four years ahead of the current diagnostic techniques [119].

1.4.2. ctDNA to monitor tumor dynamics and treatment

Tumors change in space and over time [9]. These temporal and special changes to tumor biology can result in therapeutic resistance. ctDNA is under investigation as a surrogate marker to provide clinically relevant information on cancer management [29]. Various studies have assessed non-invasive ctDNA testing to assess tumor dynamics [13, 27]. A pioneering study conducted by Diehl *et* al. [88] showed the clinical utility of longitudinal sampling of ctDNA in colorectal cancer. This study quantified ctDNA isolated from plasma from 162 advanced colorectal cancer patients through BEAMing repetitions and qPCR before and at various time points after treatment. ctDNA reflected tumor dynamics throughout treatment and at a higher sensitivity than the standard

biomarker, carcinoembryonic antigen (CEA). Moreover, high ctDNA levels were associated with a poor outcome for breast cancer patients[120] and non-small cell lung cancer patients [121]. Subsequent publications also reported ctDNA as a sensitive and specific marker to monitor tumor dynamics in cancer [47, 64, 122, 123].

1.4.2.1. ctDNA to evaluate tumor burden

The total amount of cancer, defined as tumor burden, has been reported as a predictive marker [124]. A correlation between ctDNA levels and tumor burden has been highlighted in several cancers types [125-127], For example, a retrospective study in 40 high-grade serous ovarian carcinoma patients found that ctDNA levels were associated with tumor volume [128]. In this study, the authors measured the tumor volume by computed tomography and evaluated ctDNA levels by looking at *TP53* mutations within ctDNA in plasma samples collected at serial time points. Interestingly, they found that for every cubic centimeter of a lesion, mutant alleles in plasma increased by about 0.008% and by six mutant copies per milliliter of plasma. Overall, their data showed that ctDNA decreased by about 60% after treatment and correlated with treatment response. This study suggested that ctDNA analysis provides a comprehensive view of tumor burden and treatment response [128]. In addition, a study that assessed ctDNA through plasma variant allele frequency in early stages of non-small cell lung cancer showed a linear correlation between tumor volume and ctDNA levels [129].

1.4.2.2. ctDNA to monitor treatment response

Tumors can evolve in response to therapy which can result in drug resistance in cancer patients [130]. Conducting multiple tissue biopsies to evaluate this resistance is often unfeasible

[13]. Therefore, monitoring treatment response through ctDNA is another relevant application of liquid biopsy. One example of ctDNA as a biomarker of treatment response stem from studies conducted on anti-EGFR therapies in colorectal cancer [131-134]. For example, ctDNA increases have been correlated to resistance to anti-EGFR therapies, indicating the emergence of therapy-resistant clones that emerge before clinically evident progression [131-134]. ctDNA measurement has also been used to evaluate the success of a given therapy. A study conducted by Murtaza *et* al.[135] reported the utility of ctDNA to monitor early signs of secondary drug resistance [135].

In addition, liquid biopsy has been used as a surrogate indicator for disease recurrence, for example, to identify minimal residual disease (MRD) [14]. MRD refers to the amount of remaining cancer cells during or after treatment, which may not be detectable by current diagnostics methods. Evidence has shown that detectable ctDNA levels predict relapse in early-stage disease [116]. An increase in ctDNA levels after treatment or surgery has been associated with recurrence and poor prognosis [14]. For example, a multicentre study conducted in 96 -stage III colon cancer patients observed a significant association between ctDNA detection and 3-year recurrence-free interval (RFI). While a 30% RFI was reported when ctDNA levels were detectable, a 77% RFI was noted when ctDNA was undetectable. This data supports ctDNA as a prognostic marker [136].

Overall, various studies have indicated the potential of ctDNA as a diagnostic, predictive, and prognostic tool that allows for non-invasive sampling. In most cases, ctDNA analysis is a simple, fast, and cost-efficient tool that can be a particularly useful approach in tumors with difficult access.

2. Uveal melanoma

This section contains excerpts from Bustamante *et* al.[1]

2.1. Introduction

Uveal melanoma (UM) is the most common primary intraocular tumor in adults [137], and the second most common type of melanoma, after that of the skin [138]. The tumor originates within the pigmented uveal tract which includes the iris, the ciliary body, and choroid (**Figure 1.2**). While most of the cases are located in the choroid (90%), only a few cases involve the ciliary body (6%) and iris (4%)][139, 140]. In Canada, the average-annual incidence rate of UM is 3.75 cases per million [141]. The mean age-adjusted incidence of UM in United States is 5.2 cases per million [142], while in Europe it varies according to latitude, with more than 8 cases per million in Northern countries and around 2 cases per million in Southern Europe [143]. Caucasian ethnicity is the most affected population (98% of cases), with a male predominance [144].

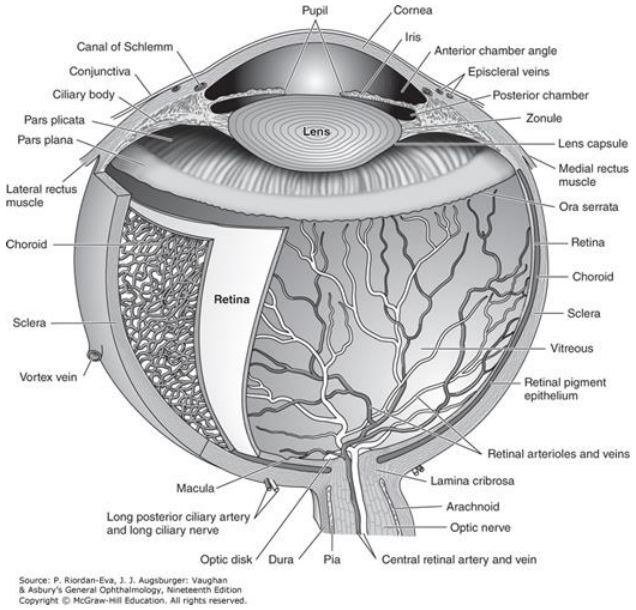

Figure 1. 2: Anatomy of the human eye.

Schematic representation of a human eye. UM involves the iris, in the anterior chamber of the eye, the ciliary body and the choroid in the posterior chamber of the eye. Figure taken from [145].

The cause of UM remains unclear. Predisposing factors have been proposed and include light iris color [146], fair skin color [147], choroidal nevus [148], and ocular melanocytosis[140]. Among environmental factors, exposure to blue light has been suggested as a risk factor [149], while the role of ultraviolet (UV) radiation remains controversial in UM[150]. Interestingly, UV-hallmark mutations were found at codon 183 of *G protein subunit alpha Q and 11* (*GNAQ*/*GNA11*), codon 182 of *GNA11*, and codon 29 of *Rac family small GTPase 1* (*RAC1*) in UM, with typical C<T transitions at dipyrimidine sites, but these mutations account only for a small percentage of those found in UM[23, 24, 151-153]. No evidence of an UV radiation mutational signature was found in molecular data from 80 primary UMs available through The Cancer Genome Atlas (TCGA) [154]. Previous studies have associated UM with welding [150], a source of artificial UV radiation and blue light.

UM tumors are often asymptomatic and are thus frequently discovered during a routine ophthalmic examination [155, 156]. The diagnosis is made primarily based on imaging modalities, including fundus photography, fluorescein angiography, fundus autofluorescence imaging, optical coherence tomography, and ultrasound imaging [157], making UM one of the few cancers generally diagnosed without a tissue biopsy.

Moreover, UM accounts for only 5% of melanoma cases but it represents 13% of mortality from melanoma [138, 158]. Therefore, this relatively rare cancer is marked by a high rate of metastasis and associated mortality. Moreover, UM has a very high predilection to metastasize to the liver, with over 90% of metastatic cases showing hepatic lesions. In this section, I will

introduce the oncogenic signalling, some prognostic indicators associated with poor prognosis, and current and prospective treatments in UM.

2.2. Molecular signaling

Hotspot mutations in the alpha subunit of G protein-coupled receptors *GNA11* [24] and *GNAQ* [23] are key initiating molecular drivers in UM. According to mutation data available through TCGA, approximately 92% of UM cases are characterized by an early mutation in one of the two genes. *GNAQ/11* play a role in activating G protein signaling cascade via inositol triphosphate (IP3), diacylglycerol (DAG), and cyclic adenosine monophosphate (cAMP), which activates the mitogen-activated protein kinase (MAPK), protein kinase B (PKB, also known as Akt), protein kinase C (PKC), phosphoinositide 3-kinase (PI3K), and mechanistic targets of rapamycin kinase (mTOR) [137, 159]. *GNAQ/11* is also involved in the Hippo-Yes-associated protein (YAP) signaling pathway [160, 161]. Mutations in *GNAQ* and *GNA11* occur mainly at the codon Q209 (Q209P/L, c.626A>C/T), within the RAS_like GTPase domain, with some rare cases seen at a second hotspot (R183) or a third codon (G48)[23, 24, 154]. Cases in which *GNAQ/11* is not observed will present alternative initiating mutations in either the G protein-coupled receptor *cysteinyl leukotriene receptor 2* (*CYSLTR2*)[26], *phospholipase C beta 4* (*PLCB4*, a downstream effector of GNAQ signaling [25]) (**Figure 1.3 A**). Overall, UM oncogenesis is linked to G alpha 11/Q pathway alterations. In particular, by a mutually exclusive mutation in *GNAQ*, *GNA11*, *PLCB4*, or *CYSLTR2*[162], also called UM early mutations. Interestingly, these mutations have been observed in choroidal nevi [163].

Subsequently to the early mutations, UM cases can present an alteration in *BAP1* (BRCA-associated protein 1 [164]), change-of-function heterozygous mutations of a splicing gene

(SF3B1[151, 165]), or an N-terminal tail mutation in EIF1AX [151]. Therefore, a *GNAQ*, *GNA11*, *PLCB4*, or *CYSLTR2* mutation is needed but insufficient for UM development.

2.3. Metastatic disease

Metastatic disease is detectable at diagnosis in less than 4% of UM cases [166]. Interestingly, UM metastasizes preferentially and almost exclusively to the liver, with up to 90% of metastatic UM associated with hepatic lesions, and in most cases, the liver is the only affected organ [167, 168]. Other sites such as the lungs (24%), bones (16%), skin/subcutaneous tissues (11%) and lymph nodes (10%) can also be affected [168], while involvement of brain and fellow eye are rare [167]. Once metastasis is found, the mortality rate is 92% within two years[168], with an overall survival of 3 to 16 months [142]. As such, high-risk cases are generally integrated into a lifetime surveillance program, which includes liver imaging and function tests [169].

UM metastasis is marked by a relatively long latency between the ocular tumor diagnosis and the detection of metastatic foci. Depending on tumor size, 3-14% of the UM patients will develop metastasis within 5 years, up to 49% in 10 years, and up to 67% in 20 years [139, 170]. The temporal variation and latency of UM metastasis could, at least in part, be explained by tumor cell dormancy. Evidence for tumor dormancy has been demonstrated by the observation of microscopic foci of melanoma cells in autopsy samples from metastatic UM patients [171]. There is evidence based on mathematical modeling of cell doubling times that subclinical and dormant hepatic micro-metastases are already present at the time of the initial ocular tumor diagnosis [19, 20]. In an effort to estimate metastasis occurrence [19, 172, 173], Eskelin *et* al. used the Schwartz formula to calculate UM tumor doubling time using three presumed sizes of metastasis at last negative follow-up. They estimated that the development of metastasis ranged from 30 to 220 days (median, 63 days) in untreated patients, while it ranged from 25 to 2,619 days in treated patients

[19]. Interestingly, this group suggested that hepatic metastatic seeding in the liver (micro-metastasis) occurred 5 years prior to clinical detection, assuming a constant growth rate [19]. Moreover, circulating tumor cells (CTCs) have been detected at the time of diagnosis, both in patient samples and in animal models [174-176]. In light of these findings, there may be a limited role for primary tumor control in improving mortality rate in UM patients.

2.4. Prognostic indicators of poor prognosis in uveal melanoma

The poor prognosis of UM is linked to the challenge in its early diagnosis due to the lack of symptoms, few sensitive biomarkers to monitor the progression of the disease, and no effective treatments for the metastatic stage [177]. In this section, I will summarize prognostic indicators of UM, including clinical/histopathological factors and genetic indicators.

2.4.1. Clinical and histopathological factors

Like in many other malignancies, tumor size has been shown to correlate with prognosis in UM[170, 178]. A meta-analysis reported that the estimated 5-year mortality rate associates negatively with tumor size (thickness and largest basal diameter), with rates of 16, 32 and 53% reported for small (<3 mm in thickness and <10 mm in basal diameter), medium (3-8 mm in thickness and <15 mm in basal diameter) and large (>8 mm in thickness and >15 mm in basal diameter) UM tumors [178]. Ciliary body involvement has also been associated with poor prognosis [179], and linked to large UM tumors [180], as well as to loss of nuclear BRCA1 associated protein 1 (*BAP1*) expression [140, 181]. Although extrascleral extension is rare [182], it has been linked to poor survival with a 10-year mortality rate doubled to 75% compared to an absence of extrascleral extension [179]. Furthermore, extraocular spread was correlated with increased mortality because of its association with large basal tumor diameter, epithelioid cells, and monosomy of chromosome 3 [180].

UM can also be classified according to cell type: epithelioid, spindle, or mixed (a combination of both)[183, 184]. Spindle cell tumors have the best prognosis, while tumors composed of epithelioid cells have the worst prognosis, with a 15-year mortality rate of 20% and 75%, respectively [183, 184]. Accordingly, metastatic UM is predominately composed of epithelioid- or mixed-cell populations [185]. Next, the tumor mitotic activity has been correlated with poor prognosis, with a 6-year mortality of 56% for tumors with high mitotic activity compared to 15% for tumors with low mitotic activity[170, 186] Highly invasive UM cells possess the ability to organize into vascular-like channels or patterned extracellular matrix (ECM) without endothelial lining, a process called vasculogenic mimicry [187-190]. The presence of these Periodic acid-Schiff positive patterns in UM primary tumors has an adverse influence on patient survival (10-year mortality rate of 50%) [188, 190], and was correlated with low BAP1 expression in primary UM tumors[188]. Finally, increased numbers of tumor-infiltrating lymphocytes (TILs) and tumor-associated macrophages (TAMs; M2 phenotype) in UM primary tumors were significantly associated with poor prognosis [191, 192].

Immunohistochemistry analyses of primary and metastatic UM cases showed that increased expression of the intermediate filament nestin is a predictor of metastatic progression and reduced survival [193]. Moreover, the nuclear expression of BAP1 determined by immunohistochemistry is currently used as a prognostic indicator in the clinic [181, 194, 195]. The loss of nuclear BAP1 protein expression is linked to poor prognosis parameters such as increasing tumor height, ciliary body involvement, and monosomy 3, whereas cytoplasmic BAP1 expression showed no association with UM overall survival [181]. Likewise, significantly lower nuclear BAP1 staining was observed in primary tumors of UM patients with metastasis compared to metastasis-free patients [194].

2.4.2. Genetic indicators

While intraocular biopsies are not generally performed to confirm UM diagnosis, they are used to predict metastasis pre-irradiation or when the affected eye is not enucleated [196]. Indeed, cytogenetic anomalies, gene expression profiling signatures, and mutations can be determined in both fine needle aspiration biopsies and tissue blocks (frozen or fixed) [197].

2.4.2.1. Cytogenetic features

Majority of UMs exhibit a low degree of aneuploidy and chromosomal rearrangements compared with other types of cancers[198-200]. The most frequent chromosomal changes found in UM are the loss of one copy of chromosome 3 (monosomy 3; almost half of UMs) and the amplification of chromosome 8q (40% of UM), both associated with a poor prognosis [201-204]. The *BAP1* gene (frequently mutated in metastatic UM) and oncogenes of interest such as *MYC*, *DDEF1*, and *NBS1* (all overexpressed in UM with poor prognosis) are located at chromosomes 3p21 and 8q24, respectively[164, 205-207]. Monosomy 3 is associated with a high risk of metastasis and remains the strongest cytogenetic indicator to predict UM metastasis[201-204]. A loss on chromosome 8p was detected in about a quarter of UMs, and the putative metastasis suppressor gene *LZTS1* is located at chromosome 8p12-22[208]. Another frequent alteration is chromosome 1p loss (25% of UMs), which occurs frequently with monosomy 3, and is correlated with decreased disease-free survival [209, 210]. The chromosomal alterations associated with UM metastasis were correlated with increasing tumor size, which suggests that these are acquired events during tumor growth and progression [211]. The other chromosomal aberrations detected in UM, such as loss on 6q and 9p or gain on 1q and 6p, are not associated with metastatic progression [212].

2.4.2.2. Mutations

UM early mutations, *GNAQ*, *GNA11*, *PLCB4*, or *CYSLTR2*, do not appear to be associated with the development of metastasis [154, 213]. However, a study performed with 30 metastatic UM patients showed an over-representation of *GNA11* mutations in metastatic cases [185]. To better understand UM progression, some reports have highlighted key somatic mutations which confer metastatic risk. One example of these mutations is a *BAP1* mutation. Somatic mutations in *BAP1*, resulting in loss of protein expression, are associated with increased risk of metastasis in UM[164]. *BAP1* encodes a nuclear ubiquitin carboxy-terminal hydrolase with a deubiquitinase activity[214], and acts as a tumor suppressor gene in UM [164]. *BAP1* is located on chromosome 3p21.1 and is frequently mutated on the only allele present in tumors with monosomy 3[154, 164]. Previous studies have shown that more than 80% of metastatic UM patients maintain only the mutated allele of *BAP1* [154, 164]. Interestingly, germline mutations in *BAP1* have been identified in about 5% of UM patients, and these were associated with larger tumor size and ciliary body involvement [215]. Germline *BAP1* mutations are frequent in familial UM (22%) [216], and are associated with earlier onset of disease [217]. BAP1 is an enzyme responsible for removing ubiquitin molecules from specific proteins to regulate their functions [214]. Histone deacetylase (HDAC) inhibitors were shown to reverse the biochemical effects of the inactivation of *BAP1*, specifically by inducing melanocytic differentiation and cell cycle arrest and blocking UM tumor growth in mice [218]. In addition to *BAP1*, other genes may confer increasing risk of UM metastasis. Metastatic UM cases wildtype for *BAP1* frequently present a mutation in the *splicing factor 3b subunit 1* (*SF3B1*) gene involved in splicing of pre-mRNAs [151]. Mutations in *SF3B1* are associated with late metastasis in UM (median of 8.2 years), as opposed to *BAP1* mutations that are linked to early metastasis [219]. In addition to *SF3B1*, a second gene related to pre-mRNA

splicing is *serine and arginine-rich splicing factor 2* (*SRSF2*) [154]. *SRSF2* is involved in the assemble of the spliceosome and mutations have been reported in hematological malignancies [220]. Similarly to *SF3B1*, *SRSF2* has been associated with Class 1B GEP, disomy 3, intermediate risk of metastasis [213]. As such, primary UM tumors mutant for *SF3B1* are classified as having a late metastatic risk [219]. Finally, a mutation in the *eukaryotic translation initiation factor 1A X-linked* (*EIF1AX*) gene is an indicator of low risk of metastasis and is associated with prolonged survival [151]. Mutations in *BAP1, SF3B1*, and *EIF1AX* are nearly mutually exclusive and are thought to be associated with early (*BAP1*), late (*SF3B1*), or no (*EIF1AX*) metastasis [154].

2.4.2.3. Prognostic classifying systems

Some classifications have been established to standardize a system to predict UM metastasis. For example, the American Joint Committee on Cancer (AJCC)'s Tumor-Node-Metastasis (TNM) staging [221], which classified patients according to tumor size, ciliary body involvement, and extraocular extension, divides UM cases into 4 tumor size categories, 17 anatomical subcategories, and 4 prognostic stages [222]. A retrospective study with 522 UM cases concluded that the TNM staging along with chromosomes 3 and 8q status enable a more accurate prognostication in UM [223].

Several studies have highlighted the prognostic value of gene expression profiling (GEP) signatures in classifying UMs into prognostic groups (Class 1 or Class 2), with low- or high-risk of developing metastasis, respectively [224, 225]. As few as 15 mRNAs are used to determine the risk of metastasis with the prognostic test DecisionDx-UM [224, 226]. Onken et at using genetic profile categorized upregulated and downregulated genes Class 1 and Class 2 [227]. Class 1 tumors retain a well-differentiated melanocytic phenotype, while Class 2 tumors demonstrate a primitive neural/ectodermal stem cell-like phenotype [228]. These two molecular classes can be subdivided

into four prognostically significant subclasses based on GEP and cytogenetic anomalies: 1A with minimal aneuploidy (longest metastasis-free survival), 1B with gain of chromosome 6p, 2A with loss of chromosome 3 and 2B with loss of chromosomes 3 and 8p (shortest metastasis-free survival) [229].

The interactive web-based tool PRiMeUM, that stands for Prediction of Risk of Metastasis in UM, predicts a patient's risk of metastasis based on individual characteristics such as clinical and chromosomal information [230].The authors reported an accuracy of 85% when clinical and chromosomal features were both taken into consideration, 80% when only the chromosomal information was considered, and 83% when only clinical data were used [230]. In addition, the Liverpool Uveal Melanoma Prognosticator Online (LUMPO) uses clinical information, histological and genetic findings, and includes normal life expectancy [231]. Interestingly, a collaborative study that analyzed data from an international cohort of UM patients using LUMPO version 3 (LUMPO3) determined that it was a valuable method to predict their 10-year survival [232].

Recently, Field *et* al. reported that preferentially expressed antigen in melanoma (PRAME) is an independent biomarker of UM, which identifies increased metastatic risk in patients with Class 1 signature or disomy 3 [233, 234]. The analysis of PRAME mRNA in 678 UM samples showed that PRAME was aberrantly hypomethylated and activated in Class 1 and Class 2 UMs, and that the PRAME+ status was associated with shorter time to metastasis in both GEP classes [233, 234]. Retrospective studies have compared PRAME expression along with GEP and TNM staging [235, 236]. They reported that GEP and PRAME showed a superior prognostic power than TNM staging, and that PRAME+ status correlated with large basal diameter, tumor volume, and worsening GEP class [235, 236].

Another classification based on RNA expression, DNA methylation and chromosomal data from TCGA separated the UM primary tumors into categories A to D based on the presence of monosomy 3 and the degree of chromosome 8q gain [154, 237]. *BAP1* mutations and immune profiles allowed the separation into prognostically favorable (A and B) or unfavorable (C and D) tumors, while *EIF1AX* mutations occurred in group A, and *SF3B1* mutations mostly in group B [154, 237] (**Figure 1.3 B**). A recent work comparing both TCGA and TNM classifications confirmed that the TCGA classification had a greater power to predict UM metastasis [238]. In addition, another team analyzed the TCGA data in order to classify primary tumors by immune subtypes, and was able to identify three distinct groups; interestingly the immune score was strongly associated with immune infiltration and poor outcomes, regardless of the level of aneuploidy in tumor samples [239].

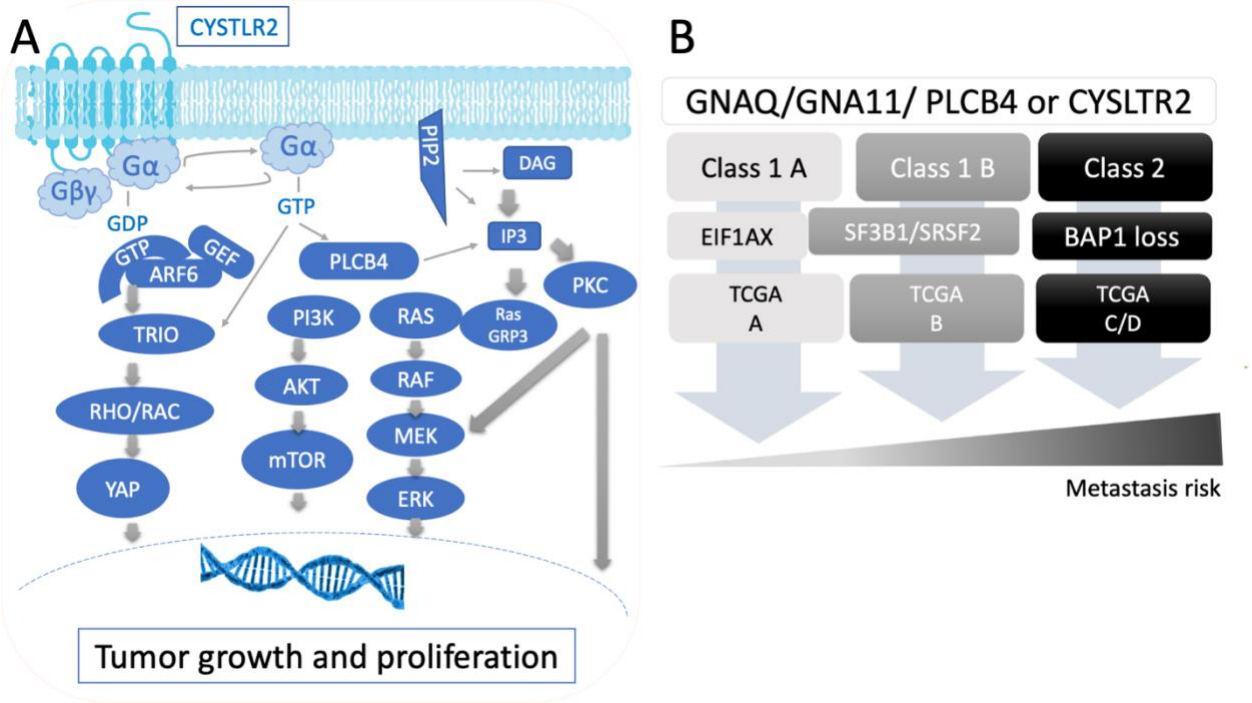

Figure 1. 3 Overview of Uveal melanoma signaling pathway and subtypes.

A) *GNA11* and *GNAQ* (GαQ/11) are the main driver mutations (rarely *PLCB4* or C*YSLTR2*) in UM oncogenesis (adapted from Patel M *et* al., 2011); it leads to activation of pathways involved in tumor growth and proliferation. **B)** Overview of UM subtypes in link with metastasis risk (adapted from Smit KN *et* al., 2019).

2.5. Current and prospective treatments for primary and metastatic uveal melanoma

2.5.1. Current treatments

Treatment modalities for the intraocular tumor comprise radiotherapy, laser therapy, which preserve the eye, or surgical resection (enucleation)[240]. The latter treatment is considered for large tumors or blind painful eyes secondary to neovascular glaucoma or post-irradiation effects, and accounts for about 30% of cases [139]. As such, eye-conserving alternatives such as radioactive plaque (brachytherapy) are the preferred approaches and result in effective control of the primary tumor. Despite current treatments that achieve excellent local tumor control, up to 50% of patients develop metastasis within 15 years, which are generally asymptomatic at detection and associated with high mortality [241].

Once metastasis is diagnosed, effective treatment options are currently limited in UM. However, some studies have reported better median survival in treated patients compared to untreated cases [242]. While UM primary tumors can be successfully controlled with radiotherapy or by surgical resection, response rates to chemotherapy or immunotherapy remain low in patients with metastases [177, 243].

A surgical approach is the gold standard for patients with resectable liver metastasis but these account for less than 10% of cases in UM since most patients present diffuse metastases

[244]. Hepatic-directed therapies are also available such as radiofrequency ablation, stereotactic radiotherapy, and regional chemotherapy; they have shown long-term survival in a few and highly selected cases [243, 245, 246]. Chemotherapeutic agents originally approved for cutaneous melanoma (e.g. dacarbazine, fotemustine) [247] have been tested in metastatic UM [243]. However, conventional systemic chemotherapy has shown poor response rates and no improvement of overall survival in UM patients [248]. Although immunotherapy has dramatically changed the treatment approach to skin melanoma, metastatic UM is resistant to current immune checkpoint blockade and only rare complete responses have been reported in metastatic UM using adoptive T-cell therapy [249, 250]. It has been suggested that UM low mutational burden [251], as well as an upregulation of immunosuppressive factors such as IDO1 and TIGIT might contribute to this limited success [154, 243].

2.5.2. Prospective treatments

In an effort to improve unresectable metastatic UM prognosis, near 20 active or recruiting clinical trials are currently outgoing according to the NIH clinical trial registry. Indeed, immunotherapy, regional chemotherapy or radiation, epigenetic drugs or inhibitors targeting specific signaling pathways are under investigation with cohorts of metastatic UM patients.

Checkpoint inhibitors (e.g. ipilimumab, nivolumab) with immunoembolization (#NCT03472586), adoptive T cell therapy (#NCT03068624, #NCT03467516, #NCT02743611), as well as vaccination with dendritic cells loaded with autologous tumor RNA (#NCT01983748) are among the tested immunotherapy strategies. Another clinical trial will test intravenous injections of a modified virus to trigger a strong immune response to kill specifically melanomic cells expressing the tyrosinase related protein 1 (#NCT03865212).

Mutations in *GNAQ/11*, present in the vast majority of UM cases, activate the central oncogenic Ras/RAF/MEK/ERK pathway, which contributes to tumor growth (Figure 1A) [137, 252]. The MEK inhibitor selumetinib was thus tested in a phase II trial, and showed clinical potency in metastatic UM patients, with an improvement in objective response rate and progression-free survival compared to chemotherapy [253]. However, significant toxicity and no improvement in overall survival were observed [253]. Moreover, treatments targeting signaling pathways involved in UM pathogenesis are still under investigation, such as inhibitors of ERK1/2 (ulixertinib, #NCT03417739), protein kinase C (LXS196, #NCT02601378; AEB071, #NCT02273219; IDE196, #NCT03947385), PI3Kα (BYL719, #NCT02273219), c-Met (crizotinib, #NCT02223819) or tyrosine kinase receptors (cabozantinib s-malate, #NCT01835145).

Additional active clinical trials involve combination of checkpoint inhibitors with regional chemotherapy (#NCT04283890), stereotactic radiation therapy and gene therapy (#NCT02831933), internal hepatic radiation (SirSpheres Yttrium-90, #NCT02913417), intralesional injection of iodinated fluorescein derivatives (#NCT00986661), VEGF receptor inhibitors (#NCT04184518), or epigenetic drugs (#NCT02697630).

Combination therapies and the targeting of the reactive hepatic stroma in addition to metastatic cell properties are becoming more and more envisioned strategies to improve the overall survival of metastatic UM patients.

3. ctDNA in Uveal melanoma

As reviewed in the previous section, UM is rare but is the most common intraocular tumor in adults. While iris melanoma, which is usually detected early, has the best prognosis [254], choroidal and ciliary body [255] have a poor prognosis, with mortality linked to a high incidence in liver metastasis. Metastasis risk can be assessed by gene expression, somatic copy number alterations, and specific gene mutation [256]. These approaches require a tissue specimen obtained by an intraocular biopsy, which is an invasive procedure with rare but important complications. A biopsy also reflects a static view of a tumor. Consequently, in an effort to surrogate a tissue biopsy and monitor the dissemination of UM cells in real-time, ctDNA-based liquid biopsy has been studied in UM patients (Table 2).

Madic *et* al in 2012 conducted one of the pioneering studies in which ctDNA was analyzed in the blood of UM patients with established metastatic disease. By using driver mutations (*GNAQ/GNA11*) to quantify ctDNA by bidirectional pyrophosphorolysisactivated polymerization (bi-PAP), the authors detected ctDNA in 20 of the 21 participants. In general, these levels correlated with tumor burden [257]. Metz *et* al also analyzed ctDNA using *GNAQ/11* mutations but employed ultradeep sequencing. Through this sequencing method, the authors identified ctDNA in 9 of the 22 cases. While ctDNA was not detected in all metastatic patients, it was associated with extensive metastasis, mainly in the bone [258]. In a study conducted by Bidard *et* al [259], in which ctDNA was analyzed through detection of *GNAQ/11* mutations using bi-PAP, ctDNA correlated with disease progression, leading the authors to suggest it as a prognostic marker. In particular, high ctDNA levels were correlated with hepatic military metastases. By using the CellSearch technique in metastatic patient blood, that study also assessed CTCs; however, CTCs showed less clinical significance compared to ctDNA analysis. In addition to this

study, CTCs and ctDNA were compared in a subsequent study performed by Beasley *et* al[260], in which CTCs were immunomagnetically captured by melanoma-associated chondroitin sulfate proteoglycan, and ctDNA was detected using *GNAQ/11* mutations by ddPCR. That study showed that ctDNA can inform about early signs of metastasis, whereas CTCs support UM prognosis. Including primary and metastatic patients, ctDNA was detectable in 8 out of 30 cases and CTCs in 15 of 26 patients. Altogether, that study highlighted the clinical utility of CTCs to distinguish between low versus high metastasis risk and ctDNA to monitor disease progression [260].

A subsequent work supported the clinical utility of ctDNA in UM, where Le Guin *et* al [261] detected ctDNA in 17 of 21 metastatic patients. Interestingly, ctDNA detection was up to 10 months before clinical confirmation of metastasis in 10 of these 17 ctDNA-positive cases. Overall, ctDNA sensitivity was 80% and specificity 96% across the study [261].

In an effort to successfully treat metastasis, new therapies have been proposed in UM. One example of these treatments is immunotherapy, in which ctDNA has been used to assess therapy response. A study conducted by Cabel, *et* al [262] in 2017 analyzed ctDNA plasma before anti-PDI treatment (pembrolizumab or nivolumab) and after 8 weeks of treatment. Using ddPCR and sequencing (when no prior knowledge of mutations was available), ctDNA was associated with treatment response, progression-free survival (PFS), and overall survival (OS) [262]. In a case study conducted in 2018, Rodrigues *et* al also reported the utility of ctDNA to monitor patient response with anti-PD1 therapy [263].

In addition to anti-PDI treatment, the analysis of ctDNA has been used to evaluate protein kinase C inhibition (PKCi) treatment. A clinical study conducted by Park *et* al in 2021[264] evaluated ctDNA levels by using ddPCR and NGS to assess PKCi. The authors found that patients with low ctDNA levels corresponded to a better response [264]. Particularly, these patients had

low disease volume and low baseline lactate dehydrogenase (LDH), an enzyme associated with tumor activity and inversely associated with good outcome [264]

In conclusion, although ctDNA has been widely studied in various cancer types, only a few studies have explored the potential of ctDNA in intraocular tumors (**Table 2**). Indeed, FDA-approval tests are currently available to screen patients suffering from non-small lung and metastatic breast, colorectal, and prostate cancer [265], but this does not extend to intraocular tumors. As we will present in the following chapters, our proposed goal was to perform a comprehensive study to assess ctDNA in human cancer cell lines, a human-rabbit animal model, and patient samples with primary disease and a premalignant lesion in the choroidal (Chapter 2). Furthermore, once we confirmed that ctDNA is a clinically relevant biomarker of tumor development and progression in UM and optimized our experimental methodologies, we aimed to better understand cfDNA release mechanisms by evaluating the release pattern of cfDNA upon cytotoxic agents (Chapter 3). In a similar way, taking advantage of our *in vitro* model to study ctDNA release, we used ctDNA to evaluate treatment response in preclinical models (Chapter 4).

Table 2 Summary of studies on clinical relevance of ctDNA in UM					
Title	Year	Patient population and n	Sample and technique of analysis	Prognostic relevance	Ref
Pyrophosphorolysis-activated polymerization detects circulating tumor DNA in metastatic uveal melanoma	2012	Metastatic n=21	5 mL/Plasma Bi-PAP	ctDNA was detected in 20 of 21 patients and correlated with tumor burden	[257]
Ultradeep sequencing detects GNAQ and GNA11 mutations in cell-free DNA from plasma of patients with uveal melanoma	2013	Metastatic n=22	1-5 mL/Plasma NGS	ctDNA was detected in 9 of 22 participants. While it was associated with metastasis, no correlation between ctDNA and primary tumor characteristics was found.	[258]
Detection rate and prognostic value of circulating tumor cells and circulating tumor DNA in metastatic uveal melanoma	2014	Metastatic n=40 (26 with ctDNA analysis)	5 mL/ Plasma Bi-PAP	Levels of ctDNA were found in 22 of 26 cases. The levels were associated with metastasis, presence of CTCs, and tumor volume.	[259]
Circulating tumor DNA changes for early monitoring of anti-PD1 immunotherapy: a proof-of-concept study	2017	Metastatic n=3	5 mL/ Plasma Bi-PAP	ctDNA assessed anti-PD1 treatment response. Lack of ctDNA detection suggested better outcome	[262]
Outlier response to anti-PD1 in uveal melanoma reveals germline MBD4 mutations in hypermutated tumors	2018	Metastatic n=1	1-5 mL/Plasma Bi-PAP	ctDNA correlated with anti-PD1 treatment	[266]
Clinical Application of Circulating Tumor	2018	Primary (n=30) and	5 mL/Plasma	ctDNA levels were found in 8/8 of	[260]

Cells and Circulating Tumor DNA in Uveal Melanoma		metastatic (n=8)	ddPCR	metastatic patients than 8/30 primary cases.	
Early detection of metastatic uveal melanoma by the analysis of tumor-specific mutations in cell-free plasma DNA	2021	Primary (n=135) and metastatic or recurrence (n=21)	1-5 mL/ Plasma NGS	ctDNA levels were detected in metastatic UM patients. ctDNA levels were detected with 80% sensitivity and 96% specificity	[261]
Circulating Tumor DNA Reflects Uveal Melanoma Responses to Protein Kinase C Inhibition	2021	Metastatic (n=17)	1-4 mL/Plasma ddPCR and NGS	ctDNA was used to assess protein kinase C inhibitor therapy. ctDNA levels were associated with tumor burden and LDH levels, both prognostic makers.	[264]

Preamble to Chapter 2

The literature review introduced ctDNA as a liquid biopsy-based biomarker and its clinical implementation in oncology. This biomarker approach is especially relevant in tumors where biopsies are difficult to perform and cannot be repeated. UM is a perfect candidate for liquid biopsy-based monitoring due to its intraocular location, its high metastatic rate linked with high mortality, and the lack of effective biomarkers to monitor disease course. UM tumors can develop asymptomatically *de novo* or from a pre-existing nevus [1] and are characterized by mutually exclusive somatic mutations in *GNAQ* [23], *GNA11* [24], *CYSLTR2* [26], and *PLCB4* [25]. Although these mutations are not sufficient to develop a tumor, they are present in all UM cases [267] and in some choroidal nevi[163]. There is a need for a method to monitor growth and malignant transformation of choroidal nevi non-or minimally invasive manner. Therefore, a liquid biopsy test that informs us about nevus growth and UM development would be clinically valuable in this context.

In this chapter, we evaluated the feasibility of using driver mutations to detect ctDNA in UM. We hypothesized that driver mutations (*GNAQ*, *GNA11*, *CYSLTR2*, and *PLCB4*) can be detected in ctDNA from a liquid biopsy and act as a biomarker of UM development and to monitor disease course in real-time. We first assessed the presence of fragments of DNA in the culture media of UM cell lines according to their parental mutations in order to establish and validate an *in vitro* model. We then validated our assay in plasma and aqueous humor isolated from rabbits of a human UM cell xenograft model. Finally, we evaluated ctDNA levels in a clinical study including healthy individuals and patients with choroidal nevi and UM.

This chapter is based on **Manuscript 2:** Bustamante, P. *et al.* Circulating tumor DNA tracking through driver mutations as a liquid biopsy-based biomarker for uveal melanoma. *J Exp Clin Cancer Res* 40, 196, doi:10.1186/s13046-021-01984-w (2021).

Chapter 2: Circulating tumor DNA tracking through driver mutations as a liquid biopsy-based biomarker for uveal melanoma

Prisca Bustamante[1]; Thupten Tsering[1]; Jacqueline Coblentz[1]; Christina Mastromonaco[1], Mohamed Abdouh[1], Cristina Fonseca[2], Rita P. Proença[3,4], Nadya Blanchard[5]; Claude Laure Dugé[5]; Rafaella Atherino Schmidt Andujar[1], Emma Youhnovska[1], Miguel N Burnier[1,5]; Sonia A. Callejo[5,6] Julia V. Burnier[1,7,8].

[1]Cancer Research Program, Research Institute of the McGill University Health Centre, Montreal, QC, Canada

[2]Department of Ophthalmology, Centro Hospitalar e Universitario de Coimbra, Coimbra, Portugal.

[3]Department of Ophthalmology, Centro Hospitalar de Lisboa Central, Lisbonm Portugal

[4]Faculdade de Medicina de Lisboa, Lisbon, Portugal

[5]McGill Academic Eye Clinic, Montreal, QC, Canada

[6]Department of Ophthalmology, Centre hospitalier de l'Université de Montréal, QC, Canada

[7]Experimental Pathology Unit, Department of Pathology, McGill University, Montreal, QC, Canada

[8]Gerald Bronfman Department of Oncology, McGill University, Montreal, QC, Canada

Correspondence

Julia V. Burnier

1001 Decarie Blvd, EM2.2218. Montreal, QC H4A 3J1

Email: Julia.burnier@mcgill.ca

Abstract

Background: Uveal melanoma (UM) is the most common intraocular tumor in adults. Despite good primary tumor control, up to 50% of patients develop metastasis, which is lethal. UM often presents asymptomatically and is usually diagnosed by clinical examination and imaging, making it one of the few cancer types diagnosed without a biopsy. Hence, alternative diagnostic tools are needed. Circulating tumor DNA (ctDNA) has shown potential as a liquid biopsy target for cancer screening and monitoring. The aim of this study was to evaluate the feasibility and clinical utility of ctDNA detection in UM using specific UM gene mutations.

Methods: We used the highly sensitive digital droplet PCR (ddPCR) assay to quantify UM driver mutations (*GNAQ, GNA11, PLCB4 and CYSTLR2*) in cell-free DNA (cfDNA). cfDNA was analyzed in six well-established human UM cell lines with known mutational status. cfDNA was analyzed in the blood and aqueous humor of an UM rabbit model and in the blood of patients. Rabbits were inoculated with human UM cells into the suprachoroidal space, and mutated ctDNA was quantified from longitudinal peripheral blood and aqueous humor draws. Blood clinical specimens were obtained from primary UM patients ($n = 14$), patients presenting with choroidal nevi ($n = 16$), and healthy individuals ($n = 15$).

Results: The *in vitro* model validated the specificity and accuracy of ddPCR to detect mutated cfDNA from UM cell supernatant. In the rabbit model, plasma and aqueous humor levels of ctDNA correlated with tumor growth. Notably, the detection of ctDNA preceded clinical detection of the intraocular tumor. In human specimens, while we did not detect any trace of ctDNA in healthy controls, we detected ctDNA in all UM patients. We observed that UM patients had significantly higher levels of ctDNA than patients with nevi, with a strong correlation between

ctDNA levels and malignancy. Noteworthy, in patients with nevi, the levels of ctDNA highly correlated with the presence of clinical risk factors.

Conclusions: We report, for the first time, compelling evidence from *in vitro* assays, and *in vivo* animal model and clinical specimens for the potential of mutated ctDNA as a biomarker of UM progression. These findings pave the way towards the implementation of a liquid biopsy to detect and monitor UM tumors.

Keywords. Circulating tumor DNA, Liquid biopsy, Uveal melanoma, Choroidal nevi, Biomarker, Mutated driver genes, *In vitro* study, Animal model, Clinical specimens.

Background

Uveal melanoma (UM) is the most common primary intraocular malignancy in adults [1, 268, 269], and the second most common form of melanoma after that of the skin [137]. While rare, with an incidence of 4.2 per million [137], it is associated with a high mortality rate[1]. Patients are most commonly treated by globe-preserving plaque radiation or by enucleation for large tumors [243]. Regardless of primary treatment and effective local tumor control, approximately 50% of patients develop metastasis, primarily to the liver via hematogenous dissemination [137]. Liver metastasis is lethal in the majority of patients, with an estimated 6-12 months survival rate [137].

Predisposing risk factors for UM development include environmental factors and intrinsic factors such us the occurrence of gene mutations (such as *GNAQ*, *GNA11*, *BAP1*, *CYSLTR2*, *PLCB4*)[23, 24, 143, 146, 270-272]. For instance, UM is characterized by constitutive activation of G protein-coupled receptor signaling, with a hotspot mutation in either G protein subunit alpha Q (*GNAQ*) or alpha 11 (*GNA11*). These mutations represent an initiating event in up to 90% of all UM cases [23, 24]. Less commonly, mutations in cysteinyl leukotriene receptor 2 (*CYSLTR2*), or phospholipase C beta 4 (*PLCB4*) have been reported [25, 26]. Pre-existing nevi in the choroid are reported as potential precursors of UM [163]. Interestingly, *GNAQ/11* mutations have also been detected in these lesions [163], suggesting that such mutations may be essential but not sufficient for malignant transformation. Choroidal nevi are the most common pigmented intraocular lesion, with a prevalence of 4.6% to 7.9% in the USA [273]. However, because these lesions are generally asymptomatic and found on ophthalmic exams performed for other reasons, it is believed that the true incidence may be much higher. Generally, a nevus remains stable over time [18]; however, a rate of malignant transformation of 2, 9; and 13% at 1, 5, and 10 years, respectively, has been

reported [139]. Although choroidal nevi are not biopsied, they are clinically followed for signs of growth or malignant transformation [139]. Risk factors for malignant transformation include tumor thickness greater than 2 mm, subretinal fluid, visual symptoms, orange lipofuscin pigment, tumor margin within 3 mm of the optic disc (i.e. peripapillary), ultrasonographic hollowness, and halo absence [139].

Moreover and due to the asymptomatic nature of the disease, UM is often detected during a routine ophthalmology examination, and its diagnosis is based on ultrasonography [137], making UM one of the few malignancies in which a biopsy is generally not used to confirm the diagnosis[274]. Detection of the classical presentations of UM generally give rise to an accurate clinical diagnosis; however, clinical diagnosis of nevi with clinical risk factors that border onto malignancy becomes a challenge [275]. In addition, an overlap of the size between small UM and benign choroidal nevi adds to this challenge [276]. Therefore, having a quantitative screening method is crucial to differentiate between benign choroidal nevi and small malignant melanomas, as both often share several features such as size, color, location, drusen, orange pigment and subretinal fluid.

While biopsies are generally not used for diagnosis, they are used in UM lesions for prognostication [274]. Important prognostic factors for metastasis have been elucidated, such as chromosomal anomalies assessed by cytogenetics, gene expression profiling, and the presence of loss of function *BAP-1* mutations [277]. However, tissue biopsies, aside from being invasive, provide a static picture of the tumor, neglecting spatial and temporal heterogeneity and do not sample disseminated disease, circulating tumor cells (CTCs), or micrometastasis [14, 278]. As such, UM remains challenging as it requires accurate profiling, proper interpretation of nevi (as nevi often share several features with UM [276] and/or right risk stratification. Given the high rate

of metastasis associated with this malignancy, more objective monitoring is needed to determine the best treatment options. An alternative approach that does not rely on a biopsy and that could non-invasively sample tumor-derived material would be paramount, especially to distinguish high risk nevi from small UM as well as to detect metastasis.

Liquid biopsy is a minimally invasive approach to detect and monitor disease progression, recurrence and response to treatment by investigation/assessing tumor features using different biofluids, most commonly blood, as well as other biofluids such as urine [279], saliva [44], and pleural effusion [280]. In the eye, aqueous and vitreous humors have been proposed as sources of circulating tumor DNA (ctDNA) in retinoblastoma [281, 282]. Cell-free DNA (cfDNA) has been widely studied as a liquid biopsy analyte. ctDNA can be detected within cfDNA using mutations inherent to a tumor lesion [34]. ctDNA represents as little as 0.1% of the total cfDNA [283], making its detection a challenge. Thus, a highly sensitive and specific method is needed not only for diagnosis, but also for monitoring disease progression. Digital droplet PCR (ddPCR) detects allele frequencies as low as 0.01% [284], making it suitable for ctDNA analysis.

Using this highly sensitive assay, we undertook this study to investigate the feasibility and clinical value of tracking UM-specific mutated ctDNA.

Material and Methods

Cell lines and culture conditions

MP41 and MP46 were purchased from American Type Culture Collection (ATCC). 92.1 cells were gifted by Dr. Martine Jager (Leiden University, Netherlands) [285]. MEL270 and OMM2.5 were gifted by Dr. Vanessa Morales (University of Tennessee). OCM1 was received from the Institute of Ophthalmology and Visual Sciences (University of Valladolid). Cells were

cultured in RPMI-1640 (Corning) supplemented with 10% Fetal Bovine Serum, 10 mM HEPES, 2mM Corning glutaGRO, 1 mM NaPyruvate, 0.1% 10 U/ml penicillin and 10 µg/ml streptomycin (all from Corning), and 10 µg/ml insulin (Roche) in a 37ºC and 5% CO_2 atmosphere.

Animal model

Fifteen female New Zealand albino rabbits (Charles River) were used in accordance with an animal use protocol (#2018-8028) approved by the Animal Care committee at the Research Institute of the McGill University Health Centre (RI-MUHC). Animals were randomly divided into three groups of five rabbits each; (i) group 1 (labeled G1:R1 to G1:R5), group 2 (labeled G2:R1 to G2:R5) and group 3 (labeled G3:R1 to G3:%5) (**Figure 2.2A**). All rabbits were immunosuppressed using daily intramuscular injections of cyclosporin A (CsA at 15 mg/kg) (Sandimmune, Novartis), starting 3 days before cell inoculation and lasting until intraocular tumor detection by fundoscopy. Following anesthesia using intramuscular injection of Acepromazine (0.75 mg/kg), Ketamine (35 mg/kg) and xylazine (5 mg/kg); 1 million living 92.1 cells (in groups 1 and 2) or MP41 cells (in group 3) were inoculated into the suprachoroidal space in the right eye [21]. All rabbits were examined weekly with fundoscopy (Keeler Vantage Plus Indirect LED Binocular Opthalmoscope, lens 20D Indirect BIO lens from Volk Optical) and ultrasound (Master-Vu, Sonomed Escalon) using drops of tropicamide and phenylephrine to dilate pupils. No anesthesia or sedation were required. At fundoscopic detection of UM lesions, CsA doses were decreased to 10 mg/Kg daily in group 1, discontinued in group 2, or reduced to 5 mg/Kg daily in group 3. During the experiment, all rabbits were monitored daily for CsA secondary effects (i.e. weight loss, loss of appetite, and gastrointestinal and respiratory complications). One rabbit (G3:5) was excluded from our study at week 3 due to early death following serious CsA secondary effects. Animals were euthanatized by intraperitoneal injection of pentobarbital sodium (120 mg/kg). After

enucleation, eyes were fixed in 10% phosphate-buffered formalin (Fisher). Using an DSX100 microscope (Olympus) gross phatology images were obtained. During fundoscopy examinations, tumors were measured and categorized into four categories based on basal diameter: 0 (no tumor formation), 1 (small: <11mm), 2 (medium: 11 to 15 mm), and 3 (large: >15 mm).

Patient recruitment and categorization

Forty-five participants were enrolled for this study (14 patients diagnosed with primary UM, 16 patients with nevi and 15 healthy individuals (controls)) at the McGill Academic Eye Clinic in accordance to an approved ethics protocol (MAEC; IRB protocol #2018-4187) approved by the Review Ethics Board of the RI-MUHC (**Table 3-5**). The enrolled healthy individuals had no symptoms or personal history of cancer at the time of consent, and no family history of cancer. Blood samples were obtained following acquisition of informed consent.

Patient medical records were retrieved and used to correlate ctDNA to disease characteristics. UM patients were classified according to the American Joint Committee on Cancer (AJCC) classification of UM (**Table 3**) [286]. In the UM cohort, no evidence of metastasis was seen in any patient. Most of the UM patients had underwent episcleral brachytherapy (plaque radiation) as a treatment, except LB36 who had not received any treatment at the time of blood withdraw (**Table 3**). Patients with nevi were categorized according to risk factors for UM: thickness, presence of subretinal fluid, visual symptoms, orange pigment, peripapillary, halo, and ultrasonographic hollowness (**Table 4**) [139].

Blood specimen collection and sample preparation

In the animal model, following anesthesia (as stated above), 8 ml of peripheral blood was collected via the central ear artery using EDTA tubes (Becton Dickinson) at the day of cell inoculation, every 2 weeks from week 4 to 16 after inoculation and at euthanasia. For human

donors, 10 ml blood samples were collected from a peripheral vein. Blood samples from all UM patients, nine patients with nevi, and eight control were collected in PAX gene Blood ccfDNA Tubes (QIAGEN/Becton Dickinson). Blood samples from the remaining seven healthy individuals and seven patient with nevi were collected in vacutainer tubes containing clot-activation additive and a barrier gel and left 60 min at room temperature to isolate serum (Becton Dickinson). Blood samples were spun at 2000 *g* for 20 min within 1 hour after collection. A second spin (2000 *g* for 20 min) was performed to ensure for the elimination of contaminating cells. Resultant plasma/serum were aliquoted and store at -80ºC until DNA isolation.

Aqueous humor collection from rabbits

At the time of cell inoculation, at tumos formation (weeks 5-8), and euthanasia (18-19 weeks), a paracentesis was conducted to withdraw 100-300 uL aqueous humor from the anterior chamber of rabbits from groups 1 and 2 using a BD Luer-Lok 1 mL syringe (Becton Dickinson). The procedure was conducted under general anesthesia (as stated above) and following topical application of proparacaine hydrochloride ophthalmic solution (Alcon).

DNA isolation

Genomic DNA (gDNA) was extracted from all cell lines using the QIAamp DNA Mini Kit (QIAGEN) according to the manufacturer's instructions. cfDNA was recoved either from (i) 3 mL cell conditioned medium: $4x10^5$ cells were seeded in a T25 flask (Corning), once culture reaches 80% confluency medium was renewed. Then, after 12 hours it was collected in 15 ml tubes (Falcon) and spun at 300 *g* for 5 min to eliminate contaminating cells and cell debris. (ii) 2 mL plasma/serum samples, or (iii) 100-300 µL aqueous humor samples using the QIAamp Circulating Nucleic Acid (CNA) Kit (QIAGEN). Isolated DNA was stored in AVE buffer (RNase-free water with 0.04% sodium azide-QIAGEN) in a 25 uL final volume and quantified using Qubit 2.0

fluorometer with Qubit dsDNA HS assay reagents (**Supplementary Figure 2A-E and 3A)** (Thermofisher Scientific).

Analysis of mutated DNA fragments

To evaluate technical reproducibility, ctDNA was quantified from 2 mL plasma in duplicate using ddPCR. The hotspot mutations analyzed were Q209P (c.626 A>C) and Q209L (c.626 A>T) in *GNAQ*, Q209P (c.626 A>C) and Q209L (c.626 A>T) in *GNA11*, L129Q (c.386 T>A) in *CYSLTR2* and D630Y (c.1888 G>T) in *PLCB4* (**Table 3**).

Primers, probes, and gBlock (synthetic double-stranded DNA fragments of 125-3000 bp used as a positive control [287]) were designed and generated by Integrated DNA technologies (**Table 3**). Serial dilutions using gBlocks were performed to obtain the minimum detection of mutant copies (**Supplementary Figure 1**). A 20 µL reaction mixture was prepared using 10 µL 2x ddPCR Supermix for probes (No UTP) (Bio-Rad), 900 nM forward/reverse primers, 250nM hydrolysis probes, 1 ng DNA sample, and RT-PCR grade water (Invitrogen). DNA samples were run in triplicates, and the no-template controls and positive controls were run in duplicates. Droplets were generated using a QX200 droplet generator (Bio-Rad), and transferred into a semi-skirted 96-well PCR plate (Bio-Rad). Using a C100 thermal cycler (Bio-Rad), PCR reactions were run as follows: 10 min at 95ºC, followed by 50 cycles of 30 sec at 95ºC, 1 min at 56-60ºC (optimized for each primer set (**Table 3**)), and 30 sec at 72ºC; finally, 10 min at 98ºC. Processed droplets were analyzed in a QX200 Droplet reader (Bio-Rad). Samples with £2 mutant droplets were considered as negative for ctDNA. Copies of target and percentage fractional abundance (%FA), which refers to the portion of the mutant allele frequencies over the wild type background) were generated by Quanta Soft software v 1.7.4.

Data analysis

Our data were analyzed using levels of ctDNA (molecules/mL) and %FA. The number of ctDNA molecules was calculated following a previous reported calculation [86, 283], where the amount of copies/µL, volume added to each reaction and amount of plasma/serum are considered, as well as assuming 3.3 pg corresponded to the weight of a human haploid.

Graphs and statistical analyses were performed using Excel or Prism GraphPad Softwares. Spearman correlation analyses were performed to measure the degree of association between data outcomes, and comparison among groups was done by Kruskal-Wallis test. $P < 0.05$ was considered statistically significant.

Results

Validation of wild type and mutant cfDNA detection in conditioned medium of human UM cell line cultures

Digital droplet PCR (ddPCR), coupled to the noninvasive blood-based liquid biopsy, has been proposed as a promising and accurate strategy to document rare variant mutations for the monitoring of cancer development and progression [284]. By targeting well-known driver mutations that characterize UM, we performed ddPCR analyses to determine its feasibility and value for UM patient staging. We assayed serial dilutions of gBlocks that mimic several UM somatic mutations to determine the minimal detection levels of mutated copies. We were able to detect as little as 0.16, 0.08, 0.09, 041, 057 and 0.09 [copies/µL] mutated DNA for *GNAQ c.646 A>T, GNAQ c.646 A>C, GNA11 c.646 A>T, and GNA11 c.646 A>C, PLCB4 c.1888 G>T,* and *CYSLTR2 c.386 T>A* mutations, respectively (**Supplementary Figure 1**).

We first sought to determine whether we could detect cfDNA in a culture system of UM. We used six well established human UM cell lines (92.1, MP41, MP46, MEL270, OMM2.5 and OCM1) with known mutational status to set up our assay by focusing on mutations at *GNAQ* and *GNA11*. By analyzing genomic DNA (gDNA), we detected the correct mutation signature in all UM cell lines, as previously reported, which strengths the validity of our test (**Figure 2.1 A-C, Supplementary Table 1**) [288]. Notably, when we assessed DNA fragments recovered from cell-free conditioned media of these cell lines, we detected both *GNAQ/11* WT and the correct parental *GNAQ/11* mutation (c.626A>C or c.626A>T), respective to the analyzed cells, indicating the release of different amounts of fragmented DNA (i.e. cfDNA) into the culture medium (**Figure 2.1A-C**). In addition, in conditioned media from OCM1, a known *GNAQ/11* wild type cell line, we did not detect any mutant copies of *GNAQ/11* (**Figure 2.1 B**) [289]. Together, these results indicate the feasibility of our assay to accurately and specifically detect fragmented mutant UM cfDNA targets.

Blood mutated ctDNA levels correlated with tumor development and progression in a UM animal model

As we had established the conditions to screen for cfDNA using the cell culture model, we applied our assay to assess the utility of *GNAQ/11* mutations in detecting ctDNA as a liquid biopsy *in vivo*. For this purpose, we first took advantage of a human UM rabbit model that we developed [21]. We used two cell lines with different driver mutations (i.e. 92.1 and MP41 cells harboring mutated *GNAQ* (c.626 A>T) and *GNA11* (c.616 A>T), respectively) (**Figure 2.2 A, Supplementary Table 1**). The goal is to insure the potential of screening for different UM specific mutations *in vivo*. During the course of the animal experiments and once ocular tumors were

detected by ultrasound and fundoscopy, we adjusted the dosage of CsA to reduce the adverse effects associated with the drug (**Supplementary Table 1**). In addition, in the cohort of rabbits injected with 92.1 cells, CsA administration was discontinued in Group 2 to determine the potential of our assay to monitor for disease progression (i.e. tumor shrinkage) (**Figure 2.2 A**).

Rabbits developed detectable subretinal tumors within 4-6 weeks as judged by ultrasound and fundoscopic examinations (**Figure 2 B, Supplementary Table 2)**. As the growth of the ocular tumors differed between rabbits, their sizes at different time points (i.e. 4, 6, 8, 10, 12, 14, and 16 weeks after cell inoculation and at euthanasia) were assessed and categorized by a clinical ophthalmologist into four categories as stated under the methods section (**Figure 2.3 A-C**). In parallel, blood samples were recovered to analyze cfDNA patterns (**Figure 2.2A and 2.3 A-D**). Total cfDNA ranged from 10.1 ng to 189 ng/ 2mL of plasma along the 20 week-study (**Supplementary Figure 2A-C)**. In these DNA samples, and as expected, we did not detect wild type nor mutant *GNAQ/11* ctDNA of human origin at the time of inoculation (**Figure 3D)**. In contrast, we detected mutated *GNAQ* ctDNA fragments in groups 1 and 2, and mutated *GNA11* ctDNA fragments in group 3 as early as 4 weeks and 6 weeks post-inoculation, respectively (**Figure 2.3 A-D**), confirming the potential of our assay to screen for different UM specific mutations *in vivo*. Interestingly, in group 1, while ctDNA was first detected 24 days after cell inoculation, in all the animals intraocular tumors were seen later; on average 31.4 days post-cell inoculation, suggesting that ctDNA was an earlier biomarker of tumor formation compared to clinical imaging. In addition, in group 2, detection of ctDNA was highest at around 6 weeks; however, levels decreased steadily and significantly afterward until animal euthanasia (**Figure 2.3B and D)**. Decreased levels of ctDNA were concomitant with the shrinkage of ocular tumors that were no longer visible (like in rabbits G2:R2 (i.e. rabbit #2 in group 2), G2:R3, and G2:R4)

or very small (like in rabbits G2:R1 and G2:R5) at autopsy (**Figure 2.3B and D**). These observations correlated with the arrest of CsA administration, suggesting the potential of our assay to monitor for disease progression**.** In group 3, where ctDNA were not detected before the 6th week, ocular tumors were detected at the 6th or 8th weeks (**Figure 2.3 C and D**), suggesting again that UM ctDNA is an earlier biomarker of tumor formation and a valuable tool to monitor UM progression. Overall, and by using Spearman correlation analyses, while no correlation was found between total DNA (not tumor specific) and ctDNA or tumor size (r = -0.045, P = 0.63, or r = -0.149, P = 0.39, respectively) (**Supplementary Figure 2F and G**), we found a significant positive correlation between ctDNA level and tumor size in all the rabbits (r = 0.60, P < 0.0001), and a negative correlation between ctDNA level and body weight (r = -0.37, P < 0.0001) (**Figure 2.3E**), suggesting that the correlation of blood cfDNA levels with tumor growth was specific to DNA originating from ocular UM tumor cells (i.e. ctDNA).

Taken together, these data bring strong evidence that blood biopsy screening for human mutated *GNA11/Q* ctDNA biomarkers is a valuable and feasible tool for the early diagnosis of UM and the monitoring of disease progression.

UM-derived cfDNA detected in the aqueous humor correlated with tumor size and progression

In parallel to the analyses done on blood biopsies, we sought to determine whether UM cfDNA could be detected in the aqueous humor (AH) of grafted animals. An AH paracentesis was conducted in rabbits from groups 1 and 2, and samples were analyzed for the presence of mutated *GNAQ* cfDNA. As expected, no detectable levels of UM cfDNA were found at the time of UM cell inoculation. In contrast, we detected mutated *GNAQ* cfDNA at the second sampling (weeks 5-

8, range 0-4 molecules/mL) in both groups. Interestingly, at the third sampling (weeks 18-19), we still detected mutated *GNAQ* cfDNA in the AH of rabbits from group 1 (range 1-3 molecules/mL), while we observed a sustained decrease in the AH of rabbits from group 2 with only minimal detectable traces (**Figure 2.3F and G**). Using Spearman correlation analyses, we did not find any correlation between total DNA (not tumor specific) and cfDNA or tumor size (**Supplementary Figure 2H and I**). In contrast, we observed a significant and positive correlation between mutated *GNAQ* cfDNA level (tumor specific) and tumor size ($r = 0.71$, $P < 0.0001$) and a negative correlation between mutated *GNAQ* cfDNA level (tumor specific) and the body weight ($r = -0.33$, $P = 0.07$) (**Figure 2.3H and I**). These data suggest that the AH is another biological analytes that can be used to screen for mutated cfDNA copies for the management of UM patients.

Mutant GNA11/Q cfDNA was detected in patient blood biopsy and correlated with the degree of lesion malignancy

GNAQ/11 mutations are present in more than 90% of UM cases and, although not sufficient, they are thought to be initiating events of the disease [23, 24]. As our assay was able to detect these mutations in an *in vivo* human UM rabbit model and correlated with disease burden, we applied this strategy to clinical samples to get more insight on its validity to screen for UM and stratify patients presenting with ocular nevi (**Tables 4-6**). In addition, for cases that were negative for *GNAQ/11* mutant DNA, we verified the presence of *PLCB4* and *CYSLTR2* mutant ctDNA. As expected, all analyzed samples (from 14 primary UM patients, 16 patients with choroidal nevi and 15 disease-free healthy controls) were positive for wild type *GNAQ, GNA11, PLCB4, CYSLTR2* ctDNA copies (**Supplementary Figure 3A).** In addition, in contrast to patient (UM and nevi)

donors, none of the 15 healthy control samples contained mutated *GNAQ/11*, *PLCB4*, *CYSLTR2* cfDNA (**Figure 2.4 A, B,and E**).

We then focused our analyses first on blood biopsies drawn from UM patients. Mutant *GNAQ*, *GNA11* or *PLCB4* ctDNA copies were detected in all 14 primary UM patients. We found that these mutations were present in a mutually exclusive manner and frequencies in the range of previously published data (i.e. 9 patients (64%) having a *GNA11* mutation (range, 0.7-26.4 molecules/mL), 4 patients (29%) having a *GNAQ* mutation (range, 3.1-31.4 molecules/mL) and 1 (7%) having a *PLCB4* mutation (2.1 molecules/mL) (**Figure 2. 4A**) [23, 24]. We did not observe any correlation between the levels of ctDNA and the age of patients or total DNA amounts (r = -0.13, P = 0.48, r = 0.07, P = 0.34, respectively) (**Supplementary Figure 3B and C**).

We searched for a relationship between the levels of mutated ctDNA copies and tumor stage. We found a positive and significant correlation between the AJCC classification and %FA (r = 0.69, P = 0.008) (**Figure 2. 4C** (left panel) **and Table 5**) [290]. In addition, and although not significant, we observed a correlation between the tumor thickness and the %FA (r = 0.38, P = 0.079) (**Figure 2.4 C and Table 3**). These data suggest that our assay combined to a blood biopsy is valuable to screen for patients with UM lesions and to monitor for disease aggressiveness.

We then sought to determine the pattern of mutated *GNAQ/11* ctDNA in the blood of patients presenting with premalignant choroidal nevi. In this cohort, we recruited 16 patients, and blood samples were processed to isolate either plasma (9 patients: LB20 – LB45) or serum (7 patients: LB06 – LB12) (**Figure 2.4 B and Table 6**).

We categorized these patients according to the presence of clinical risk factors for melanoma transformation by taking advantage of a systematic classification of clinical and imaging features [291]. Seven patients had at least 2 risk factors, and interstingly all were positive

for the presence of mutated *GNAQ* cfDNA copies. In contrast, of the two patients that had no risk factors, one (LB37) had displayed measurable levels of mutated *GNAQ* cfDNA (**Figure 2.4 B and Table 6**). This patient had bilateral nevi, one of which was 1mm thick. Notably, the levels of mutated cfDNA positively and significantly correlated with the presence of factors predisposing to nevus transformation ($r = 0.92$, $P < 0.0001$) (**Figure 2. 4D).**

Moreover, while the levels of mutated ctDNA in patients having nevi with risk factors did not differ compared to those in samples from the UM patient cohort, they were significantly higher when compared to levels in samples from patients having nevi with no risk factors and from healthy individuals ($P < 0.05$) (**Figure 2. 4E)**. This highlights that a close follow-up of the levels of mutated cfDNA in patients with choroidal nevi may be beneficial for the early detection of potential transformation into UM lesions. Altogether, our data bring evidence that plasma- rather than serum-based liquid biopsy screening for UM-specific mutated ctDNA may be a new tool for the early UM diagnosis, the staging of lesion malignancy, and the monitoring of disease progression.

Figures

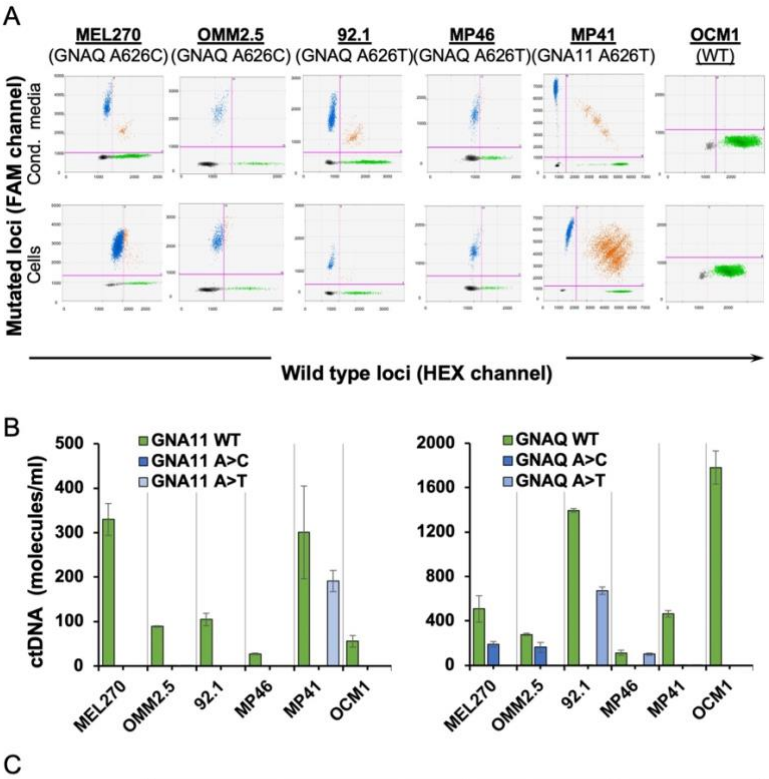

C

Cell lines	ctDNA (molecules/ml) GNAQ A626T	GNAQ A626C	GNA11 A626T	Cells total DNA (ng/25ul)	Cond. media total DNA (ng/25ul)
92.1	672.3	--		3280	112
MP41	--	--	190.9	2205	200
MP46	101.0	--	--	2750	33.8
MEL270	--	189.4	--	2350	68.5
OMM2.5	--	162.9	--	2260	105
OCM1	--	--	--	2325	129

Figure 2. 1: Wildtype and mutant cfDNA were accurately detected in human UM cell line conditioned medium.

A. Representative 2D fluorescence amplitude plots of DNA extracted from conditioned medium (Cond. Media; cfDNA) and cells (genomic DNA). GNAQ and GNA11 mutant DNA-positive droplets are shown in blue (FAM channel), wild type DNA-positive droplets are represented in green (HEX channel), droplets positive for both wild type and mutant targets are shown in orange, and the negative droplets are shown in black. B. Copy numbers of wild type and mutant cfDNA in

UM cells conditioned medium. Data are shown as number of molecules per mL of medium (mean +/− SD, n = 3 independent experiments). C. Table summarizes ctDNA (molecules/mL) isolated from condicionated medium and total DNA derived from cells and conditioned medium.

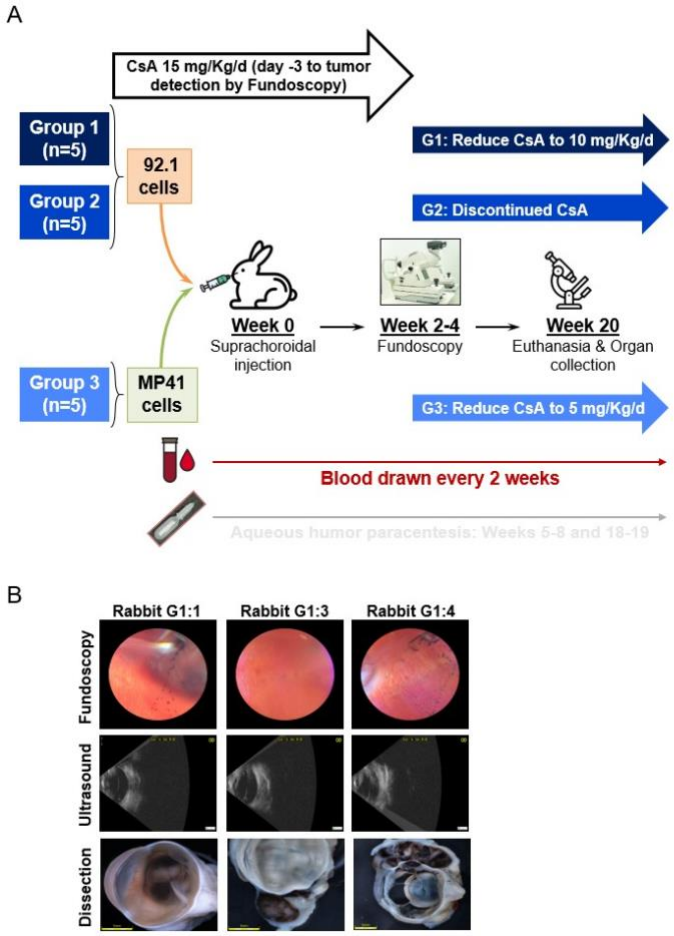

Figure 2. 2: A human UM rabbit model was used to validate the detection of mutated ctDNA in liquid biopsies.

A. Overview of the developed human UM xenograft model and animal follow-up procedures. For more details, see Material and Methods section. CsA; Cyclosporine A. B. Representative fundoscopy and ultrasound images taken at tumor formation, and post-mortem photographies of dissected eyes (scale bares: 5 mm)

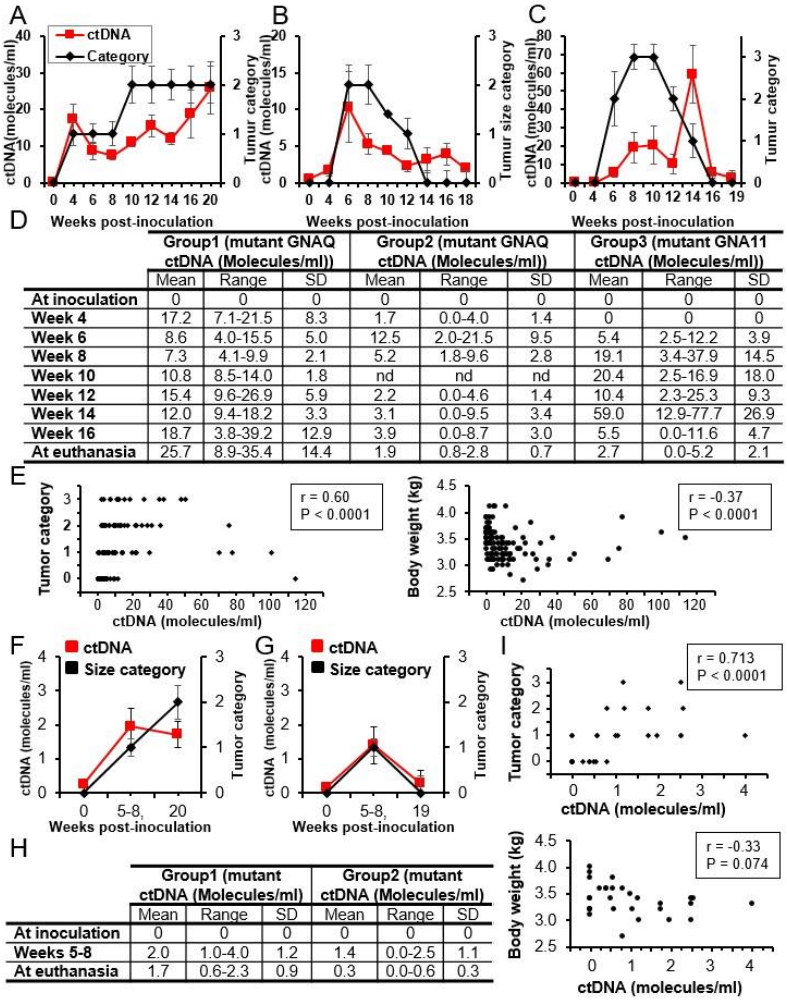

	Group1 (mutant GNAQ ctDNA (Molecules/ml))			Group2 (mutant GNAQ ctDNA (Molecules/ml))			Group3 (mutant GNA11 ctDNA (Molecules/ml))		
	Mean	Range	SD	Mean	Range	SD	Mean	Range	SD
At inoculation	0	0	0	0	0	0	0	0	0
Week 4	17.2	7.1-21.5	8.3	1.7	0.0-4.0	1.4	0	0	0
Week 6	8.6	4.0-15.5	5.0	12.5	2.0-21.5	9.5	5.4	2.5-12.2	3.9
Week 8	7.3	4.1-9.9	2.1	5.2	1.8-9.6	2.8	19.1	3.4-37.9	14.5
Week 10	10.8	8.5-14.0	1.8	nd	nd	nd	20.4	2.5-16.9	18.0
Week 12	15.4	9.6-26.9	5.9	2.2	0.0-4.6	1.4	10.4	2.3-25.3	9.3
Week 14	12.0	9.4-18.2	3.3	3.1	0.0-9.5	3.4	59.0	12.9-77.7	26.9
Week 16	18.7	3.8-39.2	12.9	3.9	0.0-8.7	3.0	5.5	0.0-11.6	4.7
At euthanasia	25.7	8.9-35.4	14.4	1.9	0.8-2.8	0.7	2.7	0.0-5.2	2.1

	Group1 (mutant ctDNA (Molecules/ml)			Group2 (mutant ctDNA (Molecules/ml)		
	Mean	Range	SD	Mean	Range	SD
At inoculation	0	0	0	0	0	0
Weeks 5-8	2.0	1.0-4.0	1.2	1.4	0.0-2.5	1.1
At euthanasia	1.7	0.6-2.3	0.9	0.3	0.0-0.6	0.3

Figure 2. 3: Mutated ctDNA plasma and aqueous humor levels mirrored the pattern of intraocular disease behavior in rabbits.

A-C. Kinetics of the levels of mutated ctDNA in rabbit plasma (left Y-axis) and tumor size categories (right Y-axis) following ocular inoculation of 92.1 cells (A and B; Groups 1 and 2) or MP41 cells (C; Group 3). The legend for all panels is shown on the top A panel. D. Table shows the number of ctDNA molecules/mL in rabbit plasma at inoculation (week 0), weeks: 4, 6, 8, 10, 12, 14, 16, and at euthanasia. E. Mutated plasma ctDNA levels were plotted against tumor size categories (left panel) or rabbit body weight (right panel). Significant positive or negative

correlations were found between ctDNA levels and size categories ($r = 0.60$, $P < 0.0001$) or body weight ($r = -37$, $P < 0.0001$). F-G. Kinetics of the levels of mutated ctDNA in rabbit aqueous humor (left Y-axis), and tumor size categories (Cat) (right Y-axis) in animals inoculated with 92.1 cells (F. Group 1, G. Group 2). H. Table shows ctDNA molecules/mL from aqueous humor at inoculation, weeks 5–8, and euthanasia. I. Top panel: Mutated ctDNA aqueous humor levels were plotted against tumor size categories, which displayed a significant positive correlation ($r = 0.713$, $P < 0.0011$). Bottom panel: Mutated ctDNA levels were plotted against rabbit body weight; no correlation was found ($r = -0.33$, $P = 0.074$). SD: Standard deviation

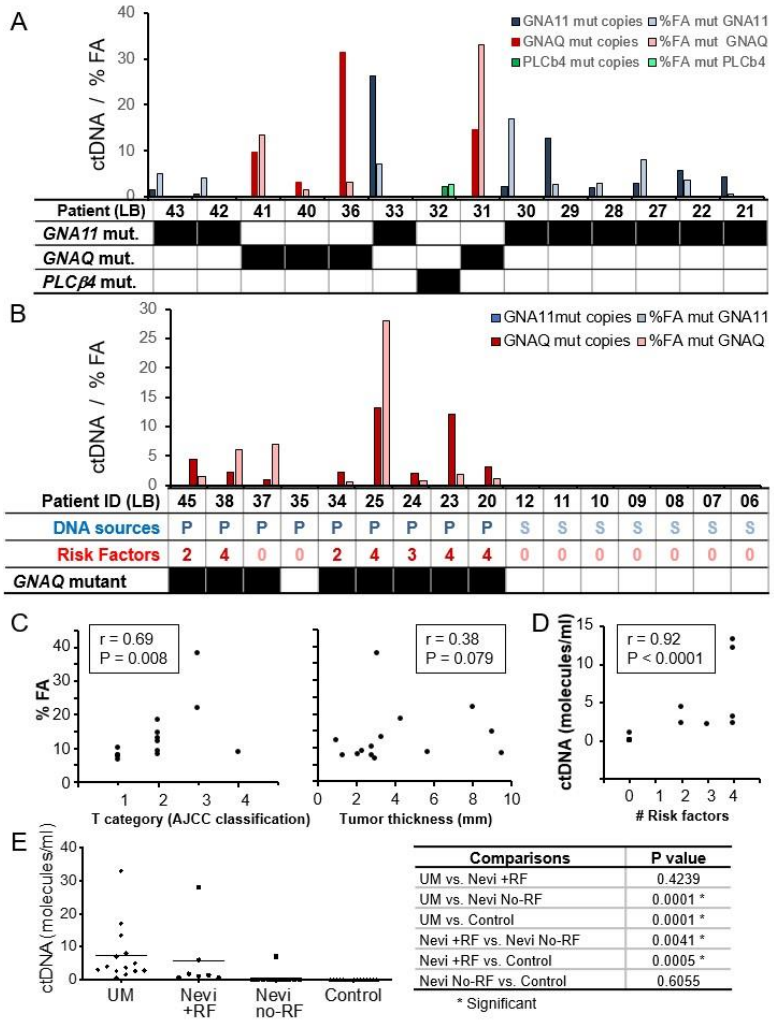

Figure 2. 4: The levels of mutated ctDNA in UM patients and patients with uveal nevi correlated with the stage of disease progression and with the presence of risk factors for malignant transformation, respectively.

A. UM patients: levels of *GNA11*, *GNAQ*, and *PLCB4* mutated ctDNA (molecules/mL of plasma) are shown in dark blue, red, and green, respectively, and %FA of *GNA11*, *GNAQ*, and *PLCB4* is shown in light color (the table shows the mutation status in the analyzed loci). B. Nevi: levels of ctDNA molecules/mL of plasma (dark) and %FA (in a light color) in patients (the table shows the mutation status in the analyzed loci). Note that in all patients, only a GNAQ mutation was detected. P:plasma. S:serum. C. Left panel: the %FA obtained with the UM samples were plotted against the T category of the AJCC staging, which displayed a significant positive correlation ($r = 0.69$, $P = 0.008$). Right panel: The %FA obtained with the UM samples were plotted against tumor thickness (mm); no correlation was found ($r = 0.38$, $P = 0.079$). D. The levels of mutated ctDNA in plasma samples obtained from patients with nevi were plotted against the number of risk factors in every patients, which displayed a significant positive correlation ($r = 0.92$, $P < 0.0001$). E Left panel: Scatter plot depicting the levels of mutated ctDNA in the plasma of UM patients and patients with nevi displaying or not risk factors for malignant transformation, and serum of healthy blood donors. Note the increased levels of ctDNA that accompany increased risk factors. The table (on the right) depicts the comparisons used and the levels of significance for differences (P value)

Tables

Table 3. ddPCR primers and probes information for this study		
	Oligos	Annealing Temperature
GNA11-F	CTTTCAGGATGGTGGATGT	
GNA11-R	ACATGATGGATGTCACGTTCT	58 C
*GNA11*_A_Allele	5HEX/AC+CGC+TGG+CC/3IABkFQ	
*GNA11*_C_Allele	56-FAM/AC+CGC+GGGCC/3IABkFQ	
*GNA11*_T_Allele	56-FAM/AC+CGC+AGG+CC/3IABkFQ	
GNAQ-F	CTTGCAGAATGGTCGATGTAG	
GNAQ-R	GCGCTACTAGAAACATGATAGAG	60 C
*GNAQ*_A_Allele	5HEX/CCT+T+T+G+GCCC/3IABkFQ	
*GNAQ*_Q209L_T_Allele	56-FAM/CCT+T+A+G+GCCC/3IABkFQ	
*GNAQ*_Q209P_C_Allele	56-FAM/ACCT+T+G+GGCC/3IABkFQ	
PLCB4-F	TAACAAACGGCAAATGAGTCG	
PLCB4-R	CAGCCAGCGTTCCAGAAA	55 C
*PLCB4*_D630Y_G_allele	5HEX/CGA+GT+C+G+ATT+CC/3IABkFQ	
*PLCB4*_D630Y_T_allele	56-FAM/CGA+GT+C+T+AT+TC+CA/3IABkFQ	
CYSLTR2-F	CCTTGTATGTCAACATGTACAGC	
CYSLTR2-R	GTGAACCATTGCCAGGAAAC	55 C
*CYSLTR2*_T_allele	5HEX/TTC+C+T+GA+CCGT/3IABkFQ	
*CYSLTR2*_A_allele	56-FAM/TTC+C+A+GA+CCGT/3IABkFQ	

Table 4 Summary of patient characteristics			
Total			45
UM	Number		14
	Sex	Female	7
		Male	7
	Age at blood draw Mean (SD) years		60.1 (15.14)
	Age at diagnosis (SD) years		51.64 (15.35)
	Follow-up (months) Mean (SD)		103 (77.8)
	Location	Choroid	13
		Iris	1
	Tumor size (mm) Mean (SD)	Base	9.42 (3.39)
		Thickness	3.83 (2.28)
Nevus	Number		16
	Sex	Female	9
		Male	7
	Age at blood draw Mean (SD) years		65.6 (13.6)
	Age at diagnosis (SD) years		62.53 (11.24)
	Follow-up (months) Mean (SD)		67.2 (61.8)
	Location	Choroid	15
		Iris	1
	Lesion size (mm) Mean (SD)	Base	3.1 (1.5)
		Thickness	1.6 (0.8)
	Risk factors		7
	No risk factors		9
Healthy individuals	Number		15
	Age at blood draw Mean (SD) years		30.2 (7.4)

F/U follow up. SD= standard deviation.

Table 5 UM patients characteristics

Code LB	Sex	Age (Y)	Location	ctDNA	FA	Lesion	T category, AJCC classification	FU	Rx
21	F	70	Choroid	4.3	9.5	3x10x9	2	77	P
22	F	60	Choroid	2.8	3.7	9x1.9x5.7	4	50	P
27	F	68	Choroid	3.0	8	9.7x9x3.3	2	39	P+
28	F	48	Choroid	1.9	2.8	7.5x5.5x2.1	1	260	TT
29	M	62	Iris	12.8	2.7	3.4x3.8x1.3	1	37	PR
30	M	69	Choroid	2.3	17	16x16x8	3	61	P+
31	M	85	Choroid	29.3	33	9.5x8.5x3.1	3	229	P
32	M	63	Choroid	2.1	2.6	11.5 x12x2.8	1	190	P+
33	F	82	Choroid	26.4	7	2.2x1x1	2	37	P+
36	M	37	Choroid	31.6	3.1	13.3x10.9x5	2	1	P
40	F	38	Choroid	3.2	1.6	10.7x8.5x3.0	1	92	SR
41	M	71	Choroid	9.8	13.5	8.2x8.7x4.3	2	164	P
42	F	38	Choroid	0.7	4	13x9.5x2.3	2	55	P+
43	M	51	Choroid	9.0	5	8.4x9.1x2.8	1	150	P

+ = anti-VEGF treatment; AJCC: AJCC classification; ctDNA (molecules/ml); FA: percentage of fractional abundance; FU: follow-up time (months); Lesion: Lesion size (small diameter x large diameter x thickness) (in mm); P: Plaque radiotherapy; PR: Proton beam radiotherapy; Rx: Treatment; SR: Stereotactic radiosurgery; T: T category; TT: Transpupillary thermotherapy.

Table 6 Characteristics of patients with nevi

Code LB	Sex	Age (Y)	Location	ctDNA	FA	B	TN	FU	RX	RF	Notes
06	F	73	Choroid	0	0	3	Flat	81	--	0	--
07	M	72	Choroid	0	0	NA	Flat	53	--	0	--
08	M	80	Choroid	0	0	2	Flat	141	--	0	--
09	M	79	Choroid	0	0	1.5	1.3	170	--	0	--
10	M	83	Choroid	0	0	3	Flat	182	--	0	Bilateral
11	M	64	Choroid	0	0	4	Flat	48	--	0	--
12	F	70	Iris	0	0	2.4	0.6	170	--	0	--
20	M	77	Choroid	3.1	1.1	1.8	NA	11	+	4	OP, S, F, PP
23	F	57	Choroid	12.1	1.8	NA	NA	5	+	4	T, OP, F, S
24	F	68	Choroid	4.3	0.7	NA	2.3	15	--	3	PP, F, T
25	F	35	Choroid	13.3	28	4.5	2.47	13	+	4	F, S, T, G
34	M	80	Choroid	2.3	0.6	NA	NA	9	--	2	OP, F
35	F	60	Choroid	0	0	2	Flat	12	--	0	--
37	F	47	Choroid	1	7	7	OD: Flat. OS: 1	82	--	0	Bilateral
38	F	45	Choroid	2.3	6	3.2	1.7	12	--	4	OP, F, PP, S
45	F	60	Choroid	4.4	1.8	NA	2.7	18	--	2	PP, T

+ = anti-VEGF treatment; B: Basal diameter (mm); ctDNA (molecules/ml). F: fluid; FA: percentage of fractional abundance; FU: follow-up time (months); G:Growth; OP: orange pigment; PP: peripapillary; RF: number of risk factors; Rx: Treatment; S: visual symptoms; T: thickness >2mm; TN: thickness (mm);

Discussion

Although rare, UM remains the most common primary ocular cancer in adults and is associated with a high mortality rate [137]. The disease often develops asymptomatically and is diagnosed following a routine ophthalmic examination or as a result of following up patients with choroidal nevi [1, 268, 269]. This argues for the development of new quantitative tools to screen for patients at risk of developing the disease [277]. By using biological analytes mainly blood, liquid biopsy has been investigated as a strategy to detect and monitor cancer progression, recurrence and response to treatment [14]. Many circulating biological materials have been proposed as a readout of tumor status, of which mutated ctDNA has gained much attention [35, 292]. The presence of specific gene mutations, like in *GNAQ* and *GNA11*, were proposed as predisposing risk factors for UM development [23, 24]. As mutated ctDNA is present at very low levels in the circulation, a highly sensitive and specific assay to detect mutated *GNAQ* and *GNA11* moieties in patient blood is needed [284]. In this study, we combined a blood-based liquid biopsy and the sensitive ddPCR assay to conduct specific UM-derived ctDNA screening [100]. We set the validity of the analysis using cfDNA from cultures of human UM cells, verified its clinical value in a human UM xenograft rabbit model, and applied it to clinical samples to correlate ctDNA levels to UM patients and patients with choroidal nevi. In summary, we bring evidence that blood biopsy permits the screening of UM-shed mutated ctDNA as a way of early diagnosis, malignancy burden staging and disease progression monitoring.

Liquid biopsy approaches using CTCs has been proposed and applied in the context of UM, where CTCs were found in 29 out of 40 UM patients (72%) at the time of diagnosis and after treatment [174]. This is in contrast to the 100% efficiency (14 out of 14 analyzed UM patients) of UM mutant ctDNA detection we report in our present study. In addition, ctDNA has been analyzed in UM samples using other assays (i.e. ultradeep sequencing and bidirectional-

pyrophosphorolysis-activated polymerization technique), but no clinical value has been reported [293]. Our patient cohort presented a hotspot mutation in *GNAQ* (Q209P and Q209L), *GNA11* (Q209P and Q209L), *PLCB4 (*D630Y), which have been reported in the majority of UM cases. However, other hotspot mutations in those genes should not be discarded. Moreover, until now, the presence of ctDNA in patients with pre-malignant intraocular nevi had not been investigated. Together, this makes our study the first to investigate the presence of ctDNA using initiating UM mutations in patients with choroidal nevi and to report positive correlations between the levels of these mutated ctDNA, and both the UM staging system and the clinical risk factor classifications [139, 286, 290, 291]. Importantly, since ddPCR requires the prior knowledge of the specific point mutation [294], it is not an ideal technique in cancer types with unknown driver events or in which various point mutations can be detected. However, in UM we were able to take advantage of the high proportion of UM cases with a mutually exclusive mutation in one of the four genes assayed. ddPCR is high sensitive (i.e. 0.01% sensitivity: 1 mutant copy in 10,000 wild type gene copies) and it does not rely on sequencing efforts, making the monitoring of ctDNA in UM patients sensitive and inexpensive [96, 283, 284, 294].

In the UM rabbit model, we conducted our assay anticipated in situ detection of UM lesions. Indeed, we observed an early presence of ctDNA days before standard clinical imaging techniques detected ocular tumors. This suggests that ctDNA screening in a blood biopsy may be an effective biomarker for early disease development when tumors are too small to be diagnosed by ophthalmological examination, such as fundoscopy. In addition, we observed that mutant ctDNA levels in the AH correlated with tumor burden, making it another analyte to test during patient follow-up, although accessing it is more invasive. This observation is supported by the finding that cytokine expression patterns in the AH discriminated between high- and low-risk UM

patients [295]. During plaque brachytherapy implantation in UM patients, an anterior chamber paracentesis is a feasible and safe procedure that can be performed [295, 296].

In our clinical study, we were unable to match the blood biopsies to ocular tumor tissue biopsies to confirm the mutational status and validate that we screened for molecules deriving from UM tumors. This limitation was overcome by the use of the UM animal model, where the rabbits were inoculated with cells of known mutations. In these experiments, we found the corresponding parental mutations in the recovered ctDNA, respective of the cell line used (92.1 *vs.* MP41). Overall, in this animal model, our assay allowed us to monitor disease progression (**Figure 3**). Notwithstanding, a well-designed study aimed to ensure matching of blood biopsy and ocular lesion genotype in clinical samples is still needed. Also, detecting ctDNA in a longitudinal study can shed light into UM dynamics and progression. A prospective study that enrolls patients from diagnosis, monitoring throughout treatment, and follow up using a single blood collection type, is needed and is currently ongoing at our center

We found that *GNAQ* and *GNA11* mutated ctDNA is present in a mutually exclusive manner and in frequencies in the range of reported data for UM [23, 24]. Notably, while *GNA11*mutated ctDNA was more frequent in samples from UM patients, only mutated *GNAQ* ctDNA fragments were detected in samples from patients with nevi presenting with risk factors. Although further samples are still required to deepen this observation, this suggests that *GNA11* mutations are more commonly initiating events in *de novo* UM, while *GNAQ*mutations trigger malignant transformation from pre-existing nevi.

The incidence of choroidal nevi is likely underestimated, as these nevi are usually only found on ophthalmic examinations for other clinical reasons. Although nevi remain generally stable over time, malignant transformation towards melanoma increases with age and the

appearance of clinical risk factors [18, 139, 148, 273, 291]. In addition, equivocal diagnosis of nevi with clinical risk factors that border onto malignancy is challenging [275]. Hence, monitoring intraocular nevi using specific ctDNA is paramount for patient follow-up. In our study, patients LB29 and LB33 were diagnosed with ocular nevi 3 and 4 years prior to the melanoma diagnosis, respectively. Furthermore, samples with undetectable levels of ctDNA may carry other hotspot mutations not included in this panel. We could not explore the correlation between ctDNA levels and thickness or base size in nevi lesions due to lack of information on medical records. However, considering clinical risk factors, our data in the nevi cohort suggest that ctDNA may indicate lesions transforming to malignant melanoma. Given the non-invasive and inexpensive nature of our testing, we propose that patients with choroidal nevus are ideal candidates to be monitored though such a liquid biopsy approach.

Preanalytical variables can influence the outcome of cfDNA [297]. Biological factors (e.g. exercise, pregnancy, inflammation, diabetes) affect the levels of cfDNA [14] [86]. Methodological variables can also impact the outcome of cfDNA [297]. For example, differences in recovery of DNA have been observed using different commercial extraction kits. In this work, the QIAamp CNA was used, which is considered as the gold standard approach [298]. In addition, higher cfDNA amounts with increased number of wild type loci copies were recovered from serum compared to plasma, likely due to the release of DNA from the lysis of white blood cells that occurs during clotting [297]. This is in line with our findings that serum was enriched in wild type *GNAQ/11* ctDNA fragments compared to plasma samples (**Supplementary Figure 3G**). This observation may explain the lack of detection of ctDNA in all serum samples despite having higher cfDNA levels, making the use of plasma more likely suitable for liquid biopsy-based platforms to screen for mutated ctDNA.

Half of UM patients will develop metastatic disease many years and even decades after primary ocular tumor diagnosis due to dormant micro-metastases foci [1, 137, 140]. Blood-based biomarkers screening, originally designed for cutaneous melanoma, have been tested in UM patients, but have shown little promise [137, 278, 299, 300]. As metastatic patients present higher ctDNA compared to patients with primary disease, our assay may be used to screen for patients at risk of UM metastasis [47].

Conclusion

Our study is of high importance to monitor UM patients and individuals at risk of developing the disease. Liquid biopsy is especially relevant to UM where classical tissue biopsies are generally not used for diagnosis. As a noninvasive strategy, its combination to sensitive and reliable technologies allows the monitoring of disease progression. By combining human UM cell culture and an *in vivo* animal model, we established the proof of principle for the validity of ddPCR to screen for specific UM mutated ctDNA in clinical UM samples. We conclude that patient plasma is an easily accessible milieu to track mutated ctDNA for the early diagnosis and staging of the patients, and the monitoring of disease progression. Further studies targeting the analysis of other UM mutations and involving a greater number of primary and metastatic UM patients, and patients with choroidal nevi are necessary, and are currently in progress in our institution.

List of abbreviations

American Joint Committee on Cancer (AJCC); aqueous humor (AH); cell-free DNA (cfDNA); circulating tumor DNA (ctDNA); cysteinyl leukotriene receptor 2 (*CYSLTR2*); confidence interval (CI); digital droplet Polymerase Chain Reaction (ddPCR); fractional abundance (FA); genomic DNA (gDNA); guanine nucleotide-binding protein G subunit alpha

(*GNAQ)*; guanine nucleotide-binding protein G subunit alpha 11 (*GNA11);* phospholipase C beta 4 (*PLCB4*) risk factors (RF); uveal melanoma (UM); wild type (WT).

Declarations

- Ethics approval and consent to participate: All participants provided informed consent to the protocol (MAEC; IRB protocol #2018-4187) was approved by the Review Ethic Board at the RI-MUHC.
- Availability of data and material: All data generated or analysed during this study are included in this published article
- Consent for publication: not applicable
- Competing interests: none

Funding: This study was supported by funding from Zeiss Canada and a Mitacs Accelerate grant. PB received CONACYT funding #739468.

- Authors' contributions: PB and TT carried out all experiments for the cell culture, animal model and analysis of human samples. JC saw patients and conducted the animal model. CM oversaw ethics review and approval, consented patients and coordinated animal study, CF and RPP conducted animal surgeries, NB and CLD took blood from patients. RASA supported the AH sample analysis, EY supported the analysis and graph generation, MNB and SAC are the attending ophthalmologists, JVB deisgned the study, provided the funding, supervised staff and students. All authors helped to draft the manuscript.

Acknowledgements: Authors thank all the participants enrolled in the study and the staff of the Animal Care facility at the RI-MUHC.

Preamble to Chapter 3

In Chapter 2, we demonstrated that UM driver mutations can be used to successfully detect ctDNA using a highly sensitive ddPCR approach. We first showed detection of ctDNA in the culture supernatant of human UM cancer cells lines. This finding was supported by the detection of ctDNA isolated from plasma and aqueous humor derived from an animal model. The translational nature of our study was highlighted in our clinical study, showing an association between the presence of ctDNA isolated through UM driver mutations in patient plasma with malignancy in UM.

Our findings showed strong evidence of ctDNA as a biomarker of UM. Other studies have also supported this biomarker role in various cancer types [12, 13, 17]. However, the biology underlying ctDNA release in cancer is still unclear. Previous literature suggests that ctDNA emission is highly linked to cell death, mainly apoptosis and necrosis [35]. ctDNA fragment size seems to inform about its origin. Necrosis releases longer DNA fragments whereas apoptosis derives shorter DNA fragments [58, 59]. Since most of ctDNA observed in the bloodstream is short, apoptosis seems to be the major contributor [34]. In addition to cell death, active cellular secretion is also a mechanism of ctDNA release [58, 301]. Moreover, a recent study reported senescence influences ctDNA levels [60].

We speculate that the kinetics of ctDNA is treatment-dependent, and treatments release different ctDNA pattern sizes. To address this hypothesis, we characterized ctDNA kinetics release using our validated UM *in vitro* system. We simultaneously assessed ctDNA from colorectal and lung cancer cells. The next chapter, thus, aims to better understand the underlying release process of cfDNA in cancer. Understanding the mechanisms and context that contribute to ctDNA release

is important to understand the kinetics of ctDNA in patients undergoing cytotoxic anti-cancer therapies, such as chemotherapy and radiation

This chapter is based on **Manuscript 3: The kinetics and fragmentation of cell-free DNA from cancer cells are influenced by anticancer treatments.** Submitted to Scientific Reports.

Chapter 3: The kinetics and fragmentation of cell-free DNA from cancer cells are influenced by anticancer treatments

Prisca Bustamante[1*], Mohamed Abdouh[1], Thupten Tsering[1], Julia V Burnier[1,2,3]

[1]Cancer Research Program, Research Institute of the McGill University Health Centre, Montreal, QC, Canada

[2]Gerald Bronfman Department of Oncology, McGill University, Montreal, QC, Canada

[3]Experimental Pathology Unit, Department of Pathology, McGill University, Montreal, Qc, Canada

*Corresponding author:

Prisca Bustamante

1001 Decarie boulevard, E01.2143. Montreal, QC H4A 3J1

514-934-1934 ext 76146

Email: prisca.bustamantealvarez@mail.mcgill.ca

Number of figures: 6 figures

Number of tables: 1 table

Submitted to Scientific Reports, 2022.

Abstract

Liquid biopsy-based detection of circulating free DNA (cfDNA) is a promising tool to monitor tumor progression and treatment response. cfDNA release is thought to result from a combination of cell death (apoptosis and necrosis), and active cellular secretion. As such, cytotoxic anti-cancer therapies can impact cfDNA kinetics. This makes the interpretation of cfDNA analyses pivotal for its applicability as a biomarker. In this study, we assessed the kinetics and fragmentation of cfDNA in cancer cells of various origins following standard anti-cancer treatments with different cytotoxic effects and mechanisms of action.

Human colorectal carcinoma, lung adenocarcinoma, and uveal melanoma cancer cells were subjected to different forms of cytotoxic stress, including induction of apoptosis (tumor necrosis factor (TNF)-related apoptosis-inducing ligand (Apo2L/TRAIL)), cell cycle arrest (Roscovitine, Valproic acid), necrosis (radiotherapy), and senescence. Following treatments, cells were analyzed for their cell cycle progression, level of senescence, and mechanism of cell death (apoptosis *vs.* necrosis). Heat treatment was used as a control for necrosis-related cell death. Total cfDNA and mutant cfDNA (based on the mutations of each parental cell line) were isolated from cultured media and quantified using the Qubit assay and digital droplet PCR targeting, respectively. Fragment length of the isolated cfDNA was visualized using the Bioanalyzer 2100.

Total and mutant cfDNA levels increased during all cytotoxic treatments in a concentration-dependent manner. Notably, cells undergoing apoptosis shed higher levels of cfDNA compared to necrotic and senescent cells. In addition, electropherogram images showed that cytotoxic conditions alter fragment size distribution, with smaller fragments of <200bp associated with apoptosis and >1000 bp with necrosis.

The kinetics and fragmentation of released cfDNA are influenced by cytotoxic insults. Determining the characteristics of cfDNA can facilitate and improve its use as a clinical biomarker during anti-cancer therapy. Our data pave the way for the establishment of criteria to apply when monitoring cfDNA for cancer management based on the anticancer therapeutic strategy.

Key words: cell-free DNA, cancer cells, Anticancer treatment, Cell death, Cell cycle, Senescence.

Background

Liquid biopsy has emerged as a minimally invasive approach and a promising tool to detect and monitor disease progression in many tumor types by using body fluids such as blood, urine, sputum, and cerebrospinal fluid [292]. One of the analytes studied in liquid biopsy is cell-free DNA (cfDNA). cfDNA is a mix of non-encapsulated DNA thought to be produced via active secretion from live cells, including via extracellular vesicles and microparticles release [61, 301-303], and as a product of cell death during apoptosis, necrosis, and autophagy [35, 58, 59, 304]. Depending on the mechanism of cell death, the size of shed cfDNA is reported to vary substantially[305]. The majority of cfDNA appears in fragments of 180 bp, consisting of internucleosomal DNA pieces resulting from apoptosis-linked caspase-dependant endonuclease cleavage[306]. In contrast, such fragmentation does not occur during necrosis, where rapid non-specific cleavage of DNA prevails and gives rise to larger fragments reaching 10,000 bp [53, 59].

While in healthy conditions, cfDNA is mainly released by hematopoietic cells [37], in cancer patients, up to 40% of cfDNA is tumor-specific (i.e. circulating tumor DNA; ctDNA) and can be detected by tumor-specific alterations, such as somatic mutations, viral sequences or epigenetic markers[29, 307-309]. The amount of released cfDNA has been shown to increase substantially in cancer patients and mirror the anatomical origin of a tumor [2, 47, 310]. Moreover, the half-life of cfDNA in circulation ranges from seconds to 15 minutes which provides real-time information on tumor spatial and temporal heterogeneity [311-314]. This makes cfDNA an ideal biomarker of cancer monitoring longitudinally for treatment response, acquired resistance, minimal residual disease, tumor recurrence, and development of metastasis [34, 315, 316].

Because cfDNA is released mainly as a result of cellular turnover, recent studies have shown a correlation between cell death and cfDNA release [35]. We and others have also

demonstrated that cfDNA in culture systems can be used to monitor drug response [3, 4, 61, 301, 303, 304]. Anti-cancer treatments such as radiation and chemotherapies are cytotoxic to tumor cells by causing a mitotic catastrophe, leading to cell death mainly via apoptosis [317, 318]. Different studies have shown a correlation between cfDNA release following drug treatments that cause apoptosis[316]. Certain chemotherapeutic agents and radiation therapy also cause cellular senescence[318]. As a result, cfDNA levels have been shown to decrease during radiation, which may be a result of cancer cells undergoing necrosis [319]. Taken together, studies suggest that different treatment types can trigger specific patterns of cfDNA release. This release has been correlated to apoptosis [58, 59]. While many studies have shown the value of ctDNA in monitoring treatment response [13], others have found that non-apoptotic fragments cause higher ctDNA fluctuations which may be related to the type of anti-cancer treatment and timing of sample analysis [320, 321]. Therefore, understanding the relationship between the cytotoxic insult and the subsequent type of cfDNA released might guide the optimization of liquid biopsy applications based on the therapeutic strategy preconized as well to elucidate the clinical utility of cfDNA as a potential biomarker for early diagnosis and management of cancer.

In addition to differences in cfDNA levels, recent studies have shown that its fragment length may provide important information on the etiology of cfDNA [74, 75, 79]. Cancer patients have shown more abundant and shorter cfDNA fragments[74, 310]. In particular, while a median fragment size of 146 bp was noted in cfDNA derived from tumors, 168 bp was the median fragment size of cfDNA release from noncancerous cells [322]. cfDNA fragment size has therefore emerged as a criterion informing of cell death-involved mechanisms in tumors [57, 75, 79].

To gain a better understanding of the characteristics of cfDNA during anticancer treatments, we assessed the levels and fragmentation of emitted cfDNA following cell death, cell

cycle arrest, and induction of senescence using *in vitro* cancer models of colorectal, lung, and melanoma cancer cells. We used clinically relevant cytotoxic conditions that mimic current therapeutic strategies for the management of cancer. We isolated and quantified mutant cfDNA from culture media and found a strong correlation between cfDNA release and cytotoxic treatments. Notably, the size of shed cfDNA depended on the cytotoxic effects of the different treatment approaches. These findings have major implications for improving the use of cfDNA as a powerful biomarker in cancer patient care.

Methods

Cell lines culture conditions

Human colorectal (HCT116 and HT29) and lung (A549) cancer cell lines were gifted by Dr. Peter Metrakos and Dr. Jonathan Cools, respectively (McGill University, Canada). Human uveal melanoma (UM) cell line MP41 (CRL-3297) was purchased from ATCC (Manassas, Va, USA). Human metastatic UM cell line OMM2.5 was kindly donated by Dr. Vanessa Morales (University of Tennessee, USA). Colorectal and lung cell lines were cultured in DMEM medium supplemented with 10% fetal bovine serum (FBS) and penicillin-streptomycin antibiotics (all from Corning). UM cell lines were maintained in RPMI-1640 medium supplemented with 10% FBS, penicillin-streptomycin antibiotics, 10 mM HEPES, 2 mM glutaGRO, 1 mM Na-Pyruvate (all from Corning), and 10 ug/ml insulin (Roche). The cells were used for all experiments at early passages ($P<20$).

Cell exposure to cytotoxic treatments

6 x 10^5 cells were seeded in their respective culture media in T25 flasks to reach 80% confluence at the time of exposure to the different treatments. These cells were treated with 2 mM

valproic acid (VA, Sigma), 40 mM roscovitine (RO, Sigma), or 100 and 300 ng/ml APO2L/TRIAL (APO, Sigma) for 48 hours. Control cell cultures were run in parallel in the presence of the respective compound vehicles. VA was dissolved in water whereas RO and APO were dissolved in DMSO.

For gamma irradiation, 1.5 x 10^5 cells were seeded in a 66 mm diameter dish to reach 80% confluence at the time of exposure. Cells were exposed to acute doses of radiation using a MultiRad225 irradiator (Precision X-Ray, Inc., Madison, CT). MP41 and OMM2.5 UM cells received 10 Gy (IR1) and 15 Gy (IR2), while colorectal (HCT116 and HT29) and lung cancer (A549) cells were exposed to 5 Gy (IR1) and 10 Gy (IR2). None-exposed cells were used as a control. Immediately after exposure, these cells were detached using 0.05% trypsin/EDTA (Corning) and re-seeded at 1:3 dilution and kept for 5 days in their respective culture media. After every treatment, the supernatants were collected, spun at 500 *g* for 5 min, and stored at -20ºC for DNA isolation.

Cell cycle analysis

To analyze the percentage of cells in each phase of the cell cycle, we fixed treated and control cells in 70% ethanol overnight. The cells were then washed with phosphate-buffered saline (PBS) and incubated in 50 µg/ml. RNase solution (Thermofisher) for 30 mins at 37ºC. After another wash with PBS, these cells were labeled with 10 µg/ml propidium iodide (PI, Sigma) and protected from light for 30 mins. These cells were analyzed using the BD FACS-CANTO II flow cytometer system at the Immunophenotyping Platform of the Research Institute of the McGill University Health Centre (RI-MUHC). Data analyses were performed using FlowJo V.10 software.

Cell death analyses

Cell death was analyzed using two assays: Annexin V/PI labeling and caspase 3/7 enzymatic activity. For the annexin V/PI labeling, dissociated cells were resuspended in Annexin V binding buffer and stained using the Alexa Fluor 488-AnnexinV/Dead Cell Apoptosis Kit (ThermoFisher Scientific) following the manufacturer's instructions. Cell acquisition was performed in an interval of no more than 1 h using the BD FACS-CANTO II system. Data analyses were performed using FlowJo V10 software to determine the fractions of cells in early or late apoptosis or necrosis. For caspase 3/7 enzymatic activity, upon irradiation, cells were plated in a 96-well plate at $2x10^3$ cells/well and incubated with the 1X medium (RPMI or DMEM enriched with FBS 10%) containing Essen Bioscience Incucyte® Caspase-3/7 activity reagent (Sartorius). The plate was subsequently placed in the Incucyte® Live-Cell analysis system for 5 consecutive days of live-cell imaging. Plates were scanned every 24 hrs for cell confluence and mean fluorescence intensity (MFI) of the caspases substrate. Pictures from the scan interval were analyzed using the IC Incucyte® software.

Senescence analysis

Cell senescence was assessed on irradiated cells using the acidic senescence-associated beta-galactosidase staining assay (Sigma) according to the manufacturer's instructions. Plates were observed under an Evos microscope (Thermofisher), and images were captured at 40X objective magnification.

DNA isolation and quantification

Following the different cell treatments, cfDNA was isolated from 3 ml of culture media, previously centrifuged at 300 *g* for 5 mins, using the QIAamp Circulating Nucleic Acid kit (QIAGEN) according to the manufacturer's instructions. The total DNA collected was kept in 50 ml AVE buffer (Qiagen; RNase-free water supplemented with 0.04% sodium azide) and quantified using the Qubit dsDNA HS assay kit on a Qubit 2.0 fluorometer (Thermofisher Scientific).

Measurement of cfDNA by ddPCR

Digital droplet PCR (ddPCR) was used to assess mutant cfDNA through the presence of specific hotspot mutations in the respective cancer cell lines (**Table 1**). ddPCR was performed as previously reported [2]. Samples were run in triplicates in the following conditions: 10 mins at 95ºC, followed by 50 cycles of 30 secs at 95ºC, 1 min at the corresponding annealing temperatures (**Table 1**), 30 secs at 72ºC and 10 mins at 98ºC in a C100 thermal cycler (Bio-Rad). The primer and probes used were designed by IDT-Technologies and are described in Table 1. Samples with ≤ 2 mutant droplets were considered negative for mutant cfDNA. Once ddPCR was performed, the number of mutant copies was generated by the Quanta Soft v 1.7.4. cfDNA is expressed in copies/µl. Water-PCR grade was used as no template control (NTC) and added to each assay.

Fragment size profiling

0.5 ng/µl of isolated cfDNA was used to determine fragment size distribution using an Agilent 2100 Bioanalyzer according to the manufacturer's instructions. The fragment size of cfDNA was defined as the mode of the main peak.

Data analysis

All experiments were performed in at least three biological replicates with three technical replicates for each cell line. Data were normalized using Excel, and statistical analyses were performed using the GraphPad Prism7.0 software (GraphPad Software) by applying an ANOVA followed by the Dunnett post-hoc test for multiple comparisons with one control group. Spearman correlation analyses were performed to measure the degree of association between total cfDNA and mutant cfDNA. Differences were considered statistically significant at $P < 0.05$.

Table 7 ddPCR primer and probes sequences			
Cell line	Mutation[a]	Primer sequence[b]	Probe[c]
MP41	*GNA11* (Q209L)	F: CCTTTCAGGATGGTGGATGT R: ACATGATGGATGTCACGTTCT	WT: 5HEX/AC+CGC+TGG+CC/3IABkFQ MUT: 56-FAM/AC+CGC+AGG+CC/3IABkFQ
OMM2.5	*GNAQ* (Q209P)	F: CTTGCAGAATGGTCGATGTAG R: GCGCTACTAGAAACATGATAGAG	WT: 5HEX/CCT+T+T+G+GCCC/3IABkFQ MUT: 56-FAM/ACCT+T+G+GGCC/3IABkFQ
A549	*KRAS* (G12S)	F: ATCGTCAAGGCACTCTTGC R: AACCTTATGTGTGACATGTTCTAA	WT: 5HEX/CGCC+A+C+CAGCT/3IABkFQ MUT: 56-FAM/CGC+CA+C+T+AGC/3IABkFQ
HCT116	*KRAS* (G13D)	F: GATTCTGAATTAGCTGTATCGTCAA R: CTGAATATAAACTTGTGGTAGTTGGA	WT: 5HEX/TA+CG+C+C+ACCA/3IABkFQ MUT: 56-FAM/CTA+C+G+T+CAC+CA/3IABkFQ
HT29	*BRAF* (V600E)	F: TTCATGAAGACCTCACAGTAAA R: ATGGGACCCACTCCATC	WT: 5HEX/AGATTT+C+A+CTG+T+AGC/3IABkFQ Mut:/56-FAM/AG+ATTT+C+T+CTGT+A+GC/3IABkFQ

[a] Hotspot mutation analyzed for the respective cell lines.
[b] F; forward primer, R; reverse primer.
[c] WT; wild type, MUT; mutant.

The annealing temperatures for the respective primers were 58°C for *GNA11* A>T (MP41), 60°C for *GNAQ* A>C (OMM2.5), and 56°C for *KRAS* G12S (A549), *KRAS* G13D (HCT116), and *BRAF* V600E (HT29).

Results

Cancer cell emission of mutant cfDNA correlates with cell viability

Tumors have been reported to shed significant amounts of cfDNA[29]. Herein, we used an *in vitro* model to assess the levels of cfDNA in culture media of different cancer cell types: colorectal cancer (HCT116 and HT49), lung cancer (A549), and uveal melanoma (UM) (MP41 and OMM2.5) cell lines. Cells were seeded at different densities (0.5 $x10^6$, $1x10^6$, and $2x10^6$ cells) and cultured for 24 hrs. We then isolated cfDNA from the conditioned media and quantified the levels of total and mutant cfDNA (according to the specific mutations of each cell line, **Table 7**) using the Qubit assay and ddPCR respectively, as we previously optimized[2-4]. We noted that the levels of total (**Figure 3.1A**) and mutant cfDNA (**Figure 3.1B**) increased proportionally to the number of cultured cells, with a positive correlation between the number of cells and the levels of mutant cfDNA ($r = 0.7687$, CI = 0.3485 to 0.9316, $p = 0.0035$). Given the use of mutant DNA to detect cfDNA-tumor specific in liquid biopsy samples[87], we utilized specific point mutations (**Table 7**) to better understand the relationship between the cytotoxic insults and the levels of mutant cfDNA released.

Cell death significantly increases cfDNA emission levels, with the largest contribution from early and late apoptosis

To better understand the relationship between the cytotoxic insults and the levels of mutant cfDNA released, we assessed the kinetics of cfDNA emission following different chemical and physical treatments. Current anticancer therapies consist of strategies to kill (i.e. induce cancer cell death) or block cancer cell growth (i.e by counteracting cell cycle progression and inducing senescence). To mirror the range of agents used in the clinic, we tested the effect of treatments that

induce cell death either by apoptosis or necrosis. We first induced apoptotic cell death through 100 ng/ml and 300 ng/ml of the TNF-related apoptosis-inducing ligand (TRAIL or APO2L; APO)[323],[324]. Following treatment of our cell lines with APO, we observed significant increases in both apoptotic and necrotic cells in a dose-dependent manner, as shown by representative plots of staining for cell death by Annexin V and PI, respectively (**Figure 3.2A**) and the flow cytometric histogram of each cell line treated with APO or vehicle (control) (**Figure 3.2B**). This corresponded to a substantial and dose-dependent increase in mutant cfDNA, engendering the greatest cfDNA release compared to other treatments (**Figure 3.2C**). This increment suggests that apoptosis triggered high cfDNA release.

In addition, we used roscovitine (CY-202 or Seliciclib; RO), a small molecule that inhibits several cyclin-dependent kinases to induce cell cycle arrest and apoptosis[325]. We observed that RO significantly increases the percentages of apoptotic cells; with both early and late apoptosis being activated (**Figure 3.2A and 3.2B**). When we assessed cfDNA release, we found that RO-treated UM cells released more mutant cfDNA compared to colorectal and lung cancer cells (**Figure 3.2D**).

We also evaluated whether mutant cfDNA was associated with necrosis. To induce necrosis, we applied heat treatment, which has been shown to mainly affect cell growth through induction of cell necrosis[326]. When we exposed the cancer cells to heat (i.e. 58ºC), cells undergo exclusively necrosis (**Figure 3.2A and 3.2B**). Heat treatment-induced necrosis caused moderate mutant cfDNA release, with the UM cell line OMM2.5 releasing the highest amounts (**Figure 3.2E**).

Cell cycle inhibition also results in cfDNA release not associated with apoptosis

Inhibitors of the cell cycle have been used as anticancer treatments[327]. To determine whether cell cycle disturbances alter cfDNA emission, we assessed the levels of mutant cfDNA upon 48 hours of treatment with 2 mM valproic acid (VA) which inhibits cell cycle progression[218]. After exposure to VA (2 mM), we analyzed these cells for their progression through the cell cycle phases. As compared to cells maintained in control medium, we found that VA-treated cells accumulate more in the G1 phase, and subsequently progress less to S and G2/M phases (**Figure 3.3A and 3.3B**). In addition, we found that it affects neither the percentage of necrotic cells nor that of apoptotic cells in A549 and MP41. In contrast, we observed an increase in cells positive to annexin in HCT116, HT29, and OMM2.5 cell lines, suggesting some levels of apoptosis (**Figure 3.3C and 3.3D**). When cfDNA release was assessed, we found that the cell cycle progression inhibitor VA also induced a release of mutant cfDNA independent of whether apoptosis was induced, as shown by substantial increases in DNA emission in cells with no apototic signal (**Figure 3.3E**).

Radiation fluctuates mutant cfDNA shedding

Radiotherapy (IR) is a standard treatment for solid cancers[328]. Irradiated cells undergo senescence and cell death[329]. We exposed the cancer cells to acute doses of gamma-radiation. When compared to non-exposed cells 5 days post-irradiation, we observed that radiation affected cell viability by increasing the percentage of both necrotic and apoptotic cells (**Figure 3.4A and 3.4B**). In addition, to further explore cell death post-irradiation, we made a follow-up of radiation-exposed cells for 5 consecutive days post-irradiation. We found that exposed cells displayed a time- and dose-dependent increase in caspases 3 and 7 activities, suggesting that cells are dying by apoptosis (**Figure 3.4C and 3.4D**). Moreover, when we analyzed these cultures for cell

senescence, we found that 5 days post-treatment the irradiation increased the acidic β-galactosidase activity in all cell lines, suggesting induction of cellular senescence (**Figure 3.4E**). Following gamma-irradiation, we detected cfDNA emission corresponding from minimally to moderate amounts of mutant cfDNA, with a kinetic release that varies substantially between the different cancer cells (**Figure 3.4F**). Further analyses are warranted to understand this variability.

Taken together, we report here that APO (apoptotic agent) induced the greatest levels of mutant cfDNA, compared to roscovitine (apoptotic agent), VA (cell cycle interfering agent), irradiation (senescence- and cell death-inducing agent), heat (necrotic agent), and irradiation. We conclude that the type of cytotoxic insults applied to cancer cells increased the levels of mutant cfDNA, with the largest contribution from cells undergoing apoptosis and to a lesser extent from cells arrested at the G1 phase of the cell cycle (**Figure 3.5**). To confirm the effect of all treatments in cfDNA isolated from conditioned media, we also evaluated total DNA (no mutation-specific). We observed that total DNA concentration was influenced by all the treatments (**Supplementary Figure 3.1A and 1B**).

All cytotoxic treatments resulted in larger cfDNA fragment

To assess whether cytotoxic conditions cause changes in DNA processing during cfDNA release, we measured the size of cfDNA isolated from conditioned media following the different treatments. Changes in cfDNA fragment size may be used to monitor responses response[78]. To this purpose, we subjected the recovered cfDNA samples to a bioanalyzer tool analysis. When we first measured cfDNA in control conditions at different time points, we noted a well-defined peak of about 200 bp, corresponding to the expected range of 266 bp resulting from apoptosis[56]. By

contrast, after 5 days in standard culture conditions, the 200 bp peak tends to dissipate, while a 10,000 bp peak emerged (**Figure 3.6A).**

Under cytotoxic treatments, we noticed various patterns of cfDNA fragmentation, with a tendency towards larger fragment lengths following treatments. In cultures treated with APO and roscovitine (apoptotic agents), we noticed the presence of a pattern of cfDNA fragments reminiscent of that derived from apoptotic cells. Specifically, while roscovitine treatment-generated electropherogram showed a 150 bp peak and larger fragments, peaks below 150 bp and above 750 bp were observed in cfDNA isolated upon APO treatment (**Figure 3.6B and 6C)**. In cultures treated with VA (cell cycle interfering agent), the electropherogram displayed mainly a DNA peak at ~5000 bp and a smear centered around 300 bp (**Figure 6D)**. In contrast, in cultures exposed to heat (necrotic agent) and in irradiated cultures (senescence- and cell death-inducing agent) we observed major peaks at 10,000 bp (**Figure 3.6 E-6 G)**, as previously reported. We conclude that cfDNA fragment sizes are associated with the type of cellular response to the cytotoxic insults, and that larger fragment sizes are associated with anti-cancer treatments. These data stipulate the presence of a link between the anticancer treatments and the length of cfDNA released during therapy.

Figures

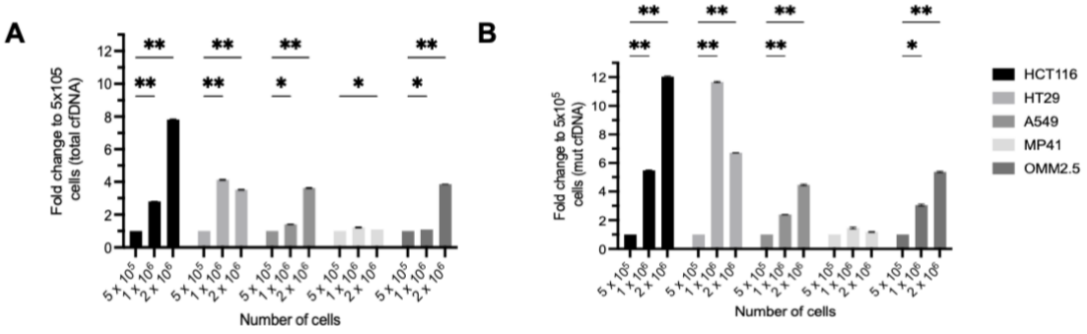

Figure 3. 1 : The levels of cancer cell-released mutant cfDNA correlated with the number of viable cells.

Cancer cells were seeded at different densities ($5x10^5$, $1x10^6$, and $2x10^6$ cells) and cultured for 24 hrs. Conditioned culture media was collected to isolate cfDNA. The levels of both (**A**) total and (**B**) mutant cfDNA were quantified using the Qubit assay and ddPCR (targeting hot spot mutations specific to each cell line), respectively. Graphs represent fold change of mutant cfDNA levels in media from the different cell cultures relative to levels in cultures with $5x10^5$ cells. Data are expressed as mean +/− SD (n = 3 independent experiments. * Indicates $p<0.05$, ** indicates $p<0.01$, whereas *** indicates $p<0.001$ compared against $0.5x10^6$ cells.

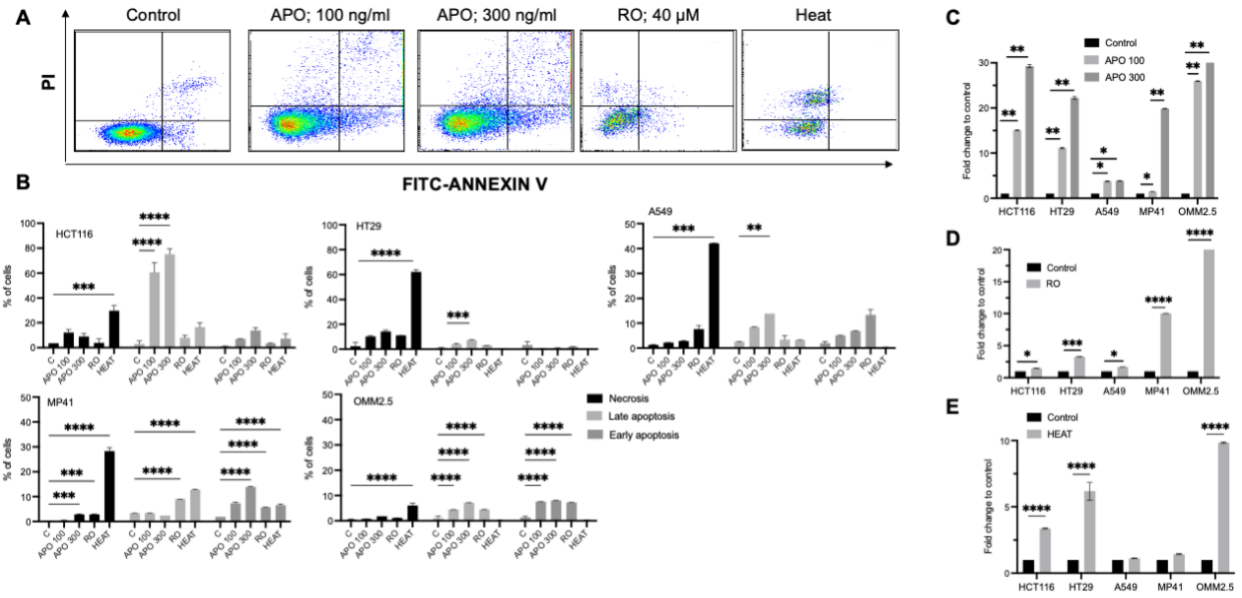

Figure 3. 2:APO2L/TRIAL induced cancer cell apoptosis and a substantially increase in cfDNA level.

Cancer cells were seeded in T25 flasks at $6x10^5$ cells/ml. At 80% Confluence, cells were left untreated (Control) or treated with 100 and 300 ng/ml APO2L (APO) for 48 hrs, 40 µM roscovitine (RO) for 48 hrs, or heat at 58ºC for 30 mins. (**A**) Plots of A549 cells labeled with Annexin V and PI. (**B**) Graphs show the percentage of cells in necrosis (Annexin V negative and PI positive, in black),), late apoptosis (Annexin V positive and PI positive, in light gray), and early apoptosis (Annexin V positive and PI negative, dark gray), and for each cell line. Cancer cells exposed to cytotoxic insults induced differential mutant cfDNA levels release. After treatments, culture media were recovered to isolate the cfDNA. Mutant cfDNA levels were evaluated using ddPCR by targeting specific hotspot mutations in the respective cancer cell lines. Cells were left untreated (Control) or exposed to (**C**) 100 and 300 ng/ml APO2L (APO) for 48 hrs, (**D**) 40 µM roscovitine

(RO) for 48 hrs, (**E**) heat at 58ºC for 30 mins. Scored data are expressed as mean +/− SD (n = 3 independent experiments. * Indicates p<0.05, ** indicates p<0.01, whereas *** indicates p<0.001 compared against control.

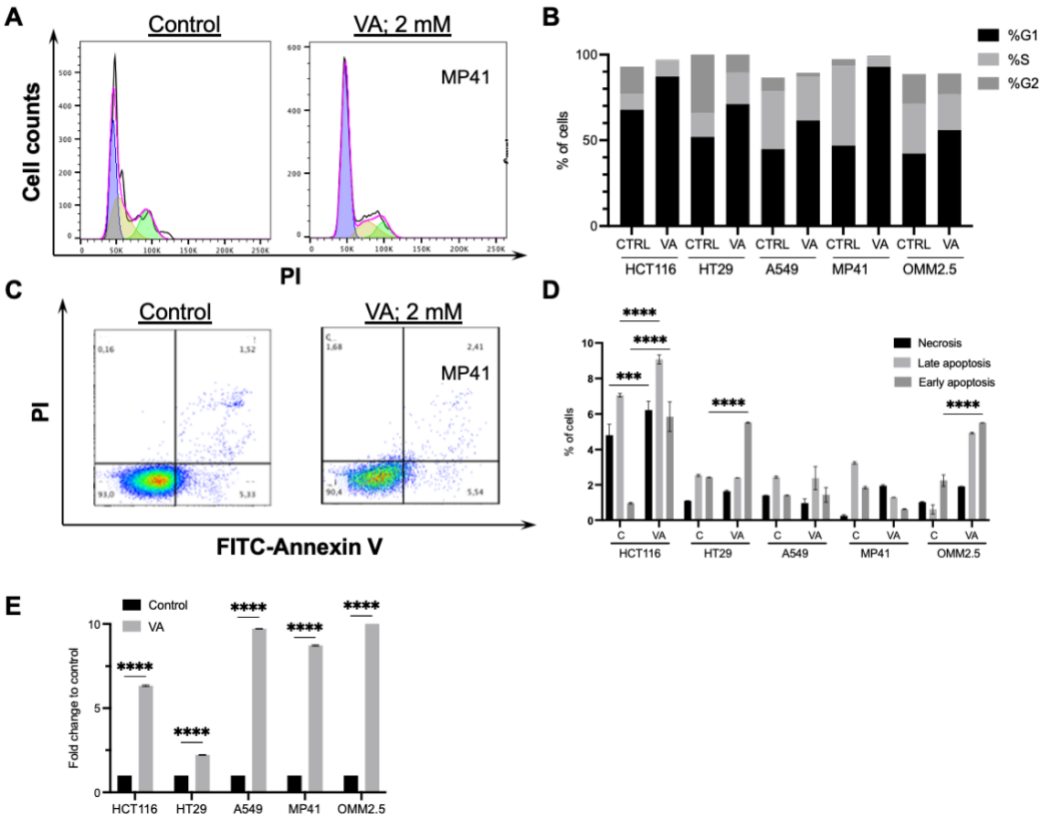

Figure 3. 3: Valproic acid-induced cancer cell accumulation at the G1 phase of cell cycle and is associated with cfDNA release.

Cancer cells were seeded at 6x10^5 cells in T25 flasks. At 80% Confluence, cells were left untreated (Control) or treated with 2 mM valproic acid (VA) for 48 hrs. (**A**) MP41 cells were loaded with PI and analyzed for their progression in the cell cycle. (**B**) Graph shows the percentage of cells in G1 (in black) phase after vehicle (C) and VA treatment. %S (synthesis) in light gray and %G2 in dark gray. Note that cells progress slowly through G1 after VA treatment. (**C**) MP41 Cells were

labeled with Annexin V and loaded with PI to determine the percentage of cells in early apoptosis (Annexin V positive and PI negative), late apoptosis (Annexin V positive and PI positive), and necrosis (Annexin V negative and PI positive). (**D**) Graph shows the percentage (%) of cells in necrosis (black), late apoptosis (light gray), and early apoptosis (dark grey). (**E**) Mutant cfDNA levels were evaluated using ddPCR by targeting specific hotspot mutations in the respective cancer cell lines after 2 mM valproic acid (VA) for 48 hrs. Scored data are expressed as mean +/− SD (n = 3 independent experiments. * Indicates $p<0.05$, ** indicates $p<0.01$, whereas *** indicates $p<0.001$ compared against control.

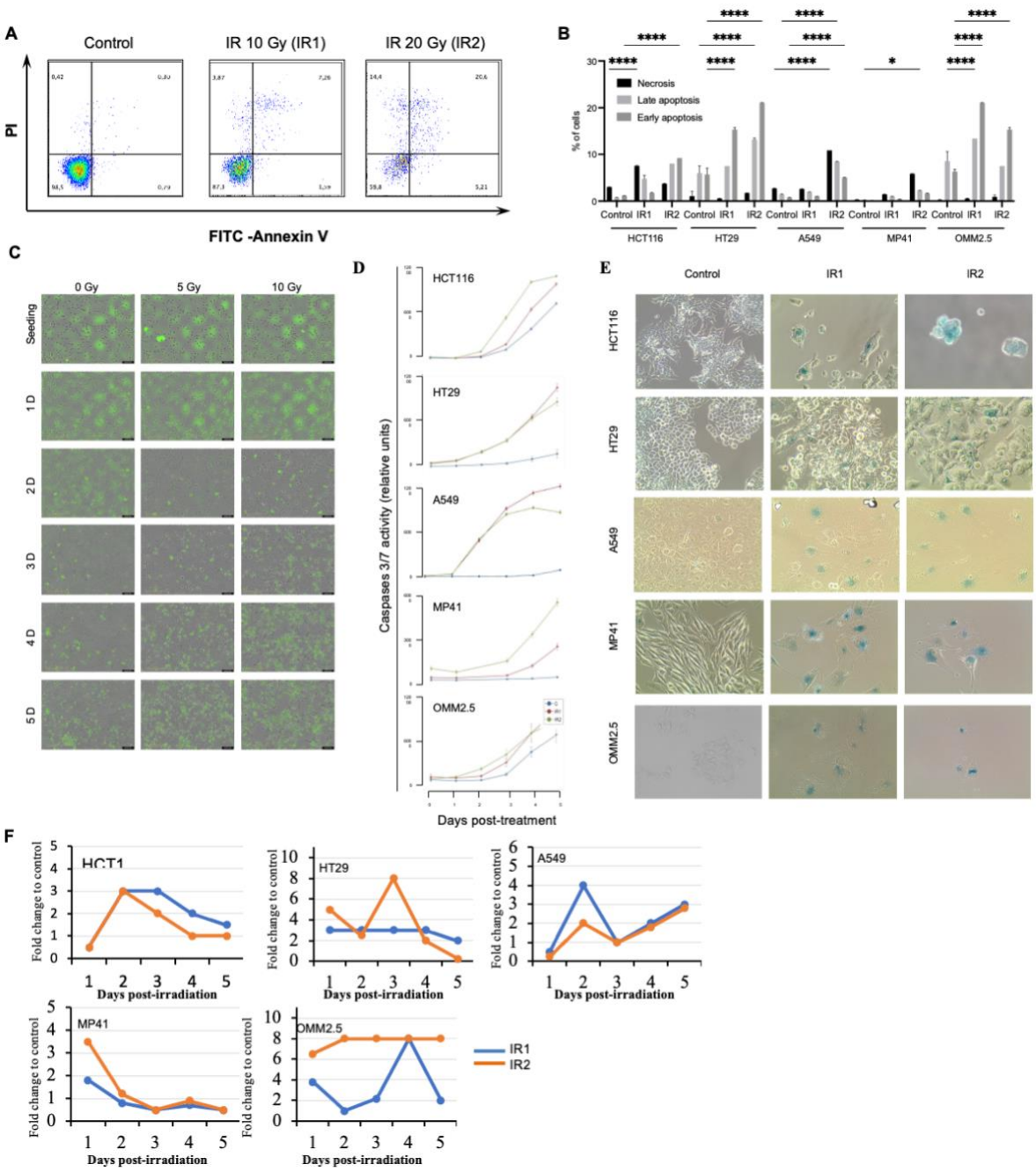

Figure 3. 4: Gamma irradiation decreased induced cell death and senescence on cancer cells.

1.5 x 10^5 cancer cells were seeded in a 66 mm dish to reach 80% confluence at the time of exposure. Cells were exposed or not to acute doses of radiation. MP41 and OMM2.5 UM cells received 10 Gy (IR1) and 15 Gy (IR2) doses, while colorectal and lung cancer cells were exposed to 5 Gy

(IR1) and 10 Gy (IR2) doses. (**A**) Representative plots of MP41 cells labeled with Annexin V and PI 5 days post-irradiation. (**B**) Graph shows the percentage of cells in necrosis (Annexin V negative and PI positive, shown in black), late apoptosis (Annexin V positive and PI positive, shown in light gray), and early apoptosis (Annexin V positive and PI negative, shown in dark gray). (**C**) Representative images of HCT116 cells analyzed for the Caspase-3/7 activity during a 5-day time-course following irradiation. Cell cultures were scanned during the 5 consecutive days at 24 hrs intervals using the Incucyte live imaging system. Representative images are shown. Scale bars: 200 µm. (**D**) Data are presented as mean fluorescence intensity (MFI) of the caspases substrate. Control (no exposure) is shown in blue, IR1 (5 or 10 Gy) in red, and IR 2 (10 or 15 Gy) in green. (**E**) 5 days post-irradiation, cells were assessed for their senescence using the acidic senescence-associated beta-galactosidase activity. (**F**) Culture media were recovered to isolate the cfDNA during the 5 consecutive days of irradiation. Mutant cfDNA levels were evaluated using ddPCR by targeting specific hotspot mutations in the respective cancer cell lines. Cells were left untreated (Control) or exposed to acute doses of radiation. HCT116, HT29, and A549 cells were exposed to 5 Gy (IR1) and 10 Gy (IR2) doses, whereas MP41 and OMM2.5 UM cells received 10 Gy (IR1) and 15 Gy (IR2) doses. Data are expressed as relative levels of mutant cfDNA after the treatments compared to levels in the respective controls set to 1 (mean +/− SD, $n = 3$ independent experiments). * Indicates $p<0.05$, ** indicates $p<0.01$, whereas *** indicates $p<0.001$ compared against control.

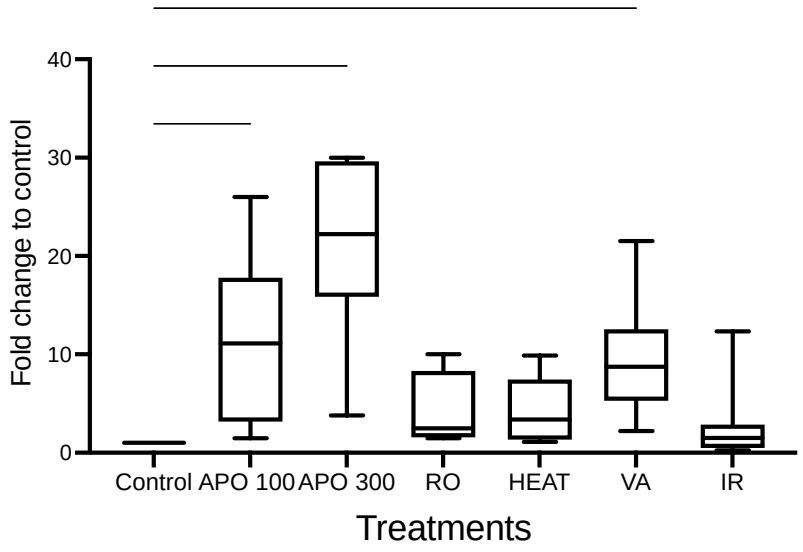

Figure 3. 5: Apoptosis is the main contributor of cfDNA release.

Levels of mutated cfDNA recovered from the different cancer cell line cultures were plotted against the different treatments. Each box in the respective treatments represents the mutant cfDNA amount recovered from the different cancer cell cultures (5 cell lines). Representative images are displayed. Scored data are expressed as mean +/− SD (n = 3 independent experiments. * Indicates $p<0.05$, ** indicates $p<0.01$, whereas *** indicates $p<0.001$ compared against control.

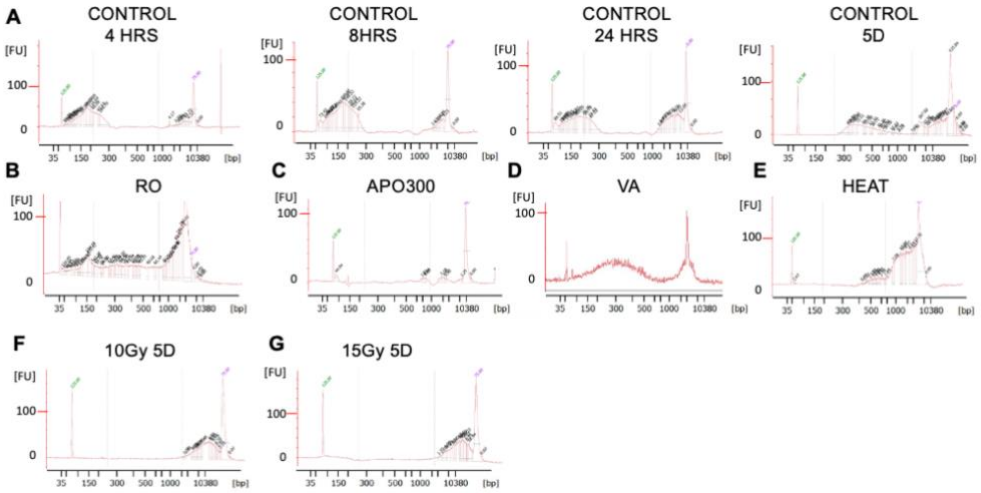

Figure 3. 6: Cancer cells exposure to cytotoxic insults released cfDNA with different sizes.

Culture media were recovered to isolate the cfDNA. Then, using an Agilent 2100 Bioanalyzer, cfDNA samples were analyzed for fragment size distribution from untreated (**A**) conditions or after treatments (**A-G**). Representative capillary electropherograms derived from MP41 are displayed from (**A**) Control and after treatment with (**B**) 40 µM roscovitine (RO) for 48 hrs, (**C**) 300 ng/ml APO2L (APO) for 48 hrs, (**D**) 2 mM valproic acid (VA) for 48 hrs, (**E**) heat at 58ºC for 30 min, and single exposure to (**F**) 10 Gy or (**G**) 15 Gy. The two reference peaks at 35 bp and 10,038 bp are shown in green and magenta, respectively.

Discussion

During cellular turnover, cells release intracytoplasmic and nuclear contents which can be detected in culture media [330]. This process has allowed various *in vitro* models to be used to study cfDNA biology [301, 302, 304, 330] and to assess drug response [3, 4, 301]. Using this model, we previously reported cfDNA release from UM cells into conditioned media [2]. We further demonstrated the presence of dose-dependent cfDNA release during drug treatments, including beta-adrenoceptors-blocker and mifepristone on UM and skin melanoma cells, both potential adjuvant antitumor drugs [3, 4]. In the present study, we used a panel of cancer cells (colorectal cancer, lung cancer, and UM cells) and different cytotoxic agents that mimic anticancer therapeutic agents to study changes in the kinetics and fragmentation of shed cfDNA. We brought evidence that the levels and fragmentation patterns of released cancer cfDNA depend on the cytotoxic treatment. These findings suggest that, depending on the anticancer therapy applied, we could predict the characteristics of the released cfDNA, which may guide the choice of suitable analytical method of these DNA fragments.

Circulating tumor DNA (ctDNA)-based liquid biopsy has emerged as an important tool to detect and monitor cancer[331] that allows for the real-time analysis of tumor cells or their products using bodily fluids[29]. Various studies have reported that ctDNA circulating in the bloodstream reflects tumor burden from primary and metastatic sites and heterogeneity by showing a spectrum of mutations that correlate with tumor size[332]. As a result, ctDNA seems to be a highly specific biomarker for non-invasive monitoring, and its fluctuations may help to guide personalized therapeutic decision-making[265]. Although ctDNA as a biomarker has been widely studied in clinical reports[14], our understanding of its etiology remains limited. Important knowledge gaps remain on how cfDNA release is influenced by anti-cancer treatments, which has

major implications for clinical interpretation of ctDNA levels in patients undergoing treatment. We undertook the present study to address this gap.

Although the biology of cfDNA release is not fully understood, studies have generally concluded that cfDNA is mainly a product of apoptosis[35]. To get more insights on the mechanisms governing cfDNA generation, we applied a battery of cytotoxic conditions to cancer cells that are similar to key effector mechanisms of several anticancer therapeutic drugs, including agents that are inducers of apoptosis, necrosis, anti-proliferative (i.e. cell cycle blocker), and senescence. In summary, we found that the levels and fragment sizes of mutant cfDNA were associated with the mechanism of cytotoxicity. In agreement with our findings, it has been reported that cytostatic treatment (i.e. cell cycle progression interference) alters cfDNA kinetics. More specifically, a cfDNA increase was observed upon the cytostatic treatment. This increase might be associated with the preparation for cell division[301]. Tumor cells that fail a transition from synthesis (S phase) to mitosis (M phases) within the cell cycle might undergo apoptosis and/or necrosis, processes that are known as a source of cfDNA[301].

Radiotherapy is one of the most common cancer treatments and is the standard of care to treat UM lesions[1, 328]. Irradiated cells undergo mitotic catastrophe, a form of cell stress that precedes apoptosis, necrosis, senescence, and autophagy[329]. However, little is known about the effect of irradiation in cfDNA release. A previous study conducted in head and neck squamous cell carcinoma and non-small lung cancer cells reported that cfDNA is modulated by a treatment-induced cell senescence[60]. Other reports identified a correlation between cfDNA levels and clonogenic survival, suggesting that cfDNA accurately quantified cell survival upon irradiation[333]. These observations are in line with our conclusions from the present study. We also noticed that the levels of cfDNA in the different cancer cells following treatments varied

substantially. This variation may be due to the carried specific mutations in the respective cancer cell type. For instance, in irradiated cells, we observed a discrepancy in the amount of cfDNA release between HT29 and HCT116 cancer cells. This discrepancy could be due to the fact that HCT116 cells harbor a wild-type *TP53* whereas HT29 cells have mutated *TP53*. As *TP53* favours radiosensitivity[334], it may also be determinant in the differential release of the cfDNA. However, this comparison was not possible in UM (OMM2.5 and MP41), in which TP53 mutations are uncommon[335], or A549 lung cancer cells that have been reported as wild-type *TP53*[336]. Further studies are therefore required to analyze the effect of specific mutations, e.g., *TP53*, in cfDNA release.

In addition to cfDNA levels, the length of cfDNA fragments may also have prognostic value[75, 79]. In both physiological and pathological conditions, a fragment length of ~266 bp has been suggested as a result of apoptosis, reflecting the length of DNA wrapped around a nucleosome, 147 bp, plus a stretch of DNA, 20 bp[56]. In contrast, necrosis has been associated with high-molecular-weight DNA. Therefore large fragment sizes of about >10,000 bp have been found[59]. However, the pattern of cfDNA fragmentation in cancer patients remains poorly characterized. While some studies have shown that cfDNA isolated from individuals with cancer is longer compared to those obtained from healthy subjects, others have reported an opposite observation[77-79, 306]. More studies are warranted and are in progress by our group to clarify this matter. Aside from this progress, our data bring evidence that the sizes of releases cfDNA depend on the anticancer treatments.

On the one hand, we show that anticancer treatments determined the levels and sizes of cancer cell-derived cfDNA. On the other hand, encapsulated DNA in extracellular vesicles such as exosomes is another major source of cfDNA, but which was not examined in the present study.

Studies targeting this specific reservoir of cfDNA are needed to complete the scheme as they will provide further information about the mechanism of cfDNA release from cancer cells[337]. In addition, the next logical step is to apply the analytical strategies we used in this *in vitro* study to our established *in vivo* model[2] by analyzing mutant cfDNA in the circulation as a preclinical step.

Our observations will help to better understand the release pattern of cfDNA under anticancer therapeutic strategies. This approach will be beneficial in leading to a better understanding of cfDNA role in cancer development and how best to utilize this indicator clinically as a biomarker of treatment response and tumor progression.

Conclusion

cfDNA is a powerful biomarker of tumor burden and treatment response. A better understanding of cfDNA kinetics is needed for the clinical applicability of liquid biopsy-based cfDNA monitoring. Our data gave evidence that cancer cells under cytotoxic conditions displayed differential cfDNA release and fragment size patterns. These data may help in tailoring targeted strategies for cfDNA analyses depending on the anticancer therapeutic strategy recognized.

Acknowledgments

This work was supported by a Canadian Cancer Society Emerging Scholar Award to JVB (#707153) and CONACyT funding to PB (#739468). The funders had no role in study design, data collection, and analysis, decision to publish, or preparation of the manuscript.

We would like to acknowledge the technical expertise and help with flow cytometry analyses from the Immunophenotyping Platform of the RI-MUHC.

Author contributions

P.B. conceived and conducted experiments, analyzed and interpreted data, and wrote manuscript; M.A. analyzed and interpreted data, supported graph generation and wrote manuscript; T.T. supported data analysis; J.V.B. designed the experiments, analyzed and interpreted data, wrote manuscript, supervised staff, and provided funding for the project. All authors have read and agreed to the published version of the manuscript.

Data Availability

All data generated or analysed during this study are included in this published article (and its Supplementary Information files).

Conflicts of Interest

The authors declare that they have no competing interests.

Preamble to Chapter 4

The previous chapter showed that cfDNA release is altered under cytotoxic conditions. In particular, using an *in vitro* system which included colorectal, lung, and melanoma cells, we observed an increase in cfDNA release in apoptotic conditions compared to untreated conditions. In addition, we observed changes in cfDNA fragment size according to release mechanism. Understanding the mechanisms underlying cfDNA release and how these are modified under different cytotoxic conditions will help to better understand cfDNA values under different treatments in clinical settings.

Given that cfDNA has a short life in the bloodstream, from 15 minutes to 2 hours, various reports have suggested cfDNA as a biomarker to monitor treatment response in real-time[13], including to monitor tumor evolution during treatment and to identify molecular relapse [14]. To further evaluate cfDNA utility, we used UM as a model to assess cfDNA release under two potential anticancer drugs that are being investigated in our laboratory. cfDNA analysis in preclinical studies allows us to better understand cfDNA release and how it is associated with cell proliferation, cycle, and death. In the next chapter, we assessed cfDNA release by UM cells treated with two drugs, propranolol and mifepristone, which have shown antiproliferation and cytotoxic effects and are being investigated as adjuvant therapies in UM. This chapter demonstrates the potential of cfDNA emission in culture systems as a biomarker of drug response in pre-clinical testing.

Data included in this chapter were taken from two manuscripts:

1. **Manuscript 4:** Alvarez, P. B. *et al.* Anticancer effects of mifepristone on human uveal melanoma cells. *Cancer Cell International* 21, 607, doi:10.1186/s12935-021-02306-y (2021).

2. **Manuscript 5:** Bustamante *et* al. Beta-blockers exert potent anti-tumor effects in cutaneous and uveal melanoma. *Cancer Med* 8, 7265-7277, doi:10.1002/cam4.2594 (2019).

Chapter 4: ctDNA as a biomarker of treatment response for potential new therapies in UM

Abstract

Our laboratory has previously shown that mifepristone (MF) and propranolol have a potent growth inhibitor role in uveal melanoma (UM). In addition, cell-free (cf) DNA suggests being a clinically relevant biomarker of tumor development and progression, including UM. However, a better understanding of cfDNA in UM is still needed to be used in the clinic. Here, we investigated the role of cfDNA as an indicator of treatment response under MF and propranolol.

Upon 72 h-MF or 24 hr propranolol treatment in human 92.1, MP41, MP46, MEL270, and OMM2.5 UM and cutaneous melanoma (WM115 and WM266.4), cytotoxicity and cell death were corroborated by CCK8 and annexin V- FITC, respectively. cfDNA was then extracted from the supernatant from 3mL supernatant. By assessing hot spot mutations (i.e. GNAQ/11, BRAF) using digital droplet (dd)PCR, we observed that cfDNA release correlated with drug treatment concentration in a dose-dependent manner.

Our work is the first study focused on understanding the pattern of release of cfDNA using in vitro model after MF and propranolol. Further studies on *in vivo* models will elucidate the role of cfDNA in UM. Understanding cfDNA kinetics can help to understand its role in UM development and how best to utilize this marker clinically.

Background

cfDNA is released into the bloodstream mainly as a result of apoptotic or necrotic death, and cellular secretions [34]. The half-life of cfDNA in blood ranges from 15 minutes to 2 hours before its clearance [338]. The mutant-specific fraction of cfDNA, ctDNA, may be a real-time marker that mirrors tumor biology and burden in cancer patients [13]. Anti-cancer treatments induce cancer cell death through several mechanisms, leading to cellular turnover, apoptosis and/or necrosis. Such treatments can therefore impact the kinetics of ctDNA levels assessed through a liquid biopsy. Indeed, studies have reported that cfDNA informs on treatment response [120, 132, 136, 339]. To develop new sustainable and effective adjuvant therapeutic options, there is a crucial need to better understand the role of cfDNA and use it as a means to understand treatment response.

Ocular melanoma is the most common primary intraocular malignancy in adults and the second most common type of melanoma. It largely arises from melanocytes of the uveal tract (uveal melanoma, UM) [146]. Local control of UM is often by local brachytherapy or enucleation[340]. Although these approaches are effective, approximately 50% of patients will develop local radiation metastasis, primarily to the liver[268]. Patients with metastatic UM have an estimated survival of 6 months [341, 342]. There is a crucial need to better understand the mechanisms involved in tumor dissemination and develop new sustainable and effective adjuvant therapeutic options.

Unfortunately, the discovery and development of new therapeutics are costly and lengthy, with high failure-to-market rates [343]. In contrast, drug repurposing studies are a cost-effective means to find new applications to approved drugs. Some of the advantages of drug repurposing are well-described safety profiles, reduced time frame for drug development, and less investment [344].

To address the limited treatment options to mitigate the progression of UM, our group is investigating the potential efficacy of two approved drugs in UM: propranolol and mifepristone (MF). MF is an antiglucocorticoid agent originally synthesized in the 1980s; yet due to its unexpected potent antiprogesterone activity, it was rapidly repurposed to the field of reproductive medicine for early termination of pregnancy, emergency contraception, and menstrual cycle regulation [345-348]. MF was further recognized for its ability to inhibit cell growth in endometriosis, uterine fibroids, and benign cases of meningioma [349]. MF has also shown a promising anti-cancer therapeutic agent in several cancer cells, for instance, cervical, breast, endometrial, ovarian, gastric, lung, brain, and prostate, regardless of progesterone, androgen, and estrogen receptor expression [347, 348]. Particularly, this drug has shown to be a potent cell cycle and DNA synthesis inhibitor [350]. We have demonstrated a potent growth inhibitory and lethal effects of MF on primary and metastatic UM cell lines in a concentration-dependent manner. These effects seem to be independent of cognate PR as no mRNA expression was detected for this receptor in any of the UM cell lines studied [4].

Another potential anticancer drug for UM is propranolol: a beta-adrenoceptor (β-AR) blocker. β-AR are membrane receptors activated by catecholamines, such as epinephrine and norepinephrine. These stress-related hormones are increased in patients with cancer and their contribution to tumor growth and disease progression has been established including in melanoma [351]. Once activated by catecholamines, β-AR stimulate several intracellular signal transduction pathways, such as the nitric oxide synthase, related to melanoma development and progression [352]. Propranolol is a non-selective β1 and β2-AR blocker that has been in use since 1964 to treat coronary insufficiency [353]. In addition to its beneficial effects on the cardiovascular system, propranolol has also been successfully used for other purposes, such as glaucoma[354] and portal

hypertension [355]. Due to its anti-proliferative properties, propranolol has become the first therapeutic choice for infantile hemangiomas [356], and has been designated an orphan drug for the treatment of glioma and angiosarcoma [357]. We have previously demonstrated that propranolol induce an anti-proliferation and pro-apoptotic effects as well as reduced migration in several UM and cutaneous melanoma (CM) cell lines. We also report the first analysis of the expression of β1 and β2-AR in tumors from UM patients and in human UM cell lines. Overall, MF and propranolol are well-established drugs with a good safety profile and few contraindications [346, 358]. In our laboratory, we previously showed that both drugs have an anticancer effect in UM [3, 4].

Here, we aimed to investigate whether cfDNA may be an indicator of treatment response under these drugs. To do that, we quantified cfDNA levels released from human UM cells with and without drug treatments in our established cell culture models. Our data provide compelling support for the use of cfDNA to assess drug efficacy in human UM cancer cells.

Methods

Cell culture

Primary human UM cell line MEL270 and metastasis human UM cell line OMM2.5, stem from the same patient and were kindly gifted by Dr. Vanessa Morales (University of Tennessee). Primary UM cells 92.1 were kindly gifted from Dr. Martine Jager [285]. MP41 and MP46 UM cell lines were acquired from American Type Culture Collection (ATCC, Manassas, VA, USA). WM115 and WM266.4 cutaneous melanoma (CM) cell lines were derived from primary and metastatic CM, respectively, from the same patient (ATCC). All cultures were maintained in RPMI + Glutamax (Gibco, ThermoFisher, USA), 10U/ml penicillin and 10 mg/ml streptomycin (Gibco)

containing 10% of Fetal Bovine Serum (FBS, Gibco). Cultures were incubated at 37ºC and supplemented with 5% CO_2 in a humidified incubator. Cells were quantified using a TC20 Automated cell counter (Bio-Rad, Irvine, CA, USA). Cells were authenticated before use by Short Tandem Repeat (University of Arizona Genetic Core).

Drug Treatments

Propranolol: Propranolol hydrochloride (Cat P0884, Sigma-Aldrich, St Louis, MO, USA) was dissolved in dimethyl sulfoxide (DMSO, Tocris, Oakville, ON, Canada) in a stock solution of 50mM. The solution was diluted freshly prior to each experiment in serum free (SF) RPMI media to different concentrations as indicated in each essay.

Mifepristone: MF (Corcept Therapeutics, Menlo Park, CA, USA) was dissolved in DMSO to generate a 40 mM stock solution that was stored at -20 ºC. Prior to each experiment, the drug was thawed and freshly prepared in media to reach a final concentration of 5, 10, 20, or 40 μM. The final concentration of DMSO (Corning) in the media was 0.1% and served as vehicle control in the absence of MF.

Cell viability assay

1.5×10^4 cells per well were seeded in a 96-well plate (Corning) 24 hours prior to treatment. Cells were kept under 5, 10, 20, or 40 μM MF treatment for 72 hours, or 0 to 200 μmol/L propranolol during 24 hours. Then, 10 μl of cell counting kit 8 solution (CCK8, Dojindo Molecular Technologies, Kumamoto, Japan) was added. After 1 hour of incubation at 37 ºC and 5% CO_2, absorbance was read at 450 nm using an Infinite M200 Pro plate reader (Tecan Trading AG). Cells with no treatment were used as a negative control. Media and CCK8 solution in the absence of cells were used as a blank control. Percentage of metabolic activity was calculated according to the following equation: sample - blank / negative control - blank * 100.

Cell-free DNA detection

cfDNA was detected using a known mutation in the cell lines. First, 3 x 10^5 cells were seeded per well in a 6-well plate. Following 72 hours of MF treatment at concentrations of 5, 10, 20, or 40 μM, 3 ml of culture supernatant was collected and spun at 300 *g* for 5 min. cfDNA was isolated using the QIAamp Circulating Nucleic Acid kit (QIAGEN, Hilden, Germany) following the urine protocol. cfDNA was kept in AVE buffer (RNase-free water with 0.04 % sodium azide; QIAGEN), and quantified by a fluorometric method using a Qubit 4 (Thermo Fisher). Droplet digital PCR (ddPCR) (Bio-Rad Laboratories) was performed to measure the number of copies of cfDNA using wild type sequences and hotspot mutations GNAQ (Q209L and Q209P) and GNA11 (Q209L) by following a previously reported protocol [2]. No template control was added in each assay. Individual runs were performed in triplicates.

Cell death assay

Early and late apoptosis, and necrosis were evaluated after 24-hour propranolol treatment (0-200 μmol/L) or 72-hour mifepristone treatment (0-40 μM). Cells were double labelling annexin V-fluorescein isothiocyanate (FITC) and propidium iodide (PI) using the Dead Cell Apoptosis Kit (Thermo Fisher Scientific, Waltham, MA, USA) following the manufacturer's instructions. Then, samples were analyzed using BD FACS Canto II Cell Analyzer (BD, Evembodegem, Belgium). Cells staining with Annexin V-FITC without PI were considered early apoptotic cells, cells with double staining were considered late apoptotic cells, whereas cells that incorporated only PI were considered necrotic cells.

Data analysis

All experiments were done in at least three biological replicates with at least four technical replicates for each cell line. Statistical analysis was performed using GraphPad Prism 5 software

(La Jolla, CA, USA). Analysis of variance (ANOVA) with a post-hoc test was performed to evaluate the number of copies of cfDNA. $P<0.05$ was considered statistically significant.

Results

Potential anticancer drugs induce the release of cell-free DNA into the culture media

We have previously shown the ability to utilize driver mutations in UM (*GNAQ* and *GNA11* c626A>T and A>C) to detect and monitor ctDNA in UM cell lines (Chapter 2). In Chapter 3, we demonstrated that cfDNA release is associated with cellular stress and cytotoxicity. Here, we evaluated whether cfDNA was an indicator of treatment response on cells treated with two anticancer drugs: propranolol or mifepristone.

To assess whether increased cell death due to either drug would result in increased cfDNA secretion into the cell culture media supernatant, we quantified cfDNA release at various concentrations of MF or propranolol using ddPCR for wildtype and mutant *GNAQ* (MP46, 92.1, MEL270, OMM2.5) and *GNA11* (MP41) in UM cells and *BRAF* (V600D) in CM cells.

The number of wild-type copies and mutant detected upon treatment of each UM cell line with increasing concentrations of MF is depicted in **Figure 4. 1 A-B**. After 72 hours of MF treatment, we detected a concentration-dependent increase in both wild-type and mutant cfDNA. A highly significant increase in cfDNA can be seen at the lethal concentration of 40 µM MF. Similarly, the release of cfDNA increased in a dose-dependent manner after 24 hours of propranolol treatment in UM (**Figure 4.1 C**) and CM (**Figure 4. 1D**) cells.

We evaluated the cytotoxicity of the drugs by CCK8, a colorimetric assay in which reduction of water-soluble tetrazolium salt (WST-8) produces orange formazan and informs about

metabolic activity. We observed that cell viability decreased with MF (**Figure 4. 2 A**) and propranolol (**Figure 4.2 B-C)** treatment.

To further assess the cytotoxic effect of treatments on the cancer cell lines, we sought to determine whether the cells were undergoing cell death (apoptosis and necrosis) by flow cytometry analysis. Cells were doubled labeling with annexin V- FITC (apoptosis) and PI (necrosis) after 72-hour MF or 24 hour-propranolol. **Figure 4.3 A** depicts the flow cytometric histograms of each one of the UM cell lines treated with vehicle or MF. We observed early (**Figure 4.3 B**) and late (**Figure 4.3 C**) apoptosis, as well as necrosis (**Figure 4.3 D)** under MF. We observed that most of the cells with MF were under early or late apoptosis. Only two cell lines, 92.1 and MEL270, displayed some degree of necrosis as denoted by the cells binding PI. Similarly, we evaluated apoptosis and necrosis in cells treated with propranolol (**Figure 4.4 A-D**). Similarly, cells under propranolol underwent mainly early and late apoptosis, except OMM2.5 which showed PI-positive staining and no Annexin V-FITC staining, suggesting that necrosis was the dominant cytotoxic mechanism.

Figures

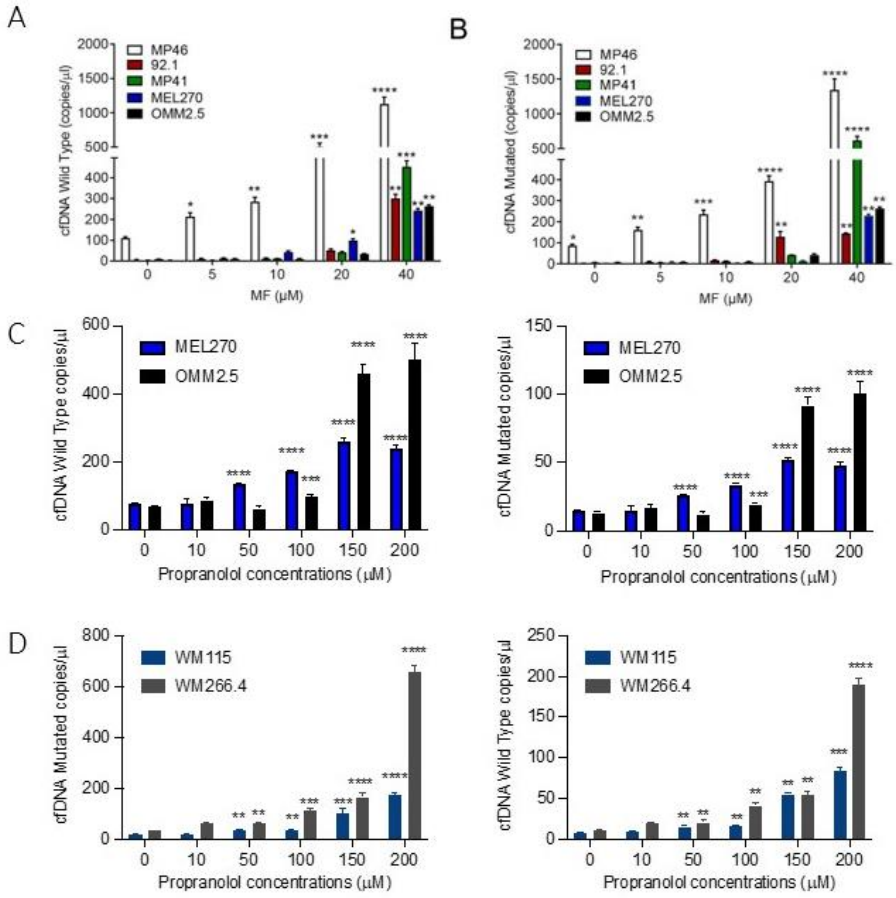

Figure 4. 1: MF treatment induces the release of cfDNA into the media supernatant.

Graphs show the number of wild type (A) and mutant (B) copies of cfDNA per ml of cell-free media obtained 72 hours after incubation with vehicle, 5, 10, 20, or 40 µM MF. Likewise, cfDNA in the supernatant was assessed following 24 h treatment with propranolol in (C) UM (Mel 270 and OMM2.5) and (D) cutaneous melanoma (WM266.4 and WM115) cell lines. *P < .05 vs control.

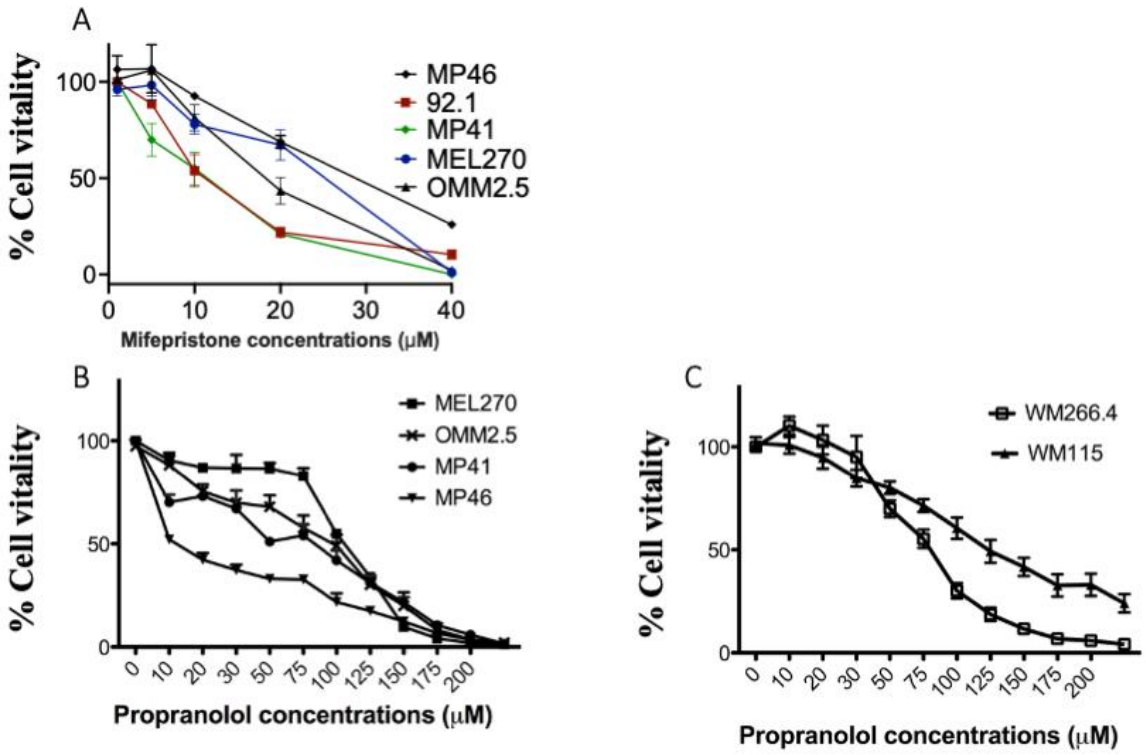

Figure 4. 2: Cell vitality decreased after drug treatment.

Graphs show cell vitality, metabolic activity of alive cells, after **(A)** MF (0, 5, 10, 20, or 40 mM) for 72 hours, and **(B)** UM and **(C)** cutaneous melanoma with propranolol (0, 12.5, 25, 50, 100, and 200 μmol) for 24 hours.

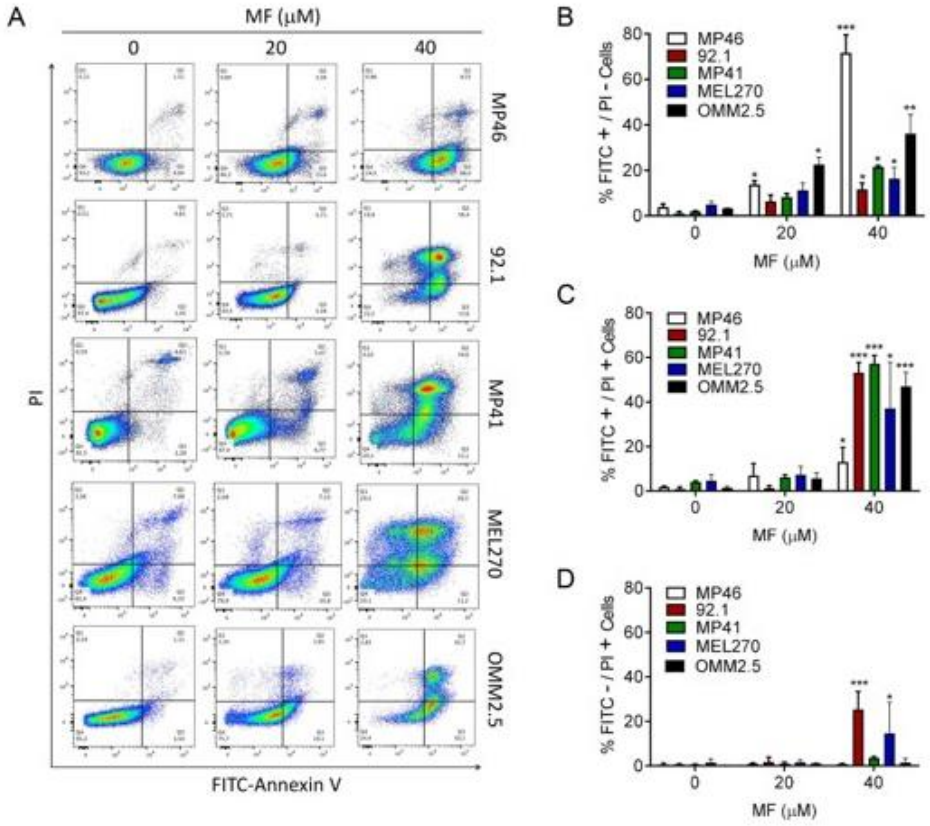

Figure 4.3: Mifepristone induces cell death.

(**A**) Representative histograms depicting the distribution of UM cells exposed to vehicle, 20, or 40 μM MF, and stained with Annexin V-FITC and/or PI after 72 hours of incubation. (**B**) The bar graphs depict the percent of UM cells undergoing early apoptosis as marked by the labeling with only Annexin V-FITC. (**C**) Results show the percent of UM cells undergoing late apoptosis represented by cells double labeled with Annexin V-FITC and PI. (**D**) The percent of cells likely undergoing necrosis is shown as PI only stained cells. Data were analyzed using two-way ANOVA followed by Dunnett's multiple comparison test. * Indicates $p<0.05$, ** indicates $p<0.01$, whereas *** indicates $p<0.001$ compared against vehicle-treated controls.

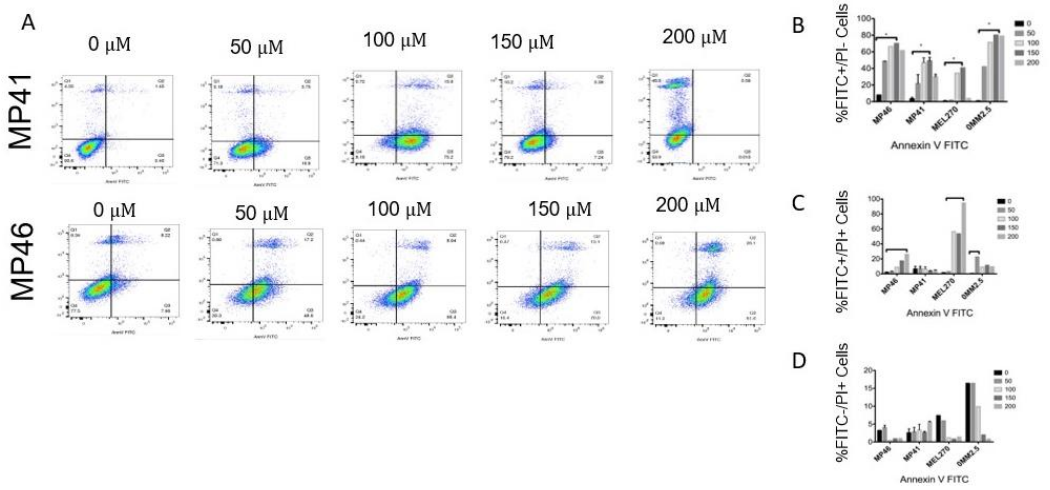

Figure 4. 4: Propranolol induces cell death.

(A) Representative flow cytometry analysis of UM with propranolol (0-200 μmol/L) using annexin V FITC (C). Bar graphs showed (B) early apoptosis, (C) late apoptosis, and (D) necrosis. Error bars represent ± 1 SD. *P < .05 vs control (0 μmol/L).

Discussion

The release of highly fragmented cell-free (cf)DNA is amplified during cellular turnover and death and can be detected in biofluids, such as the blood. In cancer, tumor-specific cfDNA, ctDNA, can be detected in a liquid biopsy. ctDNA is a promising cancer biomarker [29]. It can inform us of the current state of a tumor [13]. It also allows earlier detection, helps classify a lesion, informs on the mutational burden, and provides real-time disease monitoring in response to a treatment [9, 12, 13]. However, the mechanisms underlying cfDNA release from cancer cells, especially as it relates to cytotoxicity during anti-cancer treatment, remain largely unknown. A better understanding of cfDNA kinetics release on *in vitro* models may help to clarify the interpretation of ctDNA in clinical settings. This study aims to explore cfDNA release from tumor cells and determine its role as a biomarker of treatment response to two potential anticancer drugs.

We previously optimized a methodology to detect the dominant driver mutations in UM, using wild type and mutant *GNAQ* and *GNA11* (c626A>T and A>C) in cfDNA [2] (Chapter 2). Here we applied these methods to detect *GNAQ/11* cfDNA released by a panel of melanoma cancer cells in the presence or absence of two potential anticancer drugs: MF and propranolol. Both of these drugs have been investigated in our laboratory as potential adjuvant treatments for UM. Our findings showed MF has a growth inhibitory and lethal effects of MF on primary and metastatic UM cell lines in a dose-dependent manner [4]. We also observed a decrease in cell proliferation and migration, as well as an increase of cell death in cells treated with propranolol[3].

Consistent with the cytotoxicity of both drugs, the release of wild type and mutant cfDNA increased in a concentration-dependent manner. An increase in ctDNA could show cytotoxicity [333] or activating on cellular secretion [301, 303], whereas a decrease can be indicative of adaptive mechanisms resulting in resistant populations[14]. Conversely, the large increase in

cfDNA observed at the highest doses of MF and propranolol are most likely a consequence of widespread cell death only. This is corroborated by annexin V FITC staining positive, as cancer cells were predominately under early and late apoptosis upon drug treatment. Overall, the dose-dependent increase in ctDNA detection following MF or propranolol suggests that such an assay could be used through a liquid biopsy as a non-invasive monitoring tool for treatment response in patients.

Conclusions

cfDNA analysis could be an efficient and non-invasive tool to evaluate new treatment options for patients with UM. Our results demonstrate cfDNA levels were associated in a dose-dependent manner under MF or propranolol treatment, indicating that a significant increase in DNA release occurs when either drug is used at lethal concentrations. This lethal effect occurred in association with increased annexin V-FITC/ PI double-labelled cells. Collectively our data suggest that cfDNA may be effective biomarker in anticancer therapy, and further studies are warranted to understand its release.

Chapter 5: General discussion

5.1 Summary

Unlike a "one-size-fits-all" approach, precision oncology focuses on therapeutics according to specific molecular and cellular features of an individual patient's tumor. This strategy can guide treatment decisions and inform relapses [13, 316]. To treat patients more effectively in a personalized way, precision oncology relies on real-time molecular profiling of tumors, which requires tissue. While tissue biopsies are important for diagnosis and profiling, they have limitations, such as low tumor cell yield and quality [8]. Moreover, tissue biopsies taken at a single time point provide a static view of the tumor, and may not provide information about intratumorally heterogeneity in time or space [9]. For example, by analyzing different sites of core biopsy and regions harvested from nephrectomy and metastasectomy from metastatic renal cell carcinoma samples, a study showed that a single tumor could present genomic signatures for good as well as poor prognosis in different regions of the same tumor [359]. Sampling through one biopsy can therefore miss information about the disease, which may impact the efficacy of treatment. Multiple serial biopsies at different time points can help to better capture representative samples; however, they require significant resources, may be invasive, and confer risks [360, 361]. In addition, a tissue biopsy may cause dissemination of cancer cells [362]. Although under debate, some reports have suggested that the mechanical force of a needle biopsy may risk dislodging tumor cells into the bloodstream or tissue fluid, which could contribute to tumor dissemination [362].

A liquid biopsy-based biomarker is an alternative and complementary method to tissue biopsy [13]. Liquid biopsy provides a novel means to sample tumor-derived material repeatedly in real-time and in a non- or minimally invasive manner [29]. Nevertheless, further understanding

of liquid biopsy-based analytes is needed to fully realize the potential of liquid biopsy. In this thesis, we sought to establish a first-ever liquid biopsy-based assay for UM, the most common intraocular tumor in adults. We then aimed to understand the mechanisms underlying ctDNA release, its etiology and kinetics in response to treatment. The results of this thesis provide compelling evidence of the clinical utility of such an approach and bring us closer to the real-time monitoring of cancer patients through liquid biopsy-based ctDNA testing.

In Chapter 2, we hypothesized that ctDNA can be detected using UM early mutations and that fluctuations in ctDNA levels are an indicator of tumor formation and burden. By using a consistent methodology, we assessed and quantified the presence ctDNA in human UM cell cultures *in vitro*, an *in vivo* animal model of human UM, and in a prospective clinical study. More specifically, we used ddPCR to quantify wildtype (WT) and mutant (MUT) fragmented DNA from the supernatant of cultures of human UM cell lines. Once our assay was validated in a culture system, we conducted an animal model to test the correlation between ctDNA levels and tumor formation and progression. No detectable ctDNA levels were found at the time of UM cell inoculation. In contrast, ctDNA levels in rabbit plasma were detected as early as four weeks post-inoculation (preceding clinical detection of the tumors). Moreover, aqueous humor (AH) was evaluated as a source of ctDNA. While no detectable levels of ctDNA were found at the time of cell inoculation, ctDNA from AH was detected once tumors developed. Importantly, ctDNA levels derived from rabbit plasma and AH correlated with tumor formation and progression. To detect ctDNA levels in patient blood, we conducted a clinical study to assess ctDNA isolated from patient blood of primary UM and nevus patients, and healthy individuals, using then same methodology of detecting UM driver mutations by ddPCR. ctDNA was positive in all 14 (100%) UM patients (13 through *GNAQ/11* mutation and 1 through *PLCB4* mutation). In the choroidal nevus cohort,

ctDNA using early UM initiating mutations was detected in 8 of 18 patients, and the levels correlated with the presence of risk factors for malignant transformation into a choroidal melanoma. No ctDNA levels were found in healthy participants (N=15).

Chapter 3 aimed to explore ctDNA kinetics under cell death, cell cycle arrest, and senescence by using an *in vitro* cancer model in order to better understand ctDNA release and its correlation with tumor biology. We analyzed the effect of ctDNA on several cancer cells with cytotoxic conditions by drugs: TRIAL/APO2L, Roscovitine, and valproic acid (VA), as well as environmental stress by heat and irradiation. We observed ctDNA was increased during cytotoxic conditions in a dose-dependent manner. Apoptosis and cell cycle disturbances through anti-cancer drug treatment caused significant cfDNA release compared to untreated cells. The release of cfDNA was also induced following irradiation. In addition, electropherogram images showed that cytotoxic conditions alter fragment size distribution.

Chapter 4 explored the potential of using ctDNA as a biomarker to evaluate the response to anticancer treatments. UM human cell lines were treated with mifepristone and propranolol, two drugs under investigation for adjuvant treatment in UM. Once the cytotoxic effect was established [3, 4], we quantified mutant fragmented DNA released into the supernatant by ddPCR. We found a dose-dependent relationship between cfDNA release from UM cells and these treatments. Evaluating ctDNA in pre-clinical studies might help to better understand its fluctuations in clinical studies.

5.2 Discussion

Cancer progression encompasses dynamic molecular changes that result in cell proliferation and growth, death dysfunction, and replicative immortality [363]. These changes can contribute to metastasis, the most serious consequence of cancer. Tracking these molecular changes in real-time can provide relevant information to treat tumors, with the ultimate goal to prevent the process of metastasis. The current methodologies to monitor tumor progression include clinical examinations and imaging, which detect large changes, such as new tumors, substantial tumor growth or shrinkage. These methodologies cannot detect molecular changes, the early stages of dissemination or micrometastatic disease. To overcome this limitation, liquid biopsies have emerged as a non- or minimally invasive approach to study cancer cell progression in real-time.

5.2.1 What is the origin of cfDNA?

cfDNA may stem from a combination of cell death, predominantly apoptosis and necrosis [34, 35], but also it might be derived from NETosis, pyroptosis, phagocytosis, autophagy or mitotic catastrophe [34, 35]. Cellular secretions, such as extracellular vesicles and extracellular particles can also be a source of ctDNA [58, 305].

In cancer patients, ctDNA is derived from tumor cells and circulating tumor cells (CTCs) [364]. In this thesis, Chapters 3 and 4 showed that ctDNA is derived from dying or dead cells, confirming data from previous studies [35, 58, 59, 304, 365]. In our analysis, ctDNA release was highest during apoptosis (Chapter 3), with our fragment size analysis indicating peaks related to apoptosis. The fragments commonly found in the bloodstream are usually about 166 bp, which corresponds to 147 bp of DNA wrapped around a nucleosome plus the DNA on histone H1. This size suggests that the fragments are derived from apoptosis [56]. Our findings were confirmed

when we evaluated ctDNA under cytotoxic conditions by two potential drug treatments that induce apoptosis (Chapter 4). We observed that ctDNA levels correspond to drug concentration, indicating a strong correlation between apoptosis and ctDNA release. This was supported by other reports in which ctDNA informs treatment response [63, 116, 136, 319]. Chapter 3 also demonstrated the impact of irradiation on ctDNA release in cancer cells, which is supported by previous reports [333]. This phenomenon may attributed to irradiation causing mitotic catastrophe followed by cell death [329]. ctDNA release during apoptosis could also be related to increased cell proliferation [366]. Apoptotic cells promote the proliferation of surrounding cells, a process called apoptosis-induced proliferation [367, 368]. During apoptosis-induced proliferation, caspases cleave and activate calcium-independent phospholipases A_2. This increases arachidonic acid production to prostaglandin E2 (PGE_2), a key mediator of apoptosis-induced proliferation[247]. Moreover, proliferation might induce apoptosis[367]. Thus, signaling derived from proliferation may include compensatory signaling from proliferative cells. Altogether, the data in this thesis and in other reports [35, 53, 58-60] strongly suggest that ctDNA release is mainly attributed to cellular turnover.

In addition to apoptosis, ctDNA release from necrotic cells has also been reported [59], but the extent of its contribution remains under debate. ctDNA has been correlated with tumor burden [126], and increasing tumor size has been associated with increasing levels of necrosis [88]. Apoptotic-derived fragments are around 166 bp whereas necrotic-derived fragments are longer in length about 1,000 bp [59, 78]. Indeed, in our study, we found a peak >1,000 bp relating to necrosis. However, these large fragments may be digested in the bloodstream to similar mononucleosome-sized fragments as apoptotic ones (about 166 bp) [369]. Therefore, it is unclear

whether cfDNA fragments observed in the bloodstream are derived from apoptosis, or they are digested fragments from necrosis [369].

Cellular secretions, including active secretion from live cells, are also a source of cfDNA [301, 305, 365, 370]. These secretions are associated with various cell-derived vesicles, such as exosomes, microvesicles, and apoptotic bodies [371]. By analyzing blood, some reports have indicated that cfDNA is released via EVs and acts as an intercellular messenger, modulating the behavior of recipient cells [372, 373]. Altogether, determining the exact origin of cfDNA from each of its sources will provide further information about the clinical utility of cfDNA and its potential role in carcinogenesis and tumor progression.

5.2.2 Clinical utility of ctDNA

Numerous studies, including ours, have investigated the clinical utility of ctDNA to screen cancer, monitor tumor burden and treatment response, and detect progression and metastasis [8, 12, 13, 29].

Since an ultimate goal in cancer research is to prevent or delay metastasis, this dissertation focuses on a highly metastatic tumor: UM. UM spreads to distal organs, such as the liver, bones, and lung, through hematogenous dissemination [1]. This makes blood a suitable analyte to be explored as a liquid biopsy. Indeed, several studies have investigated circulating tumor cells (CTCs) as a liquid biopsy technique in UM [259, 260, 374]. For instance, CellSearch, an FDA-approved test, detected CTCs in 30% of samples, with CTC count associated with metastasis, progression-free survival, and overall survival [259]. A subsequent study that analyzed arterial and venous blood, showed that CTCs were identified in 100% of the arterial blood-derived samples and 53% of venous blood-derived samples [260]. By studying in parallel CTCs and ctDNA, CTCs

informed prognosis whereas ctDNA detected early metastasis [260]. Nevertheless, the clinical utility of CTCs in UM is still unclear, and few studies have explored ctDNA potential in UM (**Table 2**).

To address this knowledge gap on the role of liquid biopsy in UM, our proposed approach sought to demonstrate the utility of ctDNA as a biomarker in a comprehensive study that includes *in vitro*, *in vivo*, and clinical studies. By tracking ctDNA levels over time, we can gain invaluable insight into how UM cells regulate their molecular status to survive, sustain themselves and spread to other organs. Furthermore, we can identify molecular changes that can be useful in the diagnosis, prognosis, and detection of early metastasis and against which targeted therapy could be directed.

5.2.2.1 ctDNA as a biomarker of UM

The clinical examination of UM and a choroidal nevus is performed using the same methods: a routine slit lamp biomicroscopy, indirect ophthalmoscopy under dilated pupil, ultrasonography, fundoscopy, and optic coherence tomography [375]. While the diagnosis of small and flat nevi is generally well-established using these methods, large nevi have overlapping characteristics with UM, which may result in a more challenging diagnosis [376]. Some indeterminate pigmented tumors may carry a clinical dilemma to be treated as melanoma or be clinically observed as a nevi [377].

To identify risk factors for nevus growth to melanoma, the mnemonic *To Find Small Ocular Melanoma Doing Imaging* proposed by CL Shields *et* al [291] has been used in the clinic. This mnemonic includes identifying thickness >2 mm, subretinal fluid, symptoms (visual acuity loss to 20/50 or worse), presence of orange pigment, melanoma acoustic hollowness, and tumor diameter >5 mm (photography) [18, 148, 291]. Importantly, the combination of factors increases

the risk for tumor growth by about 4% [378]. More recently, age has been also identified as a choroidal nevus risk factor that suggests a risk of malignant transformation [379]. In addition, the *MOLES* scoring system has been proposed to distinguish melanoma from nevi. This system stands for mushroom shape, orange pigment, large tumor size, enlarging tumor, and subretinal fluid [380]. Although some factors are suggestive of malignant transformation and support clinical diagnosis, no molecular method is available to inform on malignant transformation and aid in distinguishing lesions with overlapping features. Tissue biopsies are performed for prognostication and cytogenetic testing in UM tumors, but are not generally performed to analyze nevi [277]. ctDNA could address this need, by providing a minimally invasive source of ctDNA as a biomarker to differentiate a nevus from a small melanoma. ctDNA analysis may also be important in nonmelanocytic lesions that could be misdiagnosed as melanoma [381]. Our data support further investigation of ctDNA to diagnose and monitor choroidal nevus. It would be interesting to determine in the future whether positive ctDNA is an independent diagnostic biomarker of UM or whether it could be added as a risk factor for nevus growth and transformation.

There are different approaches that could be employed to investigate whether ctDNA can serve as a biomarker to differentiate a nevus from a small melanoma. For example, ctDNA analysis can be coupled with other UM markers such as prognosis mutations (*EIF1AX, SF3B1*, and *BAP1*) or the cytogenetic analysis (loss of chromosome 3)[1]. In addition, the fragmentation of ctDNA is related to the tissue of origin[57]. Therefore, to explore the differences between ctDNA derived from nevi and UM, we can study ctDNA physical properties. First, we can characterize DNA methylation status in UM and nevus by conducting whole-genome bisulfite sequencing of DNA[382] isolated from UM cell lines and nevus-like cells (choroidal melanocytes with a point mutation in GNAQ Q209L[4]) as well as from patients with a nevus or UM. Additionally, given

that difference ctDNA fragment size has been reported in malignancies vs control [74, 78, 79], we can study whether this difference exists between both cohorts. Moreover, single-stranded DNA ends, also called jagged ends, have been reported to be increased in cancer patients compared to nontumoral DNA[383]. The characterization of jagged ends can also help us to differentiate between a nevus and melanoma.

The findings of our clinical study also support the use of ctDNA to monitor patients that are diagnosed with UM. Using the methodology outlined in this thesis, we propose a future longitudinal ctDNA assessment that would assess the impact of treatment (enucleation and radiotherapy) on the levels of ctDNA. This would allow us to determine the potential of ctDNA to monitor treatment response. This study is ongoing in our laboratory. In a similar light, ctDNA could be a valuable tool in clinical trials testing novel drug treatments for UM. Previously, response to PD-1 immunotherapy was evaluated in two studies that include 3 [262] and 42 [266] metastatic UM patients, respectively. Both studies showed that ctDNA analysis was associated with anti-PDI treatment response and patient outcomes. A more recent study corroborated the utility of ctDNA to monitor and predict UM response to PKCi-based therapy during a phase I clinical trial [264]. Additional clinical studies on ctDNA will provide further information into how a tumor evolves over time.

5.2.4 Models to study ctDNA

Several xenograft animal models have demonstrated the feasibility to detect ctDNA from blood [384-386]. Thierry *et* al 2010 [386] conducted one of the first liquid biopsy animal models, in which nude mice were xenografted with colorectal cancer cells and then analyzed for human DNA sequences in the blood originating from the tumor xenograft, showing a correlation between ctDNA and tumor burden [386]. Since then, our group and others have shown similar data,

supporting a link between primary tumor volume and ctDNA [387]. Our data in Chapter 2 revealed a strong correlation between human-specific ctDNA levels and disease development and progression, attesting to the potential of such an approach in the diagnosis and monitoring of cancer patients.

Due to ethical reasons, *in vitro* studies should be considered before the use of animal models. *In vitro* models have been shown to offer an understanding of a disease's impact at the molecular and cellular levels. This thesis and several other studies have investigated the role of cfDNA using *in vitro* models, which have allowed us to study different cfDNA aspects such as kinetics, size profiling, and epigenetics markers under normal or cytotoxic conditions [34, 61, 301, 303, 304, 330, 365, 370, 388]. One example of these studies is the characterization of cfDNA concentration in normal conditions by Ungerer *et* al [304], in which, similar to our findings in Chapters 3 and 4, cell death correlated with cfDNA concentration [304]. In our study, cell lines allowed us to study the effect of drugs on cfDNA release. Similarly, a previous study established active secretion as a source of cfDNA when treating breast cancer cells with an apoptosis inducer and cell cycle inhibitor [301]. The detection of cfDNA has recently been studied in patient-derived organoids (PDOs), which retains characteristics more similar to patient disease than two-dimensional (2D) models [389]. Using PDOs from pancreatic ductal adenocarcinoma, cfDNA has been shown to mirror genomic alterations of the primary tumor [390].

In vitro cultures have some limitations. For example, they neglect external factors which influence cfDNA release, such as the shear forces that may impact blood-derived DNA fragmentation[391]. This approach also misses the activity of Dnase1/3 that have a role in ctDNA fragmentation [369]. Moreover, cultures lack some factors that influence cfDNA elimination, for instance the binding to plasma proteins (e.g., albumin) that have a role in cfDNA clearance [391].

Nevertheless, *in vitro* models are a reliable method to evaluate ctDNA [61, 303, 304, 330, 333, 370, 388]. Indeed, results obtained from *in vitro* systems have been supported by findings in animal models [385, 387] and in human disease [2].

5.2.5 Factors that influence ctDNA analysis

Pre-and post-analytical variables can alter ctDNA results [294]. These variables include blood collection tube type, handling, and processing of specimen from blood withdrawal to cfDNA isolation (preanalytical), obtaining cfDNA (analytic), and reporting and interpreting results (post-analytical) [392, 393]. Plasma has been reported to be a preferent analyte as a source of ctDNA because serum has high background due to cfDNA released by white blood cells, with 2-24X the cfDNA concentration found in plasma. This background is mainly from wild-type signals which can dilute tumor-derived cfDNA and mask its detection [394]. Contrary to serum, plasma presents low wild-type (WT) DNA background which improves ctDNA detection. In our study, we analyzed a few healthy individuals using serum-derived samples (data not shown) that showed higher total DNA levels compared to plasma-derived samples probably due to a high WT background. For this reason, plasma isolation using tubes with EDTA anticoagulants is preferred. However, cfDNA isolation should be performed within 6 hours after blood collection [395]. This is because gDNA release increases over time which contributes to the high WT background [395]. For this reason, specialized tubes can be used to stabilize cfDNA. In this study (Chapter 2), blood was withdrawn using PAXgene tubes (BD, Qiagen) that contain fixative agents for leukocyte stabilization and cfDNA integrity preservation. Unlike EDTA blood collection tubes, PAXgene tubes allow cfDNA preservation for up to 7 days at room temperature, thereby preventing potential degradation of DNA [396].

In addition, the amount and quality of cfDNA depend on the extraction methods [395]. Indeed, cfDNA extraction protocols have reported interlaboratory variability [397]. In this project, samples were isolated by QIAGEN QIAamp CAN kit which has shown the highest cfDNA yield [397].

Postanalytical variables also alter cfDNA data. For example, quantification of cfDNA by fluorometry methods (e.g., Qubit) has been reported to be more precise than Flurospectroscopy methods (e.g., NanoDrop) [330]. Nevertheless, qPCR and ddPCR are more accurate and precise than Qubit [298]. This project used ddPCR which detects and quantifies low levels of cfDNA, as low as 0.1% mutant allele fraction, by partitioning the DNA sample into 20,000 water-in-oil droplets [98]. ddPCR uses a low input amount which may result in less consistent results than NGS [298]. However, NGS is less sensitive compared to ddPCR [398]. We observed that ddPCR provides a highly accurate and absolute measure of amplifiable DNA as noted in previous reports [298].

In an effort to mitigate the impact of experimental variables using standardized methods, some guidelines have been established. For CTC analysis, standardization and quality assurance in CANCER-ID has been established [399]. In addition, some organizations have come together as the International Alliance for Liquid Biopsy to support clinical decisions and regulatory considerations [400]. Standardizing cfDNA workflow will facilitate its integration in the clinic [400].

Overall, various variables (from collection to analysis) could affect cfDNA results [391]. Therefore, standardized workflow and validated protocol are essential. This thesis was a pioneer on best practices for blood collection, cfDNA isolation, and analysis in our laboratory, which focuses on liquid biopsy methodologies.

5.3 Limitations

Using *in vitro* and *in vivo* models as well as a clinical study, this dissertation focuses on the analysis of circulating fragmented DNA, cfDNA, and its tumor-specific fraction, ctDNA. While this project uncovered the kinetics of cfDNA *in vitro*, such analyses were not performed in patient blood samples. In the bloodstream, DNA sequences are derived from dead or dying hematopoietic [37] and tumor cells [35], CTCs [364], or EVs and extracellular particles [372]. These DNA sequences can be altered by bloodstream-related physical constraints, such as fluid-wall shear stress [401], which may impact DNA fragmentation. Further studies that investigate how shear forces of blood affect ctDNA detection are still needed.

Using different cancer cell types to evaluate the kinetics of cfDNA has increased the generalizability of our results. All previous chapters highlighted ctDNA changes after various conditions: cancer cell inoculation, exposure to cytotoxic, and potential antitumor treatments. This thesis, however, did not explore the role of cfDNA derived from normal cells. Normal cells are also killed by anti-cancer treatments [318]. In addition, cfDNA size and source released by healthy cells differ from cancer cells [74, 304]. Futures studies that investigate cfDNA origin in normal cells and how it is interconnected with ctDNA may provide useful information on cfDNA kinetics.

Another limitation in this study is that its experiments on ctDNA in UM patients (Chapter 2) have thus far been conducted only in the primary disease setting. However, its assay can be applied in the metastatic disease by comparing ctDNA levels across time points. Most of the UM patients in this clinical study had also received treatment before blood analysis, and serial time points were not included. While serial time is not used, we incorporated a patient (LB036) for whom we had before and after treatment samples, we observed that ctDNA levels decreased after

treatment. Despite being limited to only one patient, this assay can be feasibly reproduced with other patients for further analysis. Indeed, there is an ongoing study in the laboratory in sequential samples (data not shown).

Previously, some reports have compared ctDNA from blood with ctDNA from tissue biopsy. The range of concordance rate has been reported from 65 to 95% [331]. For example, a study that analyzed *KRAS* alterations by NGS in blood and tissue showed an 85% concordance rate between both specimens [402]. Although tissue biopsies were not available for our UM cohort, this present study compared blood with eye fluid (aqueous humor) and tissue tumor in rabbit-derived samples (Chapter 2). We also analyzed markers of malignancy on tissue from rabbits, which will be compared with our ctDNA data (manuscript under preparation and not included in this thesis).

5.4 Directions for future studies

Liquid biopsy could change the current paradigm in oncology for early cancer detection and screening, treatment response monitoring, and metastasis prediction [12, 14, 29, 403, 404]. Although there is promising evidence showing the potential of ctDNA as a liquid biopsy-based biomarker, little is known about the exact biological role of ctDNA in cancer patients. The results and experimental models presented in this thesis provide new avenues and additional insight into the mechanisms contributing to ctDNA levels in patients. One such future direction is to investigate how ctDNA clearance occurs. ctDNA has a short life [12] and, as such, the timing of sampling can affect ctDNA results [391]. It is known that ctDNA is cleared through uptake by the reticuloendothelial system in the liver and spleen, filtration by the renal system, and degradation

by nucleases [338]. Investigating which mechanisms play key roles in cfDNA clearance may provide useful information on ctDNA fluctuations in cancer patients.

In addition, the biological function of cfDNA remains unclear in healthy conditions and cancer. cfDNA is released by hemopoietic cells under normal conditions [37], and some reports have indicated that it may be a passive byproduct or waste product [338]. By contrast, data has suggested that cfDNA can act as a proinflammatory factor for toll-like receptors, TLR2 and TLR4, that trigger the innate immune response [405]. Further work on understanding the relationship between cfDNA in blood and immune response is needed. Moreover, evidence has suggested that cancer cell-derived EVs contain DNA. These EVs can deliver their cargo to recipient cells, modulating behaviour and contributing to cancer progression. This process suggests that cfDNA in EVs can alter the proliferation, gene expression, and functional responses of normal cells [372]. For example, by culturing two cell lines (mouse embryo fibroblasts and pluripotent stem cells) with plasma derived from colorectal cancer patients, researchers have shown that cfDNA encodes *KRAS* mutant which can induce an oncogenic transformation of these cultured cell lines [406]. Thus, cfDNA may have a functional role [407], warranting further research on the role of EVs and their cargo in cell-cell communication in cancer.

By using a consistent methodology, this thesis shows that ctDNA levels informed the disease course in UM (Chapter 2). Despite our assay demonstrating high sensitivity and specificity, it relies on prior knowledge of tumor-specific somatic alterations. While this is feasible in UM due to the high prevalence of *GNAQ/GNA11/PLCB4* and *CYSLT2* driver mutations, such an approach is not possible in other tumor types without NGS profiling. New approaches are being investigated to overcome these challenges. Epigenetic profiling has been performed in ctDNA and correlated to clinical parameters. For example, a methylation profiling method has been previously reported

in breast cancer to track cancer cell evolution without prior knowledge of mutations [408]. The FDA-approved Epi proColon 2.0 test has also assessed an epigenetic signature [72]. A complementary approach that investigates epigenetic profiles in UM may allow researchers to identify changes in ctDNA, which can be complementary to using driver mutations found in ctDNA. Indeed, our laboratory has previously demonstrated a strong association between methylation profiles and outcome in UM [409].

In cancer patients, ctDNA is also derived from CTCs [364]. Some studies have shown a correlation between the presence of CTCs and ctDNA. In most cases, both CTCs and ctDNA are detected in the same patients; however, in some cases, CTCs are not detected even when ctDNA is. In cases in which both analytes are detected, the levels of ctDNA seem to be higher than CTCs [364], reflecting the higher sensitivity of ctDNA assays. To gain insight into the potential of CTCs as a source of ctDNA, further studies to elucidate the functional characterization of CTCs in UM are still needed. Future work that compares other liquid biopsy-based analytes such as microRNAs, EVs, tumor-educated platelets, or proteins with ctDNA may support the potential of liquid biopsy in UM.

The analysis of the fragmentation patterns of ctDNA can also inform us about diagnosis and prognosis in cancer [75, 77, 82] [410]. Our data on fragmentation in *in vitro* models (Chapter 3) showed that cytotoxic conditions alter cfDNA size. We propose in the future to evaluate the ctDNA fragment size using patient blood across the disease course. This future work may elucidate the potential differences in fragment size that may inform us about treatment response or risk of metastasis.

The fragmentation of cfDNA is a non-random process [411]; however, there is a lack of knowledge about cfDNA fragmentation patterns. It could be interesting to investigate the process

of cfDNA fragmentation and the role of nucleosomes on fragment patterns. Markers focused on cfDNA fragmentation and topology have emerged recently. For example, plasma DNA motifs [73] and jagged ends [383] have been suggested as cancer biomarkers [57]. Further understanding of the fragmentation process may elucidate markers based on fragmentation patterns which can be an alternative to genetic markers for ctDNA detection in cancer.

5.4.1 Steps to the clinic

Despite this promising data, the liquid biopsy field still presents some limitations. The process of ctDNA analysis is laborious and can bring technical pre- and post-analytical variables[392] that affect ctDNA results. In order to minimize analytical validity and facilitate ctDNA workflow, we suggest looking at automatized technologies and investigating the feasibility of analyzing plasma without ctDNA isolation. A ctDNA analysis from plasma omitting ctDNA isolation has been conducted in previous studies [412-414]. By comparing this direct ctDNA testing with current commercial isolation kits, similar ctDNA concentration levels have been reported in these studies [415]. An easier workflow will facilitate ctDNA integration into the clinic [265].

BRAF and *GNAQ/11* mutations have been found in cutaneous [416] and choroidal nevi [163], respectively, indicating that driver mutations are needed but insufficient for melanoma development. Our assay relies on driver mutations to evaluate ctDNA. Integrating mutations associated with metastasis risk, such as BAP1[164], in a liquid biopsy assay would be also clinically relevant.

The integration of ctDNA into the clinic can make a difference for UM management. Recently, tebentafusp treatment showed to improve the overall survival in metastatic UM patients

(21.7 months vs 16 months for the control cohort) [417]. In addition, an observational study reported that ctDNA analysis predicted metastasis before any symptoms [418]. However, in order to ctDNA achieve the clinic, its sensitivity and specificity of cancer detection should be measured in a prospective study in which tumor biopsy tissue is collected to corroborate point mutations. The collection of serial plasma samples is also needed for therapy response monitoring. Due to the rare nature of this disease, the sample size calculation for this study should be extensively analyzed [419] and the involving various centers are warranted. Consequently, this new therapy coupled with the prognostic value of ctDNA may improve UM mortality. It is important to note that once the sensitivity and specificity of ctDNA in UM is validated, this approach must be approved by the regulatory agencies to reach the clinic [420].

Various studies have investigated liquid biopsies in cancer, including ctDNA, CTC, or EVs in different bodily fluids. To better understand this extensive data, the use of machine learning has been proposed. In particular, machine learning has been proposed to elucidate signatures of different biomarkers [421] and to capture the relationship between a biomarker and cancer subtype heterogeneity [422]. Indeed, by using machine learning, new liquid biopsy approaches have emerged. For example, the Grail's test, a multi-cancer screening test based on the cfDNA methylation profiles that uses machine-learning algorithms and NGS, appears to inform an early cancer detection [423]. Therefore, machine learning may advance the use of liquid biopsy for cancer detection and management in the clinic.

5.5 Conclusion

Collectively, the findings described in this thesis indicate that ctDNA is a potential liquid biopsy-based biomarker for UM and, as a result, provide compelling evidence for its further investigation for clinical use. It is minimally invasive, and its analysis is sensitive and specific. Using UM cancer models, which include *in vitro* and *in vivo* models as well as patient blood, has demonstrated that ctDNA is clinically relevant. By using preclinical models, we show ctDNA is altered in cytotoxic and stress conditions as well as it is a potential biomarker of drug response. The data outlined in this thesis show the importance of evaluating ctDNA in various conditions and highlight the potential role of ctDNA as a non-invasive diagnostic biomarker and monitoring tool. Altogether, these chapters validate the importance of evaluating ctDNA release in cancer. Indeed, by using our experimental approaches, our work could expand beyond UM to other cancer types.

References

1. Bustamante P, Piquet L, Landreville S, Burnier JV: **Uveal melanoma pathobiology: Metastasis to the liver**. *Semin Cancer Biol* 2021, **71**:65-85.
2. Bustamante P, Tsering T, Coblentz J, Mastromonaco C, Abdouh M, Fonseca C, Proença RP, Blanchard N, Dugé CL, Andujar RAS *et al*: **Circulating tumor DNA tracking through driver mutations as a liquid biopsy-based biomarker for uveal melanoma**. *J Exp Clin Cancer Res* 2021, **40**(1):196.
3. Bustamante P, Miyamoto D, Goyeneche A, de Alba Graue PG, Jin E, Tsering T, Dias AB, Burnier MN, Burnier JV: **Beta-blockers exert potent anti-tumor effects in cutaneous and uveal melanoma**. *Cancer Med* 2019, **8**(17):7265-7277.
4. Alvarez PB, Laskaris A, Goyeneche AA, Chen Y, Telleria CM, Burnier JV: **Anticancer effects of mifepristone on human uveal melanoma cells**. *Cancer Cell International* 2021, **21**(1):607.
5. Schwartzberg L, Kim ES, Liu D, Schrag D: **Precision Oncology: Who, How, What, When, and When Not?** *Am Soc Clin Oncol Educ Book* 2017, **37**:160-169.
6. Duraiyan J, Govindarajan R, Kaliyappan K, Palanisamy M: **Applications of immunohistochemistry**. *J Pharm Bioallied Sci* 2012, **4**(Suppl 2):S307-309.
7. Overman MJ, Modak J, Kopetz S, Murthy R, Yao JC, Hicks ME, Abbruzzese JL, Tam AL: **Use of research biopsies in clinical trials: are risks and benefits adequately discussed?** *J Clin Oncol* 2013, **31**(1):17-22.
8. Heitzer E, Haque IS, Roberts CES, Speicher MR: **Current and future perspectives of liquid biopsies in genomics-driven oncology**. *Nat Rev Genet* 2019, **20**(2):71-88.
9. Dagogo-Jack I, Shaw AT: **Tumour heterogeneity and resistance to cancer therapies**. *Nat Rev Clin Oncol* 2018, **15**(2):81-94.
10. Vanderlaan PA, Yamaguchi N, Folch E, Boucher DH, Kent MS, Gangadharan SP, Majid A, Goldstein MA, Huberman MS, Kocher ON *et al*: **Success and failure rates of tumor genotyping techniques in routine pathological samples with non-small-cell lung cancer**. *Lung Cancer* 2014, **84**(1):39-44.
11. Pantel K, Alix-Panabières C: **Circulating tumour cells in cancer patients: challenges and perspectives**. *Trends Mol Med* 2010, **16**(9):398-406.
12. Diaz LA, Jr., Bardelli A: **Liquid biopsies: genotyping circulating tumor DNA**. *J Clin Oncol* 2014, **32**(6):579-586.
13. Heitzer E, Ulz P, Geigl JB: **Circulating tumor DNA as a liquid biopsy for cancer**. *Clin Chem* 2015, **61**(1):112-123.
14. Pantel K, Alix-Panabieres C: **Liquid biopsy and minimal residual disease - latest advances and implications for cure**. *Nat Rev Clin Oncol* 2019, **16**(7):409-424.
15. Xu R, Rai A, Chen M, Suwakulsiri W, Greening DW, Simpson RJ: **Extracellular vesicles in cancer - implications for future improvements in cancer care**. *Nat Rev Clin Oncol* 2018, **15**(10):617-638.
16. Joosse Simon A, Pantel K: **Tumor-Educated Platelets as Liquid Biopsy in Cancer Patients**. *Cancer Cell* 2015, **28**(5):552-554.
17. Schwarzenbach H, Hoon DS, Pantel K: **Cell-free nucleic acids as biomarkers in cancer patients**. *Nat Rev Cancer* 2011, **11**(6):426-437.
18. Marous CL, Shields CL, Yu MD, Dalvin LA, Ancona-Lezama D, Shields JA: **Malignant transformation of choroidal nevus according to race in 3334 consecutive patients**. *Indian J Ophthalmol* 2019, **67**(12):2035-2042.

19. Eskelin S, Pyrhonen S, Summanen P, Hahka-Kemppinen M, Kivela T: **Tumor doubling times in metastatic malignant melanoma of the uvea: tumor progression before and after treatment**. *Ophthalmology* 2000, **107**(8):1443-1449.
20. Singh AD: **Uveal melanoma: implications of tumor doubling time**. *Ophthalmology* 2001, **108**(5):829-831.
21. Blanco PL, Marshall JC, Antecka E, Callejo SA, Souza Filho JP, Saraiva V, Burnier MN, Jr.: **Characterization of ocular and metastatic uveal melanoma in an animal model**. *Invest Ophthalmol Vis Sci* 2005, **46**(12):4376-4382.
22. Jin E, Burnier JV: **Liquid Biopsy in Uveal Melanoma: Are We There Yet?** *Ocul Oncol Pathol* 2021, **7**(1):1-16.
23. Van Raamsdonk CD, Bezrookove V, Green G, Bauer J, Gaugler L, O'Brien JM, Simpson EM, Barsh GS, Bastian BC: **Frequent somatic mutations of GNAQ in uveal melanoma and blue naevi**. *Nature* 2009, **457**(7229):599-602.
24. Van Raamsdonk CD, Griewank KG, Crosby MB, Garrido MC, Vemula S, Wiesner T, Obenauf AC, Wackernagel W, Green G, Bouvier N *et al*: **Mutations in GNA11 in uveal melanoma**. *N Engl J Med* 2010, **363**(23):2191-2199.
25. Johansson P, Aoude LG, Wadt K, Glasson WJ, Warrier SK, Hewitt AW, Kiilgaard JF, Heegaard S, Isaacs T, Franchina M *et al*: **Deep sequencing of uveal melanoma identifies a recurrent mutation in PLCB4**. *Oncotarget* 2016, **7**(4):4624-4631.
26. Moore AR, Ceraudo E, Sher JJ, Guan Y, Shoushtari AN, Chang MT, Zhang JQ, Walczak EG, Kazmi MA, Taylor BS *et al*: **Recurrent activating mutations of G-protein-coupled receptor CYSLTR2 in uveal melanoma**. *Nat Genet* 2016, **48**(6):675-680.
27. Wan JCM, Massie C, Garcia-Corbacho J, Mouliere F, Brenton JD, Caldas C, Pacey S, Baird R, Rosenfeld N: **Liquid biopsies come of age: towards implementation of circulating tumour DNA**. *Nature Reviews Cancer* 2017, **17**(4):223-238.
28. Sato Y, Matoba R, Kato K: **Recent Advances in Liquid Biopsy in Precision Oncology Research**. *Biol Pharm Bull* 2019, **42**(3):337-342.
29. Keller L, Belloum Y, Wikman H, Pantel K: **Clinical relevance of blood-based ctDNA analysis: mutation detection and beyond**. *Br J Cancer* 2021, **124**(2):345-358.
30. Stroun M, Anker P, Lyautey J, Lederrey C, Maurice PA: **Isolation and characterization of DNA from the plasma of cancer patients**. *Eur J Cancer Clin Oncol* 1987, **23**(6):707-712.
31. Burnham P, Kim MS, Agbor-Enoh S, Luikart H, Valantine HA, Khush KK, De Vlaminck I: **Single-stranded DNA library preparation uncovers the origin and diversity of ultrashort cell-free DNA in plasma**. *Scientific reports* 2016, **6**(1):1-9.
32. Chiu RW, Chan LY, Lam NY, Tsui NB, Ng EK, Rainer TH, Lo YD: **Quantitative analysis of circulating mitochondrial DNA in plasma**. *Clinical chemistry* 2003, **49**(5):719-726.
33. Kumar P, Dillon LW, Shibata Y, Jazaeri AA, Jones DR, Dutta A: **Normal and cancerous tissues release extrachromosomal circular DNA (eccDNA) into the circulation**. *Molecular Cancer Research* 2017, **15**(9):1197-1205.
34. Bronkhorst AJ, Ungerer V, Holdenrieder S: **The emerging role of cell-free DNA as a molecular marker for cancer management**. *Biomolecular detection and quantification* 2019, **17**:100087-100087.
35. Heitzer E, Auinger L, Speicher MR: **Cell-Free DNA and Apoptosis: How Dead Cells Inform About the Living**. *Trends in Molecular Medicine* 2020, **26**(5):519-528.

36. Hu Z, Chen H, Long Y, Li P, Gu Y: **The main sources of circulating cell-free DNA: Apoptosis, necrosis and active secretion**. *Crit Rev Oncol Hematol* 2021, **157**:103166.
37. Lui YY, Chik KW, Chiu RW, Ho CY, Lam CW, Lo YM: **Predominant hematopoietic origin of cell-free DNA in plasma and serum after sex-mismatched bone marrow transplantation**. *Clin Chem* 2002, **48**(3):421-427.
38. Lam NY, Rainer TH, Chan LY, Joynt GM, Lo YM: **Time course of early and late changes in plasma DNA in trauma patients**. *Clin Chem* 2003, **49**(8):1286-1291.
39. Tsai NW, Lin TK, Chen SD, Chang WN, Wang HC, Yang TM, Lin YJ, Jan CR, Huang CR, Liou CW *et al*: **The value of serial plasma nuclear and mitochondrial DNA levels in patients with acute ischemic stroke**. *Clin Chim Acta* 2011, **412**(5-6):476-479.
40. Gielis EM, Ledeganck KJ, De Winter BY, Del Favero J, Bosmans J-L, Claas FHJ, Abramowicz D, Eikmans M: **Cell-Free DNA: An Upcoming Biomarker in Transplantation**. *American Journal of Transplantation* 2015, **15**(10):2541-2551.
41. Long Y, Zhang Y, Gong Y, Sun R, Su L, Lin X, Shen A, Zhou J, Caiji Z, Wang X *et al*: **Diagnosis of Sepsis with Cell-free DNA by Next-Generation Sequencing Technology in ICU Patients**. *Arch Med Res* 2016, **47**(5):365-371.
42. Bianchi DW, Chiu RWK: **Sequencing of Circulating Cell-free DNA during Pregnancy**. *New England Journal of Medicine* 2018, **379**(5):464-473.
43. Fujii T, Barzi A, Sartore-Bianchi A, Cassingena A, Siravegna G, Karp DD, Piha-Paul SA, Subbiah V, Tsimberidou AM, Huang HJ *et al*: **Mutation-Enrichment Next-Generation Sequencing for Quantitative Detection of KRAS Mutations in Urine Cell-Free DNA from Patients with Advanced Cancers**. *Clin Cancer Res* 2017, **23**(14):3657-3666.
44. Wang Y, Springer S, Mulvey CL, Silliman N, Schaefer J, Sausen M, James N, Rettig EM, Guo T, Pickering CR *et al*: **Detection of somatic mutations and HPV in the saliva and plasma of patients with head and neck squamous cell carcinomas**. *Sci Transl Med* 2015, **7**(293):293ra104.
45. Sriram KB, Relan V, Clarke BE, Duhig EE, Windsor MN, Matar KS, Naidoo R, Passmore L, McCaul E, Courtney D: **Pleural fluid cell-free DNA integrity index to identify cytologically negative malignant pleural effusions including mesotheliomas**. *BMC cancer* 2012, **12**(1):1-12.
46. Pan W, Gu W, Nagpal S, Gephart MH, Quake SR: **Brain tumor mutations detected in cerebral spinal fluid**. *Clinical chemistry* 2015, **61**(3):514-522.
47. Diehl F, Schmidt K, Choti MA, Romans K, Goodman S, Li M, Thornton K, Agrawal N, Sokoll L, Szabo SA *et al*: **Circulating mutant DNA to assess tumor dynamics**. *Nat Med* 2008, **14**(9):985-990.
48. Lo YM, Zhang J, Leung TN, Lau TK, Chang AM, Hjelm NM: **Rapid clearance of fetal DNA from maternal plasma**. *Am J Hum Genet* 1999, **64**(1):218-224.
49. Kustanovich A, Schwartz R, Peretz T, Grinshpun A: **Life and death of circulating cell-free DNA**. *Cancer Biol Ther* 2019, **20**(8):1057-1067.
50. Giacona MB, Ruben GC, Iczkowski KA, Roos TB, Porter DM, Sorenson GD: **Cell-free DNA in human blood plasma: length measurements in patients with pancreatic cancer and healthy controls**. *Pancreas* 1998, **17**(1):89-97.
51. Thierry AR, El Messaoudi S, Gahan PB, Anker P, Stroun M: **Origins, structures, and functions of circulating DNA in oncology**. *Cancer Metastasis Rev* 2016, **35**(3):347-376.

52. Alcaide M, Cheung M, Hillman J, Rassekh SR, Deyell RJ, Batist G, Karsan A, Wyatt AW, Johnson N, Scott DW *et al*: **Evaluating the quantity, quality and size distribution of cell-free DNA by multiplex droplet digital PCR**. *Sci Rep* 2020, **10**(1):12564.
53. Wang BG, Huang HY, Chen YC, Bristow RE, Kassauei K, Cheng CC, Roden R, Sokoll LJ, Chan DW, Shih Ie M: **Increased plasma DNA integrity in cancer patients**. *Cancer Res* 2003, **63**(14):3966-3968.
54. McCoubrey-Hoyer A, Okarma TB, Holman HR: **Partial purification and characterization of plasma DNA and its relation to disease activity in systemic lupus erythematosus**. *Am J Med* 1984, **77**(1):23-34.
55. Fan HC, Blumenfeld YJ, Chitkara U, Hudgins L, Quake SR: **Analysis of the Size Distributions of Fetal and Maternal Cell-Free DNA by Paired-End Sequencing**. *Clinical Chemistry* 2010, **56**(8):1279-1286.
56. Sanchez C, Snyder MW, Tanos R, Shendure J, Thierry AR: **New insights into structural features and optimal detection of circulating tumor DNA determined by single-strand DNA analysis**. *npj Genomic Medicine* 2018, **3**(1):31.
57. Lo YMD, Han DSC, Jiang P, Chiu RWK: **Epigenetics, fragmentomics, and topology of cell-free DNA in liquid biopsies**. *Science* 2021, **372**(6538).
58. Stroun M, Lyautey J, Lederrey C, Olson-Sand A, Anker P: **About the possible origin and mechanism of circulating DNA apoptosis and active DNA release**. *Clin Chim Acta* 2001, **313**(1-2):139-142.
59. Jahr S, Hentze H, Englisch S, Hardt D, Fackelmayer FO, Hesch RD, Knippers R: **DNA fragments in the blood plasma of cancer patients: quantitations and evidence for their origin from apoptotic and necrotic cells**. *Cancer Res* 2001, **61**(4):1659-1665.
60. Rostami A, Lambie M, Yu CW, Stambolic V, Waldron JN, Bratman SV: **Senescence, Necrosis, and Apoptosis Govern Circulating Cell-free DNA Release Kinetics**. *Cell Rep* 2020, **31**(13):107830.
61. Aucamp J, Bronkhorst AJ, Peters DL, Van Dyk HC, Van der Westhuizen FH, Pretorius PJ: **Kinetic analysis, size profiling, and bioenergetic association of DNA released by selected cell lines in vitro**. *Cell Mol Life Sci* 2017, **74**(14):2689-2707.
62. Morbelli S, Alama A, Ferrarazzo G, Coco S, Genova C, Rijavec E, Bongioanni F, Biello F, Dal Bello MG, Barletta G *et al*: **Circulating Tumor DNA Reflects Tumor Metabolism Rather Than Tumor Burden in Chemotherapy-Naive Patients with Advanced Non-Small Cell Lung Cancer: (18)F-FDG PET/CT Study**. *J Nucl Med* 2017, **58**(11):1764-1769.
63. Uchida J, Kato K, Kukita Y, Kumagai T, Nishino K, Daga H, Nagatomo I, Inoue T, Kimura M, Oba S *et al*: **Diagnostic Accuracy of Noninvasive Genotyping of EGFR in Lung Cancer Patients by Deep Sequencing of Plasma Cell-Free DNA**. *Clinical Chemistry* 2015, **61**(9):1191-1196.
64. Thierry AR, Mouliere F, El Messaoudi S, Mollevi C, Lopez-Crapez E, Rolet F, Gillet B, Gongora C, Dechelotte P, Robert B: **Clinical validation of the detection of KRAS and BRAF mutations from circulating tumor DNA**. *Nature medicine* 2014, **20**(4):430-435.
65. Pietrasz D, Pecuchet N, Garlan F, Didelot A, Dubreuil O, Doat S, Imbert-Bismut F, Karoui M, Vaillant JC, Taly V *et al*: **Plasma Circulating Tumor DNA in Pancreatic Cancer Patients Is a Prognostic Marker**. *Clinical Cancer Research* 2017, **23**(1):116-123.
66. di Magliano MP, Logsdon CD: **Roles for KRAS in Pancreatic Tumor Development and Progression**. *Gastroenterology* 2013, **144**(6):1220-1229.

67. Therkildsen C, Bergmann TK, Henrichsen-Schnack T, Ladelund S, Nilbert M: **The predictive value of KRAS, NRAS, BRAF, PIK3CA and PTEN for anti-EGFR treatment in metastatic colorectal cancer: A systematic review and meta-analysis**. *Acta Oncologica* 2014, **53**(7):852-864.
68. Nakamura Y, Yokoyama S, Matsuda K, Tamura K, Mitani Y, Iwamoto H, Mizumoto Y, Murakami D, Kitahata Y, Yamaue H: **Preoperative detection of KRAS mutated circulating tumor DNA is an independent risk factor for recurrence in colorectal cancer**. *Scientific Reports* 2021, **11**(1):441.
69. Annala M, Vandekerkhove G, Khalaf D, Taavitsainen S, Beja K, Warner EW, Sunderland K, Kollmannsberger C, Eigl BJ, Finch D *et al*: **Circulating Tumor DNA Genomics Correlate with Resistance to Abiraterone and Enzalutamide in Prostate Cancer**. *Cancer Discov* 2018, **8**(4):444-457.
70. Ribic CM, Sargent DJ, Moore MJ, Thibodeau SN, French AJ, Goldberg RM, Hamilton SR, Laurent-Puig P, Gryfe R, Shepherd LE: **Tumor microsatellite-instability status as a predictor of benefit from fluorouracil-based adjuvant chemotherapy for colon cancer**. *New England Journal of Medicine* 2003, **349**(3):247-257.
71. Umetani N, Giuliano AE, Hiramatsu SH, Amersi F, Nakagawa T, Martino S, Hoon DS: **Prediction of breast tumor progression by integrity of free circulating DNA in serum**. *J Clin Oncol* 2006, **24**(26):4270-4276.
72. Lamb YN, Dhillon S: **Epi proColon(®) 2.0 CE: A Blood-Based Screening Test for Colorectal Cancer**. *Mol Diagn Ther* 2017, **21**(2):225-232.
73. Jiang P, Sun K, Peng W, Cheng SH, Ni M, Yeung PC, Heung MMS, Xie T, Shang H, Zhou Z *et al*: **Plasma DNA End-Motif Profiling as a Fragmentomic Marker in Cancer, Pregnancy, and Transplantation**. *Cancer Discov* 2020, **10**(5):664-673.
74. Lapin M, Oltedal S, Tjensvoll K, Buhl T, Smaaland R, Garresori H, Javle M, Glenjen NI, Abelseth BK, Gilje B *et al*: **Fragment size and level of cell-free DNA provide prognostic information in patients with advanced pancreatic cancer**. *J Transl Med* 2018, **16**(1):300.
75. Mouliere F, Chandrananda D, Piskorz AM, Moore EK, Morris J, Ahlborn LB, Mair R, Goranova T, Marass F, Heider K *et al*: **Enhanced detection of circulating tumor DNA by fragment size analysis**. *Sci Transl Med* 2018, **10**(466).
76. Mathios D, Johansen JS, Cristiano S, Medina JE, Phallen J, Larsen KR, Bruhm DC, Niknafs N, Ferreira L, Adleff V *et al*: **Detection and characterization of lung cancer using cell-free DNA fragmentomes**. *Nature Communications* 2021, **12**(1):5060.
77. Mouliere F, Smith CG, Heider K, Su J, van der Pol Y, Thompson M, Morris J, Wan JCM, Chandrananda D, Hadfield J *et al*: **Fragmentation patterns and personalized sequencing of cell-free DNA in urine and plasma of glioma patients**. *EMBO Mol Med* 2021, **13**(8):e12881.
78. Jiang P, Chan CW, Chan KC, Cheng SH, Wong J, Wong VW, Wong GL, Chan SL, Mok TS, Chan HL *et al*: **Lengthening and shortening of plasma DNA in hepatocellular carcinoma patients**. *Proc Natl Acad Sci U S A* 2015, **112**(11):E1317-1325.
79. Underhill HR, Kitzman JO, Hellwig S, Welker NC, Daza R, Baker DN, Gligorich KM, Rostomily RC, Bronner MP, Shendure J: **Fragment Length of Circulating Tumor DNA**. *PLoS Genet* 2016, **12**(7):e1006162.

80. Chen E, Cario CL, Leong L, Lopez K, Márquez CP, Chu C, Li PS, Oropeza E, Tenggara I, Cowan J *et al*: **Cell-free DNA concentration and fragment size as a biomarker for prostate cancer**. *Sci Rep* 2021, **11**(1):5040.
81. Yamamoto Y, Uemura M, Nakano K, Hayashi Y, Wang C, Ishizuya Y, Kinouchi T, Hayashi T, Matsuzaki K, Jingushi K *et al*: **Increased level and fragmentation of plasma circulating cell-free DNA are diagnostic and prognostic markers for renal cell carcinoma**. *Oncotarget* 2018, **9**(29):20467-20475.
82. Mouliere F, Robert B, Arnau Peyrotte E, Del Rio M, Ychou M, Molina F, Gongora C, Thierry AR: **High fragmentation characterizes tumour-derived circulating DNA**. *PLoS One* 2011, **6**(9):e23418.
83. Meddeb R, Dache ZAA, Thezenas S, Otandault A, Tanos R, Pastor B, Sanchez C, Azzi J, Tousch G, Azan S *et al*: **Quantifying circulating cell-free DNA in humans**. *Scientific Reports* 2019, **9**(1):5220.
84. Alborelli I, Generali D, Jermann P, Cappelletti MR, Ferrero G, Scaggiante B, Bortul M, Zanconati F, Nicolet S, Haegele J: **Cell-free DNA analysis in healthy individuals by next-generation sequencing: a proof of concept and technical validation study**. *Cell death & disease* 2019, **10**(7):1-11.
85. Catarino R, Ferreira MM, Rodrigues H, Coelho A, Nogal A, Sousa A, Medeiros R: **Quantification of free circulating tumor DNA as a diagnostic marker for breast cancer**. *DNA and cell biology* 2008, **27**(8):415-421.
86. Meddeb R, Dache ZAA, Thezenas S, Otandault A, Tanos R, Pastor B, Sanchez C, Azzi J, Tousch G, Azan S *et al*: **Quantifying circulating cell-free DNA in humans**. *Sci Rep* 2019, **9**(1):5220.
87. Bettegowda C, Sausen M, Leary RJ, Kinde I, Wang Y, Agrawal N, Bartlett BR, Wang H, Luber B, Alani RM *et al*: **Detection of circulating tumor DNA in early- and late-stage human malignancies**. *Sci Transl Med* 2014, **6**(224):224ra224.
88. Diehl F, Li M, Dressman D, He Y, Shen D, Szabo S, Diaz LA, Jr., Goodman SN, David KA, Juhl H *et al*: **Detection and quantification of mutations in the plasma of patients with colorectal tumors**. *Proc Natl Acad Sci U S A* 2005, **102**(45):16368-16373.
89. Forshew T, Murtaza M, Parkinson C, Gale D, Tsui DW, Kaper F, Dawson SJ, Piskorz AM, Jimenez-Linan M, Bentley D *et al*: **Noninvasive identification and monitoring of cancer mutations by targeted deep sequencing of plasma DNA**. *Sci Transl Med* 2012, **4**(136):136ra168.
90. Palmirotta R, Lovero D, Cafforio P, Felici C, Mannavola F, Pellè E, Quaresmini D, Tucci M, Silvestris F: **Liquid biopsy of cancer: a multimodal diagnostic tool in clinical oncology**. *Ther Adv Med Oncol* 2018, **10**:1758835918794630.
91. Pessoa LS, Heringer M, Ferrer VP: **ctDNA as a cancer biomarker: A broad overview**. *Critical Reviews in Oncology/Hematology* 2020, **155**:103109.
92. Chaudhuri AA, Binkley MS, Osmundson EC, Alizadeh AA, Diehn M: **Predicting Radiotherapy Responses and Treatment Outcomes Through Analysis of Circulating Tumor DNA**. *Seminars in Radiation Oncology* 2015, **25**(4):305-312.
93. Denis JA, Guillerm E, Coulet F, Larsen AK, Lacorte JM: **The Role of BEAMing and Digital PCR for Multiplexed Analysis in Molecular Oncology in the Era of Next-Generation Sequencing**. *Mol Diagn Ther* 2017, **21**(6):587-600.
94. Hindson BJ, Ness KD, Masquelier DA, Belgrader P, Heredia NJ, Makarewicz AJ, Bright IJ, Lucero MY, Hiddessen AL, Legler TC *et al*: **High-throughput droplet digital PCR**

system for absolute quantitation of DNA copy number. *Anal Chem* 2011, **83**(22):8604-8610.
95. **Rare Mutation Detection: Best Practices Guidelines** [https://www.bio-rad.com/fr-ca/SearchResults?search_api_fulltext=ddpcr+rare+mutation+detection]
96. Volckmar AL, Sultmann H, Riediger A, Fioretos T, Schirmacher P, Endris V, Stenzinger A, Dietz S: **A field guide for cancer diagnostics using cell-free DNA: From principles to practice and clinical applications**. *Genes Chromosomes Cancer* 2018, **57**(3):123-139.
97. Newman AM, Bratman SV, To J, Wynne JF, Eclov NCW, Modlin LA, Liu CL, Neal JW, Wakelee HA, Merritt RE *et al*: **An ultrasensitive method for quantitating circulating tumor DNA with broad patient coverage**. *Nature Medicine* 2014, **20**(5):548-554.
98. Hindson CM, Chevillet JR, Briggs HA, Gallichotte EN, Ruf IK, Hindson BJ, Vessella RL, Tewari M: **Absolute quantification by droplet digital PCR versus analog real-time PCR**. *Nat Methods* 2013, **10**(10):1003-1005.
99. Diehl F, Li M, He Y, Kinzler KW, Vogelstein B, Dressman D: **BEAMing: single-molecule PCR on microparticles in water-in-oil emulsions**. *Nat Methods* 2006, **3**(7):551-559.
100. Elazezy M, Joosse SA: **Techniques of using circulating tumor DNA as a liquid biopsy component in cancer management**. *Comput Struct Biotechnol J* 2018, **16**:370-378.
101. Dressman D, Yan H, Traverso G, Kinzler KW, Vogelstein B: **Transforming single DNA molecules into fluorescent magnetic particles for detection and enumeration of genetic variations**. *Proceedings of the National Academy of Sciences* 2003, **100**(15):8817-8822.
102. Glenn TC: **Field guide to next-generation DNA sequencers**. *Mol Ecol Resour* 2011, **11**(5):759-769.
103. Mandel P, Metais P: **[Nuclear Acids In Human Blood Plasma]**. *C R Seances Soc Biol Fil* 1948, **142**(3-4):241-243.
104. Leon SA, Shapiro B, Sklaroff DM, Yaros MJ: **Free DNA in the serum of cancer patients and the effect of therapy**. *Cancer Res* 1977, **37**(3):646-650.
105. Sorenson GD, Pribish DM, Valone FH, Memoli VA, Bzik DJ, Yao SL: **Soluble normal and mutated DNA sequences from single-copy genes in human blood**. *Cancer Epidemiol Biomarkers Prev* 1994, **3**(1):67-71.
106. Vasioukhin V, Anker P, Maurice P, Lyautey J, Lederrey C, Stroun M: **Point mutations of the N-ras gene in the blood plasma DNA of patients with myelodysplastic syndrome or acute myelogenous leukaemia**. *British Journal of Haematology* 1994, **86**(4):774-779.
107. Nones K, Patch AM: **The Impact of Next Generation Sequencing in Cancer Research**. *Cancers (Basel)* 2020, **12**(10).
108. Crosby D, Lyons N, Greenwood E, Harrison S, Hiom S, Moffat J, Quallo T, Samuel E, Walker I: **A roadmap for the early detection and diagnosis of cancer**. *Lancet Oncol* 2020, **21**(11):1397-1399.
109. Beaver JA, Jelovac D, Balukrishna S, Cochran RL, Croessmann S, Zabransky DJ, Wong HY, Toro PV, Cidado J, Blair BG: **Detection of cancer DNA in plasma of patients with early-stage breast cancer**. *Clinical cancer research* 2014, **20**(10):2643-2650.
110. Xie M, Lu C, Wang J, McLellan MD, Johnson KJ, Wendl MC, McMichael JF, Schmidt HK, Yellapantula V, Miller CA *et al*: **Age-related mutations associated with clonal hematopoietic expansion and malignancies**. *Nat Med* 2014, **20**(12):1472-1478.

111. Martincorena I, Roshan A, Gerstung M, Ellis P, Van Loo P, McLaren S, Wedge DC, Fullam A, Alexandrov LB, Tubio JM *et al*: **Tumor evolution. High burden and pervasive positive selection of somatic mutations in normal human skin**. *Science* 2015, **348**(6237):880-886.
112. Jaiswal S, Fontanillas P, Flannick J, Manning A, Grauman PV, Mar BG, Lindsley RC, Mermel CH, Burtt N, Chavez A *et al*: **Age-Related Clonal Hematopoiesis Associated with Adverse Outcomes**. *New England Journal of Medicine* 2014, **371**(26):2488-2498.
113. Fernandez-Cuesta L, Perdomo S, Avogbe PH, Leblay N, Delhomme TM, Gaborieau V, Abedi-Ardekani B, Chanudet E, Olivier M, Zaridze D *et al*: **Identification of Circulating Tumor DNA for the Early Detection of Small-cell Lung Cancer**. *EBioMedicine* 2016, **10**:117-123.
114. Chan HT, Chin YM, Nakamura Y, Low SK: **Clonal Hematopoiesis in Liquid Biopsy: From Biological Noise to Valuable Clinical Implications**. *Cancers (Basel)* 2020, **12**(8).
115. Genovese G, Kähler AK, Handsaker RE, Lindberg J, Rose SA, Bakhoum SF, Chambert K, Mick E, Neale BM, Fromer M: **Clonal hematopoiesis and blood-cancer risk inferred from blood DNA sequence**. *New England Journal of Medicine* 2014, **371**(26):2477-2487.
116. Garcia-Murillas I, Schiavon G, Weigelt B, Ng C, Hrebien S, Cutts RJ, Cheang M, Osin P, Nerurkar A, Kozarewa I *et al*: **Mutation tracking in circulating tumor DNA predicts relapse in early breast cancer**. *Sci Transl Med* 2015, **7**(302):302ra133.
117. Gormally E, Vineis P, Matullo G, Veglia F, Caboux E, Le Roux E, Peluso M, Garte S, Guarrera S, Munnia A *et al*: **TP53 and KRAS2 mutations in plasma DNA of healthy subjects and subsequent cancer occurrence: a prospective study**. *Cancer Res* 2006, **66**(13):6871-6876.
118. Phallen J, Sausen M, Adleff V, Leal A, Hruban C, White J, Anagnostou V, Fiksel J, Cristiano S, Papp E *et al*: **Direct detection of early-stage cancers using circulating tumor DNA**. *Sci Transl Med* 2017, **9**(403).
119. Chen X, Gole J, Gore A, He Q, Lu M, Min J, Yuan Z, Yang X, Jiang Y, Zhang T *et al*: **Non-invasive early detection of cancer four years before conventional diagnosis using a blood test**. *Nat Commun* 2020, **11**(1):3475.
120. Dawson SJ, Tsui DW, Murtaza M, Biggs H, Rueda OM, Chin SF, Dunning MJ, Gale D, Forshew T, Mahler-Araujo B *et al*: **Analysis of circulating tumor DNA to monitor metastatic breast cancer**. *N Engl J Med* 2013, **368**(13):1199-1209.
121. Punnoose EA, Atwal S, Liu W, Raja R, Fine BM, Hughes BG, Hicks RJ, Hampton GM, Amler LC, Pirzkall A *et al*: **Evaluation of circulating tumor cells and circulating tumor DNA in non-small cell lung cancer: association with clinical endpoints in a phase II clinical trial of pertuzumab and erlotinib**. *Clin Cancer Res* 2012, **18**(8):2391-2401.
122. Spindler KL, Pallisgaard N, Vogelius I, Jakobsen A: **Quantitative cell-free DNA, KRAS, and BRAF mutations in plasma from patients with metastatic colorectal cancer during treatment with cetuximab and irinotecan**. *Clin Cancer Res* 2012, **18**(4):1177-1185.
123. Leary RJ, Sausen M, Kinde I, Papadopoulos N, Carpten JD, Craig D, O'Shaughnessy J, Kinzler KW, Parmigiani G, Vogelstein B *et al*: **Detection of chromosomal alterations in the circulation of cancer patients with whole-genome sequencing**. *Sci Transl Med* 2012, **4**(162):162ra154.

124. Dall'Olio FG, Marabelle A, Caramella C, Garcia C, Aldea M, Chaput N, Robert C, Besse B: **Tumour burden and efficacy of immune-checkpoint inhibitors**. *Nature Reviews Clinical Oncology* 2021.
125. Figg Ii WD, Reid J: **Monitor tumor burden with circulating tumor DNA**. *Cancer Biology & Therapy* 2013, **14**(8):697-698.
126. Rago C, Huso DL, Diehl F, Karim B, Liu G, Papadopoulos N, Samuels Y, Velculescu VE, Vogelstein B, Kinzler KW *et al*: **Serial assessment of human tumor burdens in mice by the analysis of circulating DNA**. *Cancer Res* 2007, **67**(19):9364-9370.
127. Gandara DR, Paul SM, Kowanetz M, Schleifman E, Zou W, Li Y, Rittmeyer A, Fehrenbacher L, Otto G, Malboeuf C *et al*: **Blood-based tumor mutational burden as a predictor of clinical benefit in non-small-cell lung cancer patients treated with atezolizumab**. *Nature Medicine* 2018, **24**(9):1441-1448.
128. Parkinson CA, Gale D, Piskorz AM, Biggs H, Hodgkin C, Addley H, Freeman S, Moyle P, Sala E, Sayal K *et al*: **Exploratory Analysis of TP53 Mutations in Circulating Tumour DNA as Biomarkers of Treatment Response for Patients with Relapsed High-Grade Serous Ovarian Carcinoma: A Retrospective Study**. *PLoS Med* 2016, **13**(12):e1002198.
129. Abbosh C, Birkbak NJ, Wilson GA, Jamal-Hanjani M, Constantin T, Salari R, Le Quesne J, Moore DA, Veeriah S, Rosenthal R *et al*: **Phylogenetic ctDNA analysis depicts early-stage lung cancer evolution**. *Nature* 2017, **545**(7655):446-451.
130. Housman G, Byler S, Heerboth S, Lapinska K, Longacre M, Snyder N, Sarkar S: **Drug resistance in cancer: an overview**. *Cancers (Basel)* 2014, **6**(3):1769-1792.
131. Misale S, Yaeger R, Hobor S, Scala E, Janakiraman M, Liska D, Valtorta E, Schiavo R, Buscarino M, Siravegna G *et al*: **Emergence of KRAS mutations and acquired resistance to anti-EGFR therapy in colorectal cancer**. *Nature* 2012, **486**(7404):532-536.
132. Mohan S, Heitzer E, Ulz P, Lafer I, Lax S, Auer M, Pichler M, Gerger A, Eisner F, Hoefler G *et al*: **Changes in colorectal carcinoma genomes under anti-EGFR therapy identified by whole-genome plasma DNA sequencing**. *PLoS Genet* 2014, **10**(3):e1004271.
133. Valtorta E, Misale S, Sartore-Bianchi A, Nagtegaal ID, Paraf F, Lauricella C, Dimartino V, Hobor S, Jacobs B, Ercolani C *et al*: **KRAS gene amplification in colorectal cancer and impact on response to EGFR-targeted therapy**. *Int J Cancer* 2013, **133**(5):1259-1265.
134. Bardelli A, Corso S, Bertotti A, Hobor S, Valtorta E, Siravegna G, Sartore-Bianchi A, Scala E, Cassingena A, Zecchin D *et al*: **Amplification of the MET receptor drives resistance to anti-EGFR therapies in colorectal cancer**. *Cancer Discov* 2013, **3**(6):658-673.
135. Murtaza M, Dawson SJ, Tsui DW, Gale D, Forshew T, Piskorz AM, Parkinson C, Chin SF, Kingsbury Z, Wong AS *et al*: **Non-invasive analysis of acquired resistance to cancer therapy by sequencing of plasma DNA**. *Nature* 2013, **497**(7447):108-112.
136. Tie J, Cohen JD, Wang Y, Christie M, Simons K, Lee M, Wong R, Kosmider S, Ananda S, McKendrick J *et al*: **Circulating Tumor DNA Analyses as Markers of Recurrence Risk and Benefit of Adjuvant Therapy for Stage III Colon Cancer**. *JAMA Oncol* 2019, **5**(12):1710-1717.
137. Amaro A, Gangemi R, Piaggio F, Angelini G, Barisione G, Ferrini S, Pfeffer U: **The biology of uveal melanoma**. *Cancer Metastasis Rev* 2017, **36**(1):109-140.

138. Chang AE, Karnell LH, Menck HR: **The National Cancer Data Base report on cutaneous and noncutaneous melanoma: a summary of 84,836 cases from the past decade. The American College of Surgeons Commission on Cancer and the American Cancer Society**. *Cancer* 1998, **83**(8):1664-1678.
139. Shields CL, Furuta M, Thangappan A, Nagori S, Mashayekhi A, Lally DR, Kelly CC, Rudich DS, Nagori AV, Wakade OA *et al*: **Metastasis of uveal melanoma millimeter-by-millimeter in 8033 consecutive eyes**. *Arch Ophthalmol* 2009, **127**(8):989-998.
140. Kaliki S, Shields CL: **Uveal melanoma: relatively rare but deadly cancer**. *Eye (Lond)* 2017, **31**(2):241-257.
141. Ghazawi FM, Darwich R, Le M, Rahme E, Zubarev A, Moreau L, Burnier JV, Sasseville D, Burnier MN, Litvinov IV: **Uveal melanoma incidence trends in Canada: a national comprehensive population-based study**. *Br J Ophthalmol* 2019, **103**(12):1872-1876.
142. Aronow ME, Topham AK, Singh AD: **Uveal Melanoma: 5-Year Update on Incidence, Treatment, and Survival (SEER 1973-2013)**. *Ocul Oncol Pathol* 2018, **4**(3):145-151.
143. Virgili G, Gatta G, Ciccolallo L, Capocaccia R, Biggeri A, Crocetti E, Lutz JM, Paci E: **Incidence of uveal melanoma in Europe**. *Ophthalmology* 2007, **114**(12):2309-2315.
144. Singh AD, Topham A: **Incidence of uveal melanoma in the United States: 1973-1997**. *Ophthalmology* 2003, **110**(5):956-961.
145. Riordan-Eva P, Augsburger JJ: **Vaughan & Asbury's General Ophthalmology, 19e**. In., 19th ed. edn. New York, N.Y.: McGraw-Hill Education LLC.; 2018.
146. Nayman T, Bostan C, Logan P, Burnier MN, Jr.: **Uveal Melanoma Risk Factors: A Systematic Review of Meta-Analyses**. *Curr Eye Res* 2017, **42**(8):1085-1093.
147. Weis E, Shah CP, Lajous M, Shields JA, Shields CL: **The association between host susceptibility factors and uveal melanoma: a meta-analysis**. *Arch Ophthalmol* 2006, **124**(1):54-60.
148. Shields CL, Dalvin LA, Yu MD, Ancona-Lezama D, Di Nicola M, Williams BK, Lucio-Alvarez JA, Ang SM, Maloney SM, Welch RJ *et al*: **CHOROIDAL NEVUS TRANSFORMATION INTO MELANOMA PER MILLIMETER INCREMENT IN THICKNESS USING MULTIMODAL IMAGING IN 2355 CASES: The 2019 Wendell L. Hughes Lecture**. *Retina* 2019, **39**(10):1852-1860.
149. Logan P, Bernabeu M, Ferreira A, Burnier MN, Jr.: **Evidence for the Role of Blue Light in the Development of Uveal Melanoma**. *J Ophthalmol* 2015, **2015**:386986.
150. Shah CP, Weis E, Lajous M, Shields JA, Shields CL: **Intermittent and chronic ultraviolet light exposure and uveal melanoma: a meta-analysis**. *Ophthalmology* 2005, **112**(9):1599-1607.
151. Martin M, Masshofer L, Temming P, Rahmann S, Metz C, Bornfeld N, van de Nes J, Klein-Hitpass L, Hinnebusch AG, Horsthemke B *et al*: **Exome sequencing identifies recurrent somatic mutations in EIF1AX and SF3B1 in uveal melanoma with disomy 3**. *Nat Genet* 2013, **45**(8):933-936.
152. Mallet JD, Gendron SP, Drigeard Desgarnier MC, Rochette PJ: **Implication of ultraviolet light in the etiology of uveal melanoma: A review**. *Photochem Photobiol* 2014, **90**(1):15-21.
153. Krauthammer M, Kong Y, Ha BH, Evans P, Bacchiocchi A, McCusker JP, Cheng E, Davis MJ, Goh G, Choi M *et al*: **Exome sequencing identifies recurrent somatic RAC1 mutations in melanoma**. *Nat Genet* 2012, **44**(9):1006-1014.

154. Robertson AG, Shih J, Yau C, Gibb EA, Oba J, Mungall KL, Hess JM, Uzunangelov V, Walter V, Danilova L *et al*: **Integrative Analysis Identifies Four Molecular and Clinical Subsets in Uveal Melanoma**. *Cancer Cell* 2017, **32**(2):204-220.e215.
155. Bove R, Char DH: **Nondiagnosed uveal melanomas**. *Ophthalmology* 2004, **111**(3):554-557.
156. Damato EM, Damato BE: **Detection and time to treatment of uveal melanoma in the United Kingdom: an evaluation of 2,384 patients**. *Ophthalmology* 2012, **119**(8):1582-1589.
157. Branisteanu DC, Bogdanici CM, Branisteanu DE, Maranduca MA, Zemba M, Balta F, Branisteanu CI, Moraru AD: **Uveal melanoma diagnosis and current treatment options (Review)**. *Exp Ther Med* 2021, **22**(6):1428.
158. Kaliki S, Shields CL, Shields JA: **Uveal melanoma: estimating prognosis**. *Indian J Ophthalmol* 2015, **63**(2):93-102.
159. Neves SR, Ram PT, Iyengar R: **G protein pathways**. *Science* 2002, **296**(5573):1636-1639.
160. Feng X, Degese MS, Iglesias-Bartolome R, Vaque JP, Molinolo AA, Rodrigues M, Zaidi MR, Ksander BR, Merlino G, Sodhi A *et al*: **Hippo-independent activation of YAP by the GNAQ uveal melanoma oncogene through a trio-regulated rho GTPase signaling circuitry**. *Cancer Cell* 2014, **25**(6):831-845.
161. Chen X, Wu Q, Depeille P, Chen P, Thornton S, Kalirai H, Coupland SE, Roose JP, Bastian BC: **RasGRP3 Mediates MAPK Pathway Activation in GNAQ Mutant Uveal Melanoma**. *Cancer Cell* 2017, **31**(5):685-696.e686.
162. Bakhoum MF, Esmaeli B: **Molecular Characteristics of Uveal Melanoma: Insights from the Cancer Genome Atlas (TCGA) Project**. *Cancers (Basel)* 2019, **11**(8).
163. Vader MJC, Madigan MC, Versluis M, Suleiman HM, Gezgin G, Gruis NA, Out-Luiting JJ, Bergman W, Verdijk RM, Jager MJ *et al*: **GNAQ and GNA11 mutations and downstream YAP activation in choroidal nevi**. *Br J Cancer* 2017, **117**(6):884-887.
164. Harbour JW, Onken MD, Roberson ED, Duan S, Cao L, Worley LA, Council ML, Matatall KA, Helms C, Bowcock AM: **Frequent mutation of BAP1 in metastasizing uveal melanomas**. *Science* 2010, **330**(6009):1410-1413.
165. Furney SJ, Pedersen M, Gentien D, Dumont AG, Rapinat A, Desjardins L, Turajlic S, Piperno-Neumann S, de la Grange P, Roman-Roman S *et al*: **SF3B1 mutations are associated with alternative splicing in uveal melanoma**. *Cancer Discov* 2013, **3**(10):1122-1129.
166. Finger PT, Kurli M, Reddy S, Tena LB, Pavlick AC: **Whole body PET/CT for initial staging of choroidal melanoma**. *Br J Ophthalmol* 2005, **89**(10):1270-1274.
167. **Assessment of metastatic disease status at death in 435 patients with large choroidal melanoma in the Collaborative Ocular Melanoma Study (COMS): COMS report no. 15**. *Arch Ophthalmol* 2001, **119**(5):670-676.
168. Diener-West M, Reynolds SM, Agugliaro DJ, Caldwell R, Cumming K, Earle JD, Hawkins BS, Hayman JA, Jaiyesimi I, Jampol LM *et al*: **Development of metastatic disease after enrollment in the COMS trials for treatment of choroidal melanoma: Collaborative Ocular Melanoma Study Group Report No. 26**. *Arch Ophthalmol* 2005, **123**(12):1639-1643.
169. Nathan P, Cohen V, Coupland S, Curtis K, Damato B, Evans J, Fenwick S, Kirkpatrick L, Li O, Marshall E *et al*: **Uveal Melanoma UK National Guidelines**. *Eur J Cancer* 2015, **51**(16):2404-2412.

170. Singh AD, Shields CL, Shields JA: **Prognostic factors in uveal melanoma**. *Melanoma Res* 2001, **11**(3):255-263.
171. Borthwick NJ, Thombs J, Polak M, Gabriel FG, Hungerford JL, Damato B, Rennie IG, Jager MJ, Cree IA: **The biology of micrometastases from uveal melanoma**. *J Clin Pathol* 2011, **64**(8):666-671.
172. Manschot WA, van Strik R: **Uveal melanoma: therapeutic consequences of doubling times and irradiation results; a review**. *Int Ophthalmol* 1992, **16**(2):91-99.
173. Singh AD, Rennie IG, Kivela T, Seregard S, Grossniklaus H: **The Zimmerman-McLean-Foster hypothesis: 25 years later**. *Br J Ophthalmol* 2004, **88**(7):962-967.
174. Callejo SA, Antecka E, Blanco PL, Edelstein C, Burnier MN, Jr.: **Identification of circulating malignant cells and its correlation with prognostic factors and treatment in uveal melanoma. A prospective longitudinal study**. *Eye (Lond)* 2007, **21**(6):752-759.
175. Paula L. Blanco J-CAM, Sonia A. Callejo, Emilia Antecka and Miguel N. Burnier Jr.: **Detection of circulating malignant cells in a uveal melanoma animal model**. *ARVO preceedings* 2004, **5110**.
176. Logan PT, Fernandes BF, Di Cesare S, Marshall JC, Maloney SC, Burnier MN, Jr.: **Single-cell tumor dormancy model of uveal melanoma**. *Clin Exp Metastasis* 2008, **25**(5):509-516.
177. Carvajal RD, Schwartz GK, Tezel T, Marr B, Francis JH, Nathan PD: **Metastatic disease from uveal melanoma: treatment options and future prospects**. *Br J Ophthalmol* 2017, **101**(1):38-44.
178. Diener-West M, Hawkins BS, Markowitz JA, Schachat AP: **A review of mortality from choroidal melanoma. II. A meta-analysis of 5-year mortality rates following enucleation, 1966 through 1988**. *Arch Ophthalmol* 1992, **110**(2):245-250.
179. Seddon JM, Albert DM, Lavin PT, Robinson N: **A prognostic factor study of disease-free interval and survival following enucleation for uveal melanoma**. *Arch Ophthalmol* 1983, **101**(12):1894-1899.
180. Coupland SE, Campbell I, Damato B: **Routes of extraocular extension of uveal melanoma: risk factors and influence on survival probability**. *Ophthalmology* 2008, **115**(10):1778-1785.
181. Farquhar N, Thornton S, Coupland SE, Coulson JM, Sacco JJ, Krishna Y, Heimann H, Taktak A, Cebulla CM, Abdel-Rahman MH *et al*: **Patterns of BAP1 protein expression provide insights into prognostic significance and the biology of uveal melanoma**. *J Pathol Clin Res* 2018, **4**(1):26-38.
182. **Histopathologic characteristics of uveal melanomas in eyes enucleated from the Collaborative Ocular Melanoma Study. COMS report no. 6**. *Am J Ophthalmol* 1998, **125**(6):745-766.
183. Gamel JW, McLean IW, Foster WD, Zimmerman LE: **Uveal melanomas: correlation of cytologic features with prognosis**. *Cancer* 1978, **41**(5):1897-1901.
184. McLean IW, Foster WD, Zimmerman LE, Gamel JW: **Modifications of Callender's Classification of Uveal Melanoma at the Armed Forces Institute of Pathology**. *Am J Ophthalmol* 2018, **195**:lvi-lx.
185. Griewank KG, van de Nes J, Schilling B, Moll I, Sucker A, Kakavand H, Haydu LE, Asher M, Zimmer L, Hillen U *et al*: **Genetic and clinico-pathologic analysis of metastatic uveal melanoma**. *Mod Pathol* 2014, **27**(2):175-183.

186. McLean MJ, Foster WD, Zimmerman LE: **Prognostic factors in small malignant melanomas of choroid and ciliary body**. *Arch Ophthalmol* 1977, **95**(1):48-58.
187. Folberg R, Pe'er J, Gruman LM, Woolson RF, Jeng G, Montague PR, Moninger TO, Yi H, Moore KC: **The morphologic characteristics of tumor blood vessels as a marker of tumor progression in primary human uveal melanoma: a matched case-control study**. *Hum Pathol* 1992, **23**(11):1298-1305.
188. Stalhammar G, See TRO, Phillips SS, Grossniklaus HE: **Density of PAS positive patterns in uveal melanoma: Correlation with vasculogenic mimicry, gene expression class, BAP-1 expression, macrophage infiltration, and risk for metastasis**. *Mol Vis* 2019, **25**:502-516.
189. Maniotis AJ, Folberg R, Hess A, Seftor EA, Gardner LM, Pe'er J, Trent JM, Meltzer PS, Hendrix MJ: **Vascular channel formation by human melanoma cells in vivo and in vitro: vasculogenic mimicry**. *Am J Pathol* 1999, **155**(3):739-752.
190. Makitie T, Summanen P, Tarkkanen A, Kivela T: **Microvascular loops and networks as prognostic indicators in choroidal and ciliary body melanomas**. *J Natl Cancer Inst* 1999, **91**(4):359-367.
191. de la Cruz PO, Jr., Specht CS, McLean IW: **Lymphocytic infiltration in uveal malignant melanoma**. *Cancer* 1990, **65**(1):112-115.
192. Bronkhorst IH, Ly LV, Jordanova ES, Vrolijk J, Versluis M, Luyten GP, Jager MJ: **Detection of M2-macrophages in uveal melanoma and relation with survival**. *Invest Ophthalmol Vis Sci* 2011, **52**(2):643-650.
193. Djirackor L, Shakir D, Kalirai H, Petrovski G, Coupland SE: **Nestin expression in primary and metastatic uveal melanoma - possible biomarker for high-risk uveal melanoma**. *Acta Ophthalmol* 2018, **96**(5):503-509.
194. Szalai E, Wells JR, Ward L, Grossniklaus HE: **Uveal Melanoma Nuclear BRCA1-Associated Protein-1 Immunoreactivity Is an Indicator of Metastasis**. *Ophthalmology* 2018, **125**(2):203-209.
195. Glasgow BJ, McCannel TA: **Correlation of Immunocytochemistry of BRCA1-associated Protein-1 (BAP1) With Other Prognostic Markers in Uveal Melanoma**. *Am J Ophthalmol* 2018, **189**:122-126.
196. Shields CL, Ganguly A, Bianciotto CG, Turaka K, Tavallali A, Shields JA: **Prognosis of uveal melanoma in 500 cases using genetic testing of fine-needle aspiration biopsy specimens**. *Ophthalmology* 2011, **118**(2):396-401.
197. Hastings RJ, Bown N, Tibiletti MG, Debiec-Rychter M, Vanni R, Espinet B, van Roy N, Roberts P, van den Berg-de-Ruiter E, Bernheim A *et al*: **Guidelines for cytogenetic investigations in tumours**. *Eur J Hum Genet* 2016, **24**(1):6-13.
198. Papadopoulos S, Benter T, Anastassiou G, Pape M, Gerhard S, Bornfeld N, Ludwig WD, Dorken B: **Assessment of genomic instability in breast cancer and uveal melanoma by random amplified polymorphic DNA analysis**. *Int J Cancer* 2002, **99**(2):193-200.
199. Cross NA, Murray AK, Rennie IG, Ganesh A, Sisley K: **Instability of microsatellites is an infrequent event in uveal melanoma**. *Melanoma Res* 2003, **13**(5):435-440.
200. Coleman K, Baak JP, van Diest PJ, Curran B, Mullaney J, Fenton M, Leader M: **DNA ploidy status in 84 ocular melanomas: a study of DNA quantitation in ocular melanomas by flow cytometry and automatic and interactive static image analysis**. *Hum Pathol* 1995, **26**(1):99-105.

201. Horsman DE, Sroka H, Rootman J, White VA: **Monosomy 3 and isochromosome 8q in a uveal melanoma**. *Cancer Genet Cytogenet* 1990, **45**(2):249-253.
202. Prescher G, Bornfeld N, Hirche H, Horsthemke B, Jockel KH, Becher R: **Prognostic implications of monosomy 3 in uveal melanoma**. *Lancet* 1996, **347**(9010):1222-1225.
203. Damato B, Duke C, Coupland SE, Hiscott P, Smith PA, Campbell I, Douglas A, Howard P: **Cytogenetics of uveal melanoma: a 7-year clinical experience**. *Ophthalmology* 2007, **114**(10):1925-1931.
204. Sisley K, Rennie IG, Parsons MA, Jacques R, Hammond DW, Bell SM, Potter AM, Rees RC: **Abnormalities of chromosomes 3 and 8 in posterior uveal melanoma correlate with prognosis**. *Genes Chromosomes Cancer* 1997, **19**(1):22-28.
205. Parrella P, Caballero OL, Sidransky D, Merbs SL: **Detection of c-myc amplification in uveal melanoma by fluorescent in situ hybridization**. *Invest Ophthalmol Vis Sci* 2001, **42**(8):1679-1684.
206. Ehlers JP, Harbour JW: **NBS1 expression as a prognostic marker in uveal melanoma**. *Clin Cancer Res* 2005, **11**(5):1849-1853.
207. Ehlers JP, Worley L, Onken MD, Harbour JW: **DDEF1 is located in an amplified region of chromosome 8q and is overexpressed in uveal melanoma**. *Clin Cancer Res* 2005, **11**(10):3609-3613.
208. Onken MD, Worley LA, Harbour JW: **A metastasis modifier locus on human chromosome 8p in uveal melanoma identified by integrative genomic analysis**. *Clin Cancer Res* 2008, **14**(12):3737-3745.
209. Kilic E, Naus NC, van Gils W, Klaver CC, van Til ME, Verbiest MM, Stijnen T, Mooy CM, Paridaens D, Beverloo HB *et al*: **Concurrent loss of chromosome arm 1p and chromosome 3 predicts a decreased disease-free survival in uveal melanoma patients**. *Invest Ophthalmol Vis Sci* 2005, **46**(7):2253-2257.
210. Hausler T, Stang A, Anastassiou G, Jockel KH, Mrzyk S, Horsthemke B, Lohmann DR, Zeschnigk M: **Loss of heterozygosity of 1p in uveal melanomas with monosomy 3**. *Int J Cancer* 2005, **116**(6):909-913.
211. Damato BE, Heimann H, Kalirai H, Coupland SE: **Age, survival predictors, and metastatic death in patients with choroidal melanoma: tentative evidence of a therapeutic effect on survival**. *JAMA Ophthalmol* 2014, **132**(5):605-613.
212. Smit KN, Jager MJ, de Klein A, Kili E: **Uveal melanoma: Towards a molecular understanding**. *Prog Retin Eye Res* 2019:100800.
213. Park JJ, Diefenbach RJ, Joshua AM, Kefford RF, Carlino MS, Rizos H: **Oncogenic signaling in uveal melanoma**. *Pigment Cell Melanoma Res* 2018, **31**(6):661-672.
214. Jensen DE, Proctor M, Marquis ST, Gardner HP, Ha SI, Chodosh LA, Ishov AM, Tommerup N, Vissing H, Sekido Y *et al*: **BAP1: a novel ubiquitin hydrolase which binds to the BRCA1 RING finger and enhances BRCA1-mediated cell growth suppression**. *Oncogene* 1998, **16**(9):1097-1112.
215. Gupta MP, Lane AM, DeAngelis MM, Mayne K, Crabtree M, Gragoudas ES, Kim IK: **Clinical Characteristics of Uveal Melanoma in Patients With Germline BAP1 Mutations**. *JAMA Ophthalmol* 2015, **133**(8):881-887.
216. Rai K, Pilarski R, Boru G, Rehman M, Saqr AH, Massengill JB, Singh A, Marino MJ, Davidorf FH, Cebulla CM *et al*: **Germline BAP1 alterations in familial uveal melanoma**. *Genes Chromosomes Cancer* 2017, **56**(2):168-174.

217. Cebulla CM, Binkley EM, Pilarski R, Massengill JB, Rai K, Liebner DA, Marino MJ, Singh AD, Abdel-Rahman MH: **Analysis of BAP1 Germline Gene Mutation in Young Uveal Melanoma Patients**. *Ophthalmic Genet* 2015, **36**(2):126-131.
218. Landreville S, Agapova OA, Matatall KA, Kneass ZT, Onken MD, Lee RS, Bowcock AM, Harbour JW: **Histone deacetylase inhibitors induce growth arrest and differentiation in uveal melanoma**. *Clin Cancer Res* 2012, **18**(2):408-416.
219. Yavuzyigitoglu S, Koopmans AE, Verdijk RM, Vaarwater J, Eussen B, van Bodegom A, Paridaens D, Kilic E, de Klein A: **Uveal Melanomas with SF3B1 Mutations: A Distinct Subclass Associated with Late-Onset Metastases**. *Ophthalmology* 2016, **123**(5):1118-1128.
220. Zhang J, Lieu YK, Ali AM, Penson A, Reggio KS, Rabadan R, Raza A, Mukherjee S, Manley JL: **Disease-associated mutation in SRSF2 misregulates splicing by altering RNA-binding affinities**. *Proc Natl Acad Sci U S A* 2015, **112**(34):E4726-4734.
221. Amin MB, Greene FL, Edge SB, Compton CC, Gershenwald JE, Brookland RK, Meyer L, Gress DM, Byrd DR, Winchester DP: **The Eighth Edition AJCC Cancer Staging Manual: Continuing to build a bridge from a population-based to a more "personalized" approach to cancer staging**. *CA Cancer J Clin* 2017, **67**(2):93-99.
222. **International Validation of the American Joint Committee on Cancer's 7th Edition Classification of Uveal Melanoma**. *JAMA Ophthalmol* 2015, **133**(4):376-383.
223. Dogrusoz M, Bagger M, van Duinen SG, Kroes WG, Ruivenkamp CA, Bohringer S, Andersen KK, Luyten GP, Kiilgaard JF, Jager MJ: **The Prognostic Value of AJCC Staging in Uveal Melanoma Is Enhanced by Adding Chromosome 3 and 8q Status**. *Invest Ophthalmol Vis Sci* 2017, **58**(2):833-842.
224. Harbour JW, Chen R: **The DecisionDx-UM Gene Expression Profile Test Provides Risk Stratification and Individualized Patient Care in Uveal Melanoma**. *PLoS Curr* 2013, **5**.
225. Tschentscher F, Husing J, Holter T, Kruse E, Dresen IG, Jockel KH, Anastassiou G, Schilling H, Bornfeld N, Horsthemke B *et al*: **Tumor classification based on gene expression profiling shows that uveal melanomas with and without monosomy 3 represent two distinct entities**. *Cancer Res* 2003, **63**(10):2578-2584.
226. Onken MD, Worley LA, Char DH, Augsburger JJ, Correa ZM, Nudleman E, Aaberg TM, Jr., Altaweel MM, Bardenstein DS, Finger PT *et al*: **Collaborative Ocular Oncology Group report number 1: prospective validation of a multi-gene prognostic assay in uveal melanoma**. *Ophthalmology* 2012, **119**(8):1596-1603.
227. Onken MD, Worley LA, Ehlers JP, Harbour JW: **Gene expression profiling in uveal melanoma reveals two molecular classes and predicts metastatic death**. *Cancer Res* 2004, **64**(20):7205-7209.
228. Chang SH, Worley LA, Onken MD, Harbour JW: **Prognostic biomarkers in uveal melanoma: evidence for a stem cell-like phenotype associated with metastasis**. *Melanoma Res* 2008, **18**(3):191-200.
229. Landreville S, Agapova OA, Harbour JW: **Emerging insights into the molecular pathogenesis of uveal melanoma**. *Future Oncol* 2008, **4**(5):629-636.
230. Vaquero-Garcia J, Lalonde E, Ewens KG, Ebrahimzadeh J, Richard-Yutz J, Shields CL, Barrera A, Green CJ, Barash Y, Ganguly A: **PRiMeUM: A Model for Predicting Risk of Metastasis in Uveal Melanoma**. *Invest Ophthalmol Vis Sci* 2017, **58**(10):4096-4105.

231. Damato B, Eleuteri A, Taktak AF, Coupland SE: **Estimating prognosis for survival after treatment of choroidal melanoma**. *Prog Retin Eye Res* 2011, **30**(5):285-295.
232. Cunha Rola A, Taktak A, Eleuteri A, Kalirai H, Heimann H, Hussain R, Bonnett LJ, Hill CJ, Traynor M, Jager MJ *et al*: **Multicenter External Validation of the Liverpool Uveal Melanoma Prognosticator Online: An OOG Collaborative Study**. *Cancers (Basel)* 2020, **12**(2).
233. Field MG, Decatur CL, Kurtenbach S, Gezgin G, van der Velden PA, Jager MJ, Kozak KN, Harbour JW: **PRAME as an Independent Biomarker for Metastasis in Uveal Melanoma**. *Clin Cancer Res* 2016, **22**(5):1234-1242.
234. Field MG, Durante MA, Decatur CL, Tarlan B, Oelschlager KM, Stone JF, Kuznetsov J, Bowcock AM, Kurtenbach S, Harbour JW: **Epigenetic reprogramming and aberrant expression of PRAME are associated with increased metastatic risk in Class 1 and Class 2 uveal melanomas**. *Oncotarget* 2016, **7**(37):59209-59219.
235. Cai L, Paez-Escamilla M, Walter SD, Tarlan B, Decatur CL, Perez BM, Harbour JW: **Gene Expression Profiling and PRAME Status Versus Tumor-Node-Metastasis Staging for Prognostication in Uveal Melanoma**. *Am J Ophthalmol* 2018, **195**:154-160.
236. Schefler AC, Koca E, Bernicker EH, Correa ZM: **Relationship between clinical features, GEP class, and PRAME expression in uveal melanoma**. *Graefes Arch Clin Exp Ophthalmol* 2019, **257**(7):1541-1545.
237. Jager MJ, Brouwer NJ, Esmaeli B: **The Cancer Genome Atlas Project: An Integrated Molecular View of Uveal Melanoma**. *Ophthalmology* 2018, **125**(8):1139-1142.
238. Mazloumi M, Vichitvejpaisal P, Dalvin LA, Yaghy A, Ewens KG, Ganguly A, Shields CL: **Accuracy of The Cancer Genome Atlas Classification vs American Joint Committee on Cancer Classification for Prediction of Metastasis in Patients With Uveal Melanoma**. *JAMA Ophthalmol* 2020.
239. Pan H, Lu L, Cui J, Yang Y, Wang Z, Fan X: **Immunological analyses reveal an immune subtype of uveal melanoma with a poor prognosis**. *Aging (Albany NY)* 2020, **12**(2):1446-1464.
240. Damato B: **Ocular treatment of choroidal melanoma in relation to the prevention of metastatic death - A personal view**. *Prog Retin Eye Res* 2018, **66**:187-199.
241. Xu L.T. FP, Tarhini A.A., Singh A.D.: **Uveal Melanoma: Metastases**. In: *Clinical Ophthalmic Oncology.* edn. Edited by Damato B. SA: Springer Cham; 2019.
242. Lane AM, Kim IK, Gragoudas ES: **Survival Rates in Patients After Treatment for Metastasis From Uveal Melanoma**. *JAMA Ophthalmol* 2018, **136**(9):981-986.
243. Yang J, Manson DK, Marr BP, Carvajal RD: **Treatment of uveal melanoma: where are we now?** *Ther Adv Med Oncol* 2018, **10**:1758834018757175.
244. Violanti SS, Bononi I, Gallenga CE, Martini F, Tognon M, Perri P: **New Insights into Molecular Oncogenesis and Therapy of Uveal Melanoma**. *Cancers (Basel)* 2019, **11**(5).
245. Servois V, Bouhadiba T, Dureau S, Da Costa C, Almubarak MM, Foucher R, Savignoni A, Cassoux N, Pierron G, Mariani P: **Iterative treatment with surgery and radiofrequency ablation of uveal melanoma liver metastasis: Retrospective analysis of a series of very long-term survivors**. *Eur J Surg Oncol* 2019, **45**(9):1717-1722.
246. Mariani P, Almubarak MM, Kollen M, Wagner M, Plancher C, Audollent R, Piperno-Neumann S, Cassoux N, Servois V: **Radiofrequency ablation and surgical resection of liver metastases from uveal melanoma**. *Eur J Surg Oncol* 2016, **42**(5):706-712.

247. Rozeman EA, Dekker TJA, Haanen J, Blank CU: **Advanced Melanoma: Current Treatment Options, Biomarkers, and Future Perspectives**. *Am J Clin Dermatol* 2018, **19**(3):303-317.
248. Rowcroft A, Loveday BPT, Thomson BNJ, Banting S, Knowles B: **Systematic review of liver directed therapy for uveal melanoma hepatic metastases**. *HPB (Oxford)* 2019.
249. Wessely A, Steeb T, Erdmann M, Heinzerling L, Vera J, Schlaak M, Berking C, Heppt MV: **The Role of Immune Checkpoint Blockade in Uveal Melanoma**. *Int J Mol Sci* 2020, **21**(3).
250. Chandran SS, Somerville RPT, Yang JC, Sherry RM, Klebanoff CA, Goff SL, Wunderlich JR, Danforth DN, Zlott D, Paria BC *et al*: **Treatment of metastatic uveal melanoma with adoptive transfer of tumour-infiltrating lymphocytes: a single-centre, two-stage, single-arm, phase 2 study**. *Lancet Oncol* 2017, **18**(6):792-802.
251. Chalmers ZR, Connelly CF, Fabrizio D, Gay L, Ali SM, Ennis R, Schrock A, Campbell B, Shlien A, Chmielecki J *et al*: **Analysis of 100,000 human cancer genomes reveals the landscape of tumor mutational burden**. *Genome Med* 2017, **9**(1):34.
252. Patel M, Smyth E, Chapman PB, Wolchok JD, Schwartz GK, Abramson DH, Carvajal RD: **Therapeutic implications of the emerging molecular biology of uveal melanoma**. *Clin Cancer Res* 2011, **17**(8):2087-2100.
253. Carvajal RD, Sosman JA, Quevedo JF, Milhem MM, Joshua AM, Kudchadkar RR, Linette GP, Gajewski TF, Lutzky J, Lawson DH *et al*: **Effect of selumetinib vs chemotherapy on progression-free survival in uveal melanoma: a randomized clinical trial**. *Jama* 2014, **311**(23):2397-2405.
254. Shields CL, Kaliki S, Shah SU, Luo W, Furuta M, Shields JA: **Iris melanoma: features and prognosis in 317 children and adults**. *J aapos* 2012, **16**(1):10-16.
255. Oittinen HA, O'Shaughnessy M, Cullinane AB, Keohane C: **Malignant melanoma of the ciliary body presenting as extraocular metastasis in the temporalis muscle**. *J Clin Pathol* 2007, **60**(7):834-835.
256. Toro MD, Gozzo L, Tracia L, Cicciù M, Drago F, Bucolo C, Avitabile T, Rejdak R, Nowomiejska K, Zweifel S *et al*: **New Therapeutic Perspectives in the Treatment of Uveal Melanoma: A Systematic Review**. *Biomedicines* 2021, **9**(10).
257. Madic J, Piperno-Neumann S, Servois V, Rampanou A, Milder M, Trouiller B, Gentien D, Saada S, Assayag F, Thuleau A *et al*: **Pyrophosphorolysis-activated polymerization detects circulating tumor DNA in metastatic uveal melanoma**. *Clin Cancer Res* 2012, **18**(14):3934-3941.
258. Metz CH, Scheulen M, Bornfeld N, Lohmann D, Zeschnigk M: **Ultradeep sequencing detects GNAQ and GNA11 mutations in cell-free DNA from plasma of patients with uveal melanoma**. *Cancer Med* 2013, **2**(2):208-215.
259. Bidard FC, Madic J, Mariani P, Piperno-Neumann S, Rampanou A, Servois V, Cassoux N, Desjardins L, Milder M, Vaucher I *et al*: **Detection rate and prognostic value of circulating tumor cells and circulating tumor DNA in metastatic uveal melanoma**. *Int J Cancer* 2014, **134**(5):1207-1213.
260. Beasley A, Isaacs T, Khattak MA, Freeman JB, Allcock R, Chen FK, Pereira MR, Yau K, Bentel J, Vermeulen T *et al*: **Clinical Application of Circulating Tumor Cells and Circulating Tumor DNA in Uveal Melanoma**. *JCO Precision Oncology* 2018(2):1-12.

261. Le Guin CHD, Bornfeld N, Bechrakis NE, Jabbarli L, Richly H, Lohmann DR, Zeschnigk M: **Early detection of metastatic uveal melanoma by the analysis of tumor-specific mutations in cell-free plasma DNA**. *Cancer Med* 2021, **10**(17):5974-5982.
262. Cabel L, Riva F, Servois V, Livartowski A, Daniel C, Rampanou A, Lantz O, Romano E, Milder M, Buecher B *et al*: **Circulating tumor DNA changes for early monitoring of anti-PD1 immunotherapy: a proof-of-concept study**. *Ann Oncol* 2017, **28**(8):1996-2001.
263. Rodrigues T, Kundu B, Silva-Correia J, Kundu SC, Oliveira JM, Reis RL, Correlo VM: **Emerging tumor spheroids technologies for 3D in vitro cancer modeling**. *Pharmacol Ther* 2018, **184**:201-211.
264. Park JJ, Diefenbach RJ, Byrne N, Long GV, Scolyer RA, Gray ES, Carlino MS, Rizos H: **Circulating Tumor DNA Reflects Uveal Melanoma Responses to Protein Kinase C Inhibition**. *Cancers (Basel)* 2021, **13**(7).
265. Ignatiadis M, Sledge GW, Jeffrey SS: **Liquid biopsy enters the clinic — implementation issues and future challenges**. *Nature Reviews Clinical Oncology* 2021, **18**(5):297-312.
266. Rodrigues M, Mobuchon L, Houy A, Fiévet A, Gardrat S, Barnhill RL, Popova T, Servois V, Rampanou A, Mouton A *et al*: **Outlier response to anti-PD1 in uveal melanoma reveals germline MBD4 mutations in hypermutated tumors**. *Nat Commun* 2018, **9**(1):1866.
267. Jager MJ, Shields CL, Cebulla CM, Abdel-Rahman MH, Grossniklaus HE, Stern MH, Carvajal RD, Belfort RN, Jia R, Shields JA *et al*: **Uveal melanoma**. *Nat Rev Dis Primers* 2020, **6**(1):24.
268. Jovanovic P, Mihajlovic M, Djordjevic-Jocic J, Vlajkovic S, Cekic S, Stefanovic V: **Ocular melanoma: an overview of the current status**. *Int J Clin Exp Pathol* 2013, **6**(7):1230-1244.
269. Smit KN, Jager MJ, de Klein A, Kiliç E: **Uveal melanoma: Towards a molecular understanding**. *Prog Retin Eye Res* 2020, **75**:100800.
270. Hammer H, Oláh J, Tóth-Molnár E: **Dysplastic nevi are a risk factor for uveal melanoma**. *Eur J Ophthalmol* 1996, **6**(4):472-474.
271. Shields CL, Kaliki S, Livesey M, Walker B, Garoon R, Bucci M, Feinstein E, Pesch A, Gonzalez C, Lally SE *et al*: **Association of ocular and oculodermal melanocytosis with the rate of uveal melanoma metastasis: analysis of 7872 consecutive eyes**. *JAMA Ophthalmol* 2013, **131**(8):993-1003.
272. Abdel-Rahman MH, Pilarski R, Cebulla CM, Massengill JB, Christopher BN, Boru G, Hovland P, Davidorf FH: **Germline BAP1 mutation predisposes to uveal melanoma, lung adenocarcinoma, meningioma, and other cancers**. *J Med Genet* 2011, **48**(12):856-859.
273. Singh AD, Kalyani P, Topham A: **Estimating the risk of malignant transformation of a choroidal nevus**. *Ophthalmology* 2005, **112**(10):1784-1789.
274. Frizziero L, Midena E, Trainiti S, Londei D, Bonaldi L, Bini S, Parrozzani R: **Uveal Melanoma Biopsy: A Review**. *Cancers (Basel)* 2019, **11**(8).
275. Mccannel T: **Choroidal Melanoma: Updates for a Challenging Disease**. *Retinal Physician* 2014, **12**:35-37.
276. Augsburger JJ, Corrêa ZlM, Trichopoulos N, Shaikh A: **Size Overlap between Benign Melanocytic Choroidal Nevi and Choroidal Malignant Melanomas**. *Investigative Ophthalmology & Visual Science* 2008, **49**(7):2823-2828.

277. Shields CL, Say EAT, Hasanreisoglu M, Saktanasate J, Lawson BM, Landy JE, Badami AU, Sivalingam MD, Hauschild AJ, House RJ *et al*: **Personalized Prognosis of Uveal Melanoma Based on Cytogenetic Profile in 1059 Patients over an 8-Year Period: The 2017 Harry S. Gradle Lecture**. *Ophthalmology* 2017, **124**(10):1523-1531.
278. Bande Rodriguez MF, Fernandez Marta B, Lago Baameiro N, Santiago-Varela M, Silva-Rodriguez P, Blanco-Teijeiro MJ, Pardo Perez M, Pineiro Ces A: **Blood Biomarkers of Uveal Melanoma: Current Perspectives**. *Clin Ophthalmol* 2020, **14**:157-169.
279. Yu H, Han L, Yuan J, Sun Y: **Circulating tumor cell free DNA from plasma and urine in the clinical management of colorectal cancer**. *Cancer Biomark* 2020, **27**(1):29-37.
280. Zhang P, Wu X, Tang M, Nie X, Li L: **Detection of EGFR gene mutation status from pleural effusions and other body fluid specimens in patients with lung adenocarcinoma**. *Thorac Cancer* 2019, **10**(12):2218-2224.
281. Jin E, Burnier JV: **Liquid Biopsy in Uveal Melanoma: Are We There Yet?** *Ocular Oncology and Pathology* 2020.
282. Zhou Y, Ren H, Dai B, Li J, Shang L, Huang J, Shi X: **Hepatocellular carcinoma-derived exosomal miRNA-21 contributes to tumor progression by converting hepatocyte stellate cells to cancer-associated fibroblasts**. *J Exp Clin Cancer Res* 2018, **37**(1):324.
283. Johansson G, Andersson D, Filges S, Li J, Muth A, Godfrey TE, Stahlberg A: **Considerations and quality controls when analyzing cell-free tumor DNA**. *Biomol Detect Quantif* 2019, **17**:100078.
284. Busser B, Lupo J, Sancey L, Mouret S, Faure P, Plumas J, Chaperot L, Leccia MT, Coll JL, Hurbin A *et al*: **Plasma Circulating Tumor DNA Levels for the Monitoring of Melanoma Patients: Landscape of Available Technologies and Clinical Applications**. *Biomed Res Int* 2017, **2017**:5986129.
285. De Waard-Siebinga I, Blom DJ, Griffioen M, Schrier PI, Hoogendoorn E, Beverstock G, Danen EH, Jager MJ: **Establishment and characterization of an uveal-melanoma cell line**. *Int J Cancer* 1995, **62**(2):155-161.
286. Baron EDNMS, Carol.: **Update AJCC classification for posteroir uveal melanoma**. *Oncular Oncology* 2018, **Retina Today**:30-34.
287. Tossberg JT, Esmond TM, Aune TM: **A simplified method to produce mRNAs and functional proteins from synthetic double-stranded DNA templates**. *Biotechniques* 2020, **69**(4):281-288.
288. Amirouchene-Angelozzi N, Nemati F, Gentien D, Nicolas A, Dumont A, Carita G, Camonis J, Desjardins L, Cassoux N, Piperno-Neumann S *et al*: **Establishment of novel cell lines recapitulating the genetic landscape of uveal melanoma and preclinical validation of mTOR as a therapeutic target**. *Mol Oncol* 2014, **8**(8):1508-1520.
289. Yu FX, Luo J, Mo JS, Liu G, Kim YC, Meng Z, Zhao L, Peyman G, Ouyang H, Jiang W *et al*: **Mutant Gq/11 promote uveal melanoma tumorigenesis by activating YAP**. *Cancer Cell* 2014, **25**(6):822-830.
290. Mellen PL, Morton SJ, Shields CL: **American joint committee on cancer staging of uveal melanoma**. *Oman J Ophthalmol* 2013, **6**(2):116-118.
291. Dalvin LA, Shields CL, Ancona-Lezama DA, Yu MD, Di Nicola M, Williams BK, Jr., Lucio-Alvarez JA, Ang SM, Maloney SM, Welch RJ *et al*: **Combination of multimodal imaging features predictive of choroidal nevus transformation into melanoma**. *Br J Ophthalmol* 2019, **103**(10):1441-1447.

292. Siravegna G, Mussolin B, Venesio T, Marsoni S, Seoane J, Dive C, Papadopoulos N, Kopetz S, Corcoran RB, Siu LL *et al*: **How liquid biopsies can change clinical practice in oncology**. *Ann Oncol* 2019, **30**(10):1580-1590.
293. Bidard FC, Peeters DJ, Fehm T, Nolé F, Gisbert-Criado R, Mavroudis D, Grisanti S, Generali D, Garcia-Saenz JA, Stebbing J *et al*: **Clinical validity of circulating tumour cells in patients with metastatic breast cancer: a pooled analysis of individual patient data**. *Lancet Oncol* 2014, **15**(4):406-414.
294. Geeurickx E, Hendrix A: **Targets, pitfalls and reference materials for liquid biopsy tests in cancer diagnostics**. *Mol Aspects Med* 2019:100828.
295. Wierenga APA, Cao J, Mouthaan H, van Weeghel C, Verdijk RM, van Duinen SG, Kroes WGM, Dogrusöz M, Marinkovic M, van der Burg SSH *et al*: **Aqueous Humor Biomarkers Identify Three Prognostic Groups in Uveal Melanoma**. *Invest Ophthalmol Vis Sci* 2019, **60**(14):4740-4747.
296. Chen MX, Liu YM, Li Y, Yang X, Wei WB: **Elevated VEGF-A & PLGF concentration in aqueous humor of patients with uveal melanoma following Iodine-125 plaque radiotherapy**. *Int J Ophthalmol* 2020, **13**(4):599-605.
297. van Ginkel JH, van den Broek DA, van Kuik J, Linders D, de Weger R, Willems SM, Huibers MMH: **Preanalytical blood sample workup for cell-free DNA analysis using Droplet Digital PCR for future molecular cancer diagnostics**. *Cancer Med* 2017, **6**(10):2297-2307.
298. Lampignano R, Neumann MHD, Weber S, Kloten V, Herdean A, Voss T, Groelz D, Babayan A, Tibbesma M, Schlumpberger M *et al*: **Multicenter Evaluation of Circulating Cell-Free DNA Extraction and Downstream Analyses for the Development of Standardized (Pre)analytical Work Flows**. *Clin Chem* 2020, **66**(1):149-160.
299. Barak V, Pe'er J, Kalickman I, Frenkel S: **VEGF as a biomarker for metastatic uveal melanoma in humans**. *Curr Eye Res* 2011, **36**(4):386-390.
300. Schaller UC, Bosserhoff AK, Neubauer AS, Buettner R, Kampik A, Mueller AJ: **Melanoma inhibitory activity: a novel serum marker for uveal melanoma**. *Melanoma Res* 2002, **12**(6):593-599.
301. Wang W, Kong P, Ma G, Li L, Zhu J, Xia T, Xie H, Zhou W, Wang S: **Characterization of the release and biological significance of cell-free DNA from breast cancer cell lines**. *Oncotarget* 2017, **8**(26):43180-43191.
302. Panagopoulou M, Karaglani M, Balgkouranidou I, Pantazi C, Kolios G, Kakolyris S, Chatzaki E: **Circulating cell-free DNA release in vitro: kinetics, size profiling, and cancer-related gene methylation**. *J Cell Physiol* 2019, **234**(8):14079-14089.
303. Bronkhorst AJ, Wentzel JF, Aucamp J, van Dyk E, du Plessis L, Pretorius PJ: **Characterization of the cell-free DNA released by cultured cancer cells**. *Biochim Biophys Acta* 2016, **1863**(1):157-165.
304. Ungerer V, Bronkhorst AJ, Van den Ackerveken P, Herzog M, Holdenrieder S: **Serial profiling of cell-free DNA and nucleosome histone modifications in cell cultures**. *Sci Rep* 2021, **11**(1):9460.
305. Grabuschnig S, Bronkhorst AJ, Holdenrieder S, Rosales Rodriguez I, Schliep KP, Schwendenwein D, Ungerer V, Sensen CW: **Putative Origins of Cell-Free DNA in Humans: A Review of Active and Passive Nucleic Acid Release Mechanisms**. *Int J Mol Sci* 2020, **21**(21).

306. Mouliere F, Rosenfeld N: **Circulating tumor-derived DNA is shorter than somatic DNA in plasma**. *Proc Natl Acad Sci U S A* 2015, **112**(11):3178-3179.
307. Ziegler A, Zangemeister-Wittke U, Stahel RA: **Circulating DNA: a new diagnostic gold mine?** *Cancer Treat Rev* 2002, **28**(5):255-271.
308. Khakoo S, Georgiou A, Gerlinger M, Cunningham D, Starling N: **Circulating tumour DNA, a promising biomarker for the management of colorectal cancer**. *Crit Rev Oncol Hematol* 2018, **122**:72-82.
309. Hanna GJ, Supplee JG, Kuang Y, Mahmood U, Lau CJ, Haddad RI, Jänne PA, Paweletz CP: **Plasma HPV cell-free DNA monitoring in advanced HPV-associated oropharyngeal cancer**. *Ann Oncol* 2018, **29**(9):1980-1986.
310. Wu TL, Zhang D, Chia JH, Tsao K, Sun CF, Wu JT: **Cell-free DNA: measurement in various carcinomas and establishment of normal reference range**. *Clin Chim Acta* 2002, **321**(1-2):77-87.
311. Murtaza M, Dawson SJ, Pogrebniak K, Rueda OM, Provenzano E, Grant J, Chin SF, Tsui DWY, Marass F, Gale D *et al*: **Multifocal clonal evolution characterized using circulating tumour DNA in a case of metastatic breast cancer**. *Nat Commun* 2015, **6**:8760.
312. Jiang P, Chan KC, Liao GJ, Zheng YW, Leung TY, Chiu RW, Lo YM, Sun H: **FetalQuant: deducing fractional fetal DNA concentration from massively parallel sequencing of DNA in maternal plasma**. *Bioinformatics* 2012, **28**(22):2883-2890.
313. De Mattos-Arruda L, Weigelt B, Cortes J, Won HH, Ng CK, Nuciforo P, Bidard FC, Aura C, Saura C, Peg V *et al*: **Capturing intra-tumor genetic heterogeneity by de novo mutation profiling of circulating cell-free tumor DNA: a proof-of-principle**. *Ann Oncol* 2014, **25**(9):1729-1735.
314. Sun K, Jiang P, Chan KC, Wong J, Cheng YK, Liang RH, Chan WK, Ma ES, Chan SL, Cheng SH *et al*: **Plasma DNA tissue mapping by genome-wide methylation sequencing for noninvasive prenatal, cancer, and transplantation assessments**. *Proc Natl Acad Sci U S A* 2015, **112**(40):E5503-5512.
315. Huang SK, Hoon DS: **Liquid biopsy utility for the surveillance of cutaneous malignant melanoma patients**. *Mol Oncol* 2016, **10**(3):450-463.
316. Kilgour E, Rothwell DG, Brady G, Dive C: **Liquid Biopsy-Based Biomarkers of Treatment Response and Resistance**. *Cancer Cell* 2020, **37**(4):485-495.
317. Milner AE, Palmer DH, Hodgkin EA, Eliopoulos AG, Knox PG, Poole CJ, Kerr DJ, Young LS: **Induction of apoptosis by chemotherapeutic drugs: the role of FADD in activation of caspase-8 and synergy with death receptor ligands in ovarian carcinoma cells**. *Cell Death Differ* 2002, **9**(3):287-300.
318. Eriksson D, Stigbrand T: **Radiation-induced cell death mechanisms**. *Tumour Biol* 2010, **31**(4):363-372.
319. Nygård L, Ahlborn LB, Persson GF, Chandrananda D, Langer JW, Fischer BM, Langer SW, Gabrielaite M, Kjær A, Rosenfeld N *et al*: **Circulating cell free DNA during definitive chemo-radiotherapy in non-small cell lung cancer patients - initial observations**. *PLoS One* 2020, **15**(4):e0231884.
320. Deligezer U, Eralp Y, Akisik EE, Akisik EZ, Saip P, Topuz E, Dalay N: **Size distribution of circulating cell-free DNA in sera of breast cancer patients in the course of adjuvant chemotherapy**. *Clin Chem Lab Med* 2008, **46**(3):311-317.

321. Chen Z, Fadiel A, Naftolin F, Eichenbaum KD, Xia Y: **Circulation DNA: biological implications for cancer metastasis and immunology**. *Med Hypotheses* 2005, **65**(5):956-961.
322. Leung E, Han K, Zou J, Zhao Z, Zheng Y, Wang TT, Rostami A, Siu LL, Pugh TJ, Bratman SV: **HPV Sequencing Facilitates Ultrasensitive Detection of HPV Circulating Tumor DNA**. *Clin Cancer Res* 2021, **27**(21):5857-5868.
323. Ren DH, Mayhew E, Hay C, Li H, Alizadeh H, Niederkorn JY: **Uveal melanoma expression of tumor necrosis factor-related apoptosis-inducing ligand (TRAIL) receptors and susceptibility to TRAIL-induced apoptosis**. *Invest Ophthalmol Vis Sci* 2004, **45**(4):1162-1168.
324. Huang Y, Yang X, Xu T, Kong Q, Zhang Y, Shen Y, Wei Y, Wang G, Chang KJ: **Overcoming resistance to TRAIL-induced apoptosis in solid tumor cells by simultaneously targeting death receptors, c-FLIP and IAPs**. *Int J Oncol* 2016, **49**(1):153-163.
325. Cicenas J, Kalyan K, Sorokinas A, Stankunas E, Levy J, Meskinyte I, Stankevicius V, Kaupinis A, Valius M: **Roscovitine in cancer and other diseases**. *Ann Transl Med* 2015, **3**(10):135.
326. Janko C, Munoz L, Chaurio R, Maueröder C, Berens C, Lauber K, Herrmann M: **Navigation to the graveyard-induction of various pathways of necrosis and their classification by flow cytometry**. *Methods Mol Biol* 2013, **1004**:3-15.
327. Klein ME, Kovatcheva M, Davis LE, Tap WD, Koff A: **CDK4/6 Inhibitors: The Mechanism of Action May Not Be as Simple as Once Thought**. *Cancer Cell* 2018, **34**(1):9-20.
328. Häfner MF, Debus J: **Radiotherapy for Colorectal Cancer: Current Standards and Future Perspectives**. *Visc Med* 2016, **32**(3):172-177.
329. Sia J, Szmyd R, Hau E, Gee HE: **Molecular Mechanisms of Radiation-Induced Cancer Cell Death: A Primer**. *Front Cell Dev Biol* 2020, **8**:41.
330. Bronkhorst AJ, Ungerer V, Holdenrieder S: **Comparison of methods for the quantification of cell-free DNA isolated from cell culture supernatant**. *Tumour Biol* 2019, **41**(8):1010428319866369.
331. Adashek JJ, Janku F, Kurzrock R: **Signed in Blood: Circulating Tumor DNA in Cancer Diagnosis, Treatment and Screening**. *Cancers (Basel)* 2021, **13**(14).
332. Mao X, Zhang Z, Zheng X, Xie F, Duan F, Jiang L, Chuai S, Han-Zhang H, Han B, Sun J: **Capture-Based Targeted Ultradeep Sequencing in Paired Tissue and Plasma Samples Demonstrates Differential Subclonal ctDNA-Releasing Capability in Advanced Lung Cancer**. *J Thorac Oncol* 2017, **12**(4):663-672.
333. Deig CR, Thowe RT, Frye ED, Chin-Sinex HJ, Mendonca MS, Lautenschlaeger T: **In Vitro Cell-free DNA Quantification: A Novel Method to Accurately Quantify Cell Survival after Irradiation**. *Radiat Res* 2018, **190**(1):22-27.
334. Adamsen BL, Kravik L, De Angelis PM: **Cellular response to chemoradiotherapy, radiotherapy and chemotherapy in two colorectal cancer cell lines**. *Radiat Res* 2009, **171**(5):562-571.
335. de Lange J, Teunisse AF, Vries MV, Lodder K, Lam S, Luyten GP, Bernal F, Jager MJ, Jochemsen AG: **High levels of Hdmx promote cell growth in a subset of uveal melanomas**. *Am J Cancer Res* 2012, **2**(5):492-507.

336. Leroy B, Girard L, Hollestelle A, Minna JD, Gazdar AF, Soussi T: **Analysis of TP53 mutation status in human cancer cell lines: a reassessment**. *Hum Mutat* 2014, **35**(6):756-765.
337. Kahlert C: **Liquid Biopsy: Is There an Advantage to Analyzing Circulating Exosomal DNA Compared to cfDNA or Are They the Same?** *Cancer Res* 2019, **79**(10):2462-2465.
338. Han DSC, Lo YMD: **The Nexus of cfDNA and Nuclease Biology**. *Trends Genet* 2021, **37**(8):758-770.
339. Knebel FH, Bettoni F, da Fonseca LG, Camargo AA, Sabbaga J, Jardim DL: **Circulating Tumor DNA Detection in the Management of Anti-EGFR Therapy for Advanced Colorectal Cancer**. *Front Oncol* 2019, **9**:170.
340. Xu LT, Funchain PF, Bena JF, Li M, Tarhini A, Berber E, Singh AD: **Uveal Melanoma Metastatic to the Liver: Treatment Trends and Outcomes**. *Ocul Oncol Pathol* 2019, **5**(5):323-332.
341. Eldh M, Olofsson Bagge R, Lasser C, Svanvik J, Sjostrand M, Mattsson J, Lindner P, Choi DS, Gho YS, Lotvall J: **MicroRNA in exosomes isolated directly from the liver circulation in patients with metastatic uveal melanoma**. *BMC Cancer* 2014, **14**:962.
342. Tsai KK, Bollin KB, Patel SP: **Obstacles to improving outcomes in the treatment of uveal melanoma**. *Cancer* 2018, **124**(13):2693-2703.
343. Pushpakom S, Iorio F, Eyers PA, Escott KJ, Hopper S, Wells A, Doig A, Guilliams T, Latimer J, McNamee C *et al*: **Drug repurposing: progress, challenges and recommendations**. *Nature Reviews Drug Discovery* 2019, **18**(1):41-58.
344. Cha Y, Erez T, Reynolds IJ, Kumar D, Ross J, Koytiger G, Kusko R, Zeskind B, Risso S, Kagan E *et al*: **Drug repurposing from the perspective of pharmaceutical companies**. *Br J Pharmacol* 2018, **175**(2):168-180.
345. Baulieu EE, Segal,S.J.: **The antiprogestin steroid RU 486 and human fertility control**. *New York: Plenum Press* 1985.
346. Goldstone P, Walker C, Hawtin K: **Efficacy and safety of mifepristone-buccal misoprostol for early medical abortion in an Australian clinical setting**. *Aust N Z J Obstet Gynaecol* 2017, **57**(3):366-371.
347. Schaff EA: **Mifepristone: ten years later**. *Contraception* 2010, **81**(1):1-7.
348. Spitz IM, Bardin CW: **Clinical pharmacology of RU 486--an antiprogestin and antiglucocorticoid**. *Contraception* 1993, **48**(5):403-444.
349. Goyeneche AA, Telleria CM: **Antiprogestins in gynecological diseases**. *Reproduction* 2015, **149**(1):R15-33.
350. Goyeneche AA, Seidel EE, Telleria CM: **Growth inhibition induced by antiprogestins RU-38486, ORG-31710, and CDB-2914 in ovarian cancer cells involves inhibition of cyclin dependent kinase 2**. *Invest New Drugs* 2012, **30**(3):967-980.
351. Armaiz-Pena GN, Lutgendorf SK, Cole SW, Sood AK: **Neuroendocrine modulation of cancer progression**. *Brain Behav Immun* 2009, **23**(1):10-15.
352. Palmieri G, Ombra M, Colombino M, Casula M, Sini M, Manca A, Paliogiannis P, Ascierto PA, Cossu A: **Multiple Molecular Pathways in Melanomagenesis: Characterization of Therapeutic Targets**. *Front Oncol* 2015, **5**:183.
353. Kern MJ, Ganz P, Horowitz JD, Gaspar J, Barry WH, Lorell BH, Grossman W, Mudge GH, Jr.: **Potentiation of coronary vasoconstriction by beta-adrenergic blockade in patients with coronary artery disease**. *Circulation* 1983, **67**(6):1178-1185.

354. Borthne A: **The treatment of glaucoma with propranolol (Inderal). A clinical trial**. *Acta Ophthalmol (Copenh)* 1976, **54**(3):291-300.
355. La Mura V, Abraldes JG, Raffa S, Retto O, Berzigotti A, García-Pagán JC, Bosch J: **Prognostic value of acute hemodynamic response to i.v. propranolol in patients with cirrhosis and portal hypertension**. *J Hepatol* 2009, **51**(2):279-287.
356. Fuchsmann C, Quintal MC, Giguere C, Ayari-Khalfallah S, Guibaud L, Powell J, McCone C, Froehlich P: **Propranolol as first-line treatment of head and neck hemangiomas**. *Arch Otolaryngol Head Neck Surg* 2011, **137**(5):471-478.
357. Chow W, Amaya CN, Rains S, Chow M, Dickerson EB, Bryan BA: **Growth Attenuation of Cutaneous Angiosarcoma With Propranolol-Mediated β-Blockade**. *JAMA Dermatol* 2015, **151**(11):1226-1229.
358. Pantziarka P, Bouche G, Sukhatme V, Meheus L, Rooman I, Sukhatme VP: **Repurposing Drugs in Oncology (ReDO)-Propranolol as an anti-cancer agent**. *Ecancermedicalscience* 2016, **10**:680.
359. Gerlinger M, Rowan AJ, Horswell S, Math M, Larkin J, Endesfelder D, Gronroos E, Martinez P, Matthews N, Stewart A *et al*: **Intratumor heterogeneity and branched evolution revealed by multiregion sequencing**. *N Engl J Med* 2012, **366**(10):883-892.
360. Monaco SE: **Fine Needle Aspiration Cytology**. In: *Pathobiology of Human Disease.* edn. Edited by McManus LM, Mitchell RN. San Diego: Academic Press; 2014: 3379-3398.
361. Malone ER, Oliva M, Sabatini PJB, Stockley TL, Siu LL: **Molecular profiling for precision cancer therapies**. *Genome Medicine* 2020, **12**(1):8.
362. Bai RY, Staedtke V, Xia X, Riggins GJ: **Prevention of tumor seeding during needle biopsy by chemotherapeutic-releasing gelatin sticks**. *Oncotarget* 2017, **8**(16):25955-25962.
363. Hanahan D, Weinberg RA: **Hallmarks of cancer: the next generation**. *Cell* 2011, **144**(5):646-674.
364. Papadopoulos N: **Pathophysiology of ctDNA Release into the Circulation and Its Characteristics: What Is Important for Clinical Applications**. *Recent Results Cancer Res* 2020, **215**:163-180.
365. Panagopoulou M, Karaglani M, Balgkouranidou I, Biziota E, Koukaki T, Karamitrousis E, Nena E, Tsamardinos I, Kolios G, Lianidou E *et al*: **Circulating cell-free DNA in breast cancer: size profiling, levels, and methylation patterns lead to prognostic and predictive classifiers**. *Oncogene* 2019, **38**(18):3387-3401.
366. Pérez-Garijo A: **When dying is not the end: Apoptotic caspases as drivers of proliferation**. *Semin Cell Dev Biol* 2018, **82**:86-95.
367. Ichim G, Tait SWG: **A fate worse than death: apoptosis as an oncogenic process**. *Nature Reviews Cancer* 2016, **16**(8):539-548.
368. Fogarty CE, Bergmann A: **Killers creating new life: caspases drive apoptosis-induced proliferation in tissue repair and disease**. *Cell Death Differ* 2017, **24**(8):1390-1400.
369. Serpas L, Chan RWY, Jiang P, Ni M, Sun K, Rashidfarrokhi A, Soni C, Sisirak V, Lee WS, Cheng SH *et al*: **Dnase1l3 deletion causes aberrations in length and end-motif frequencies in plasma DNA**. *Proc Natl Acad Sci U S A* 2019, **116**(2):641-649.
370. Bronkhorst AJ, Wentzel JF, Aucamp J, van Dyk E, du Plessis LH, Pretorius PJ: **An Enquiry Concerning the Characteristics of Cell-Free DNA Released by Cultured Cancer Cells**. *Adv Exp Med Biol* 2016, **924**:19-24.

371. Bu H, He D, He X, Wang K: **Exosomes: Isolation, Analysis, and Applications in Cancer Detection and Therapy**. *Chembiochem* 2019, **20**(4):451-461.
372. Malkin EZ, Bratman SV: **Bioactive DNA from extracellular vesicles and particles**. *Cell Death & Disease* 2020, **11**(7):584.
373. Klump J, Phillipp U, Follo M, Eremin A, Lehmann H, Nestel S, von Bubnoff N, Nazarenko I: **Extracellular vesicles or free circulating DNA: where to search for BRAF and cKIT mutations?** *Nanomedicine* 2018, **14**(3):875-882.
374. Beasley AB, Isaacs TW, Vermeulen T, Freeman J, DeSousa J-L, Bhikoo R, Hennessy D, Reid A, Chen FK, Bentel J *et al*: **Analysis of Circulating Tumour Cells in Early-Stage Uveal Melanoma: Evaluation of Tumour Marker Expression to Increase Capture**. *Cancers* 2021, **13**(23):5990.
375. Rashid AB, Grossniklaus HE: **Clinical, pathologic, and imaging features and biological markers of uveal melanoma**. *Methods Mol Biol* 2014, **1102**:397-425.
376. Chien JL, Sioufi K, Surakiatchanukul T, Shields JA, Shields CL: **Choroidal nevus: a review of prevalence, features, genetics, risks, and outcomes**. *Curr Opin Ophthalmol* 2017, **28**(3):228-237.
377. Singh AD, Grossniklaus HE: **What's in a Name? Large Choroidal Nevus, Small Choroidal Melanoma, or Indeterminate Melanocytic Tumor**. *Ocul Oncol Pathol* 2021, **7**(4):235-238.
378. Shields CL, Cater J, Shields JA, Singh AD, Santos MC, Carvalho C: **Combination of clinical factors predictive of growth of small choroidal melanocytic tumors**. *Arch Ophthalmol* 2000, **118**(3):360-364.
379. Grossniklaus HE, Van Meir EG: **Are Risk Factors for Growth of Choroidal Nevi Associated With Malignant Transformation? Assessment With a Validated Genomic Biomarker**. *Am J Ophthalmol* 2019, **203**:117-118.
380. Al Harby L, Sagoo MS, O'Day R, Hay G, Arora AK, Keane PA, Cohen VM, Damato B: **Distinguishing Choroidal Nevi from Melanomas Using the MOLES Algorithm: Evaluation in an Ocular Nevus Clinic**. *Ocul Oncol Pathol* 2021, **7**(4):294-302.
381. Bellerive C, Binkley E, Singh AD: **Class 2 Gene Expression Profile of a Hemorrhagic Pigment Epithelial Detachment Misdiagnosed as Melanoma**. *Ophthalmol Retina* 2019, **3**(5):453-455.
382. Jensen TJ, Kim SK, Zhu Z, Chin C, Gebhard C, Lu T, Deciu C, van den Boom D, Ehrich M: **Whole genome bisulfite sequencing of cell-free DNA and its cellular contributors uncovers placenta hypomethylated domains**. *Genome Biol* 2015, **16**(1):78.
383. Jiang P, Xie T, Ding SC, Zhou Z, Cheng SH, Chan RWY, Lee WS, Peng W, Wong J, Wong VWS *et al*: **Detection and characterization of jagged ends of double-stranded DNA in plasma**. *Genome Res* 2020, **30**(8):1144-1153.
384. Wei L, Xie L, Wang X, Ma H, Lv L, Liu L, Song X: **Circulating tumor DNA measurement provides reliable mutation detection in mice with human lung cancer xenografts**. *Lab Invest* 2018, **98**(7):935-946.
385. Gasparello J, Allegretti M, Tremante E, Fabbri E, Amoreo CA, Romania P, Melucci E, Messana K, Borgatti M, Giacomini P *et al*: **Liquid biopsy in mice bearing colorectal carcinoma xenografts: gateways regulating the levels of circulating tumor DNA (ctDNA) and miRNA (ctmiRNA)**. *J Exp Clin Cancer Res* 2018, **37**(1):124.

386. Thierry AR, Mouliere F, Gongora C, Ollier J, Robert B, Ychou M, Del Rio M, Molina F: **Origin and quantification of circulating DNA in mice with human colorectal cancer xenografts**. *Nucleic Acids Res* 2010, **38**(18):6159-6175.
387. Muhanna N, Di Grappa MA, Chan HHL, Khan T, Jin CS, Zheng Y, Irish JC, Bratman SV: **Cell-Free DNA Kinetics in a Pre-Clinical Model of Head and Neck Cancer**. *Sci Rep* 2017, **7**(1):16723.
388. Aucamp J, Van Dyk HC, Bronkhorst AJ, Pretorius PJ: **Valproic acid alters the content and function of the cell-free DNA released by hepatocellular carcinoma (HepG2) cells in vitro**. *Biochimie* 2017, **140**:93-105.
389. Rae C, Amato F, Braconi C: **Patient-Derived Organoids as a Model for Cancer Drug Discovery**. *Int J Mol Sci* 2021, **22**(7).
390. Dantes Z, Yen HY, Pfarr N, Winter C, Steiger K, Muckenhuber A, Hennig A, Lange S, Engleitner T, Öllinger R *et al*: **Implementing cell-free DNA of pancreatic cancer patient-derived organoids for personalized oncology**. *JCI Insight* 2020, **5**(15).
391. Khier S, Lohan L: **Kinetics of circulating cell-free DNA for biomedical applications: critical appraisal of the literature**. *Future Sci OA* 2018, **4**(4):Fso295.
392. Meddeb R, Pisareva E, Thierry AR: **Guidelines for the Preanalytical Conditions for Analyzing Circulating Cell-Free DNA**. *Clin Chem* 2019, **65**(5):623-633.
393. Cavallone L, Aldamry M, Lafleur J, Lan C, Gonzalez Ginestet P, Alirezaie N, Ferrario C, Aguilar-Mahecha A, Basik M: **A Study of Pre-Analytical Variables and Optimization of Extraction Method for Circulating Tumor DNA Measurements by Digital Droplet PCR**. *Cancer Epidemiol Biomarkers Prev* 2019, **28**(5):909-916.
394. Chan KC, Yeung SW, Lui WB, Rainer TH, Lo YM: **Effects of preanalytical factors on the molecular size of cell-free DNA in blood**. *Clin Chem* 2005, **51**(4):781-784.
395. El Messaoudi S, Rolet F, Mouliere F, Thierry AR: **Circulating cell free DNA: Preanalytical considerations**. *Clin Chim Acta* 2013, **424**:222-230.
396. Warton K, Yuwono NL, Cowley MJ, McCabe MJ, So A, Ford CE: **Evaluation of Streck BCT and PAXgene Stabilised Blood Collection Tubes for Cell-Free Circulating DNA Studies in Plasma**. *Mol Diagn Ther* 2017, **21**(5):563-570.
397. Tsui DWY, Barnett E, Scher HI: **Toward Standardization of Preanalytical Procedures for Cell-Free DNA Profiling**. *Clin Chem* 2020, **66**(1):3-5.
398. Chen M, Zhao H: **Next-generation sequencing in liquid biopsy: cancer screening and early detection**. *Human Genomics* 2019, **13**(1):34.
399. Neves RPL, Ammerlaan W, Andree KC, Bender S, Cayrefourcq L, Driemel C, Koch C, Luetke-Eversloh MV, Oulhen M, Rossi E *et al*: **Proficiency Testing to Assess Technical Performance for CTC-Processing and Detection Methods in CANCER-ID**. *Clin Chem* 2021, **67**(4):631-641.
400. Connors D, Allen J, Alvarez JD, Boyle J, Cristofanilli M, Hiller C, Keating S, Kelloff G, Leiman L, McCormack R *et al*: **International liquid biopsy standardization alliance white paper**. *Crit Rev Oncol Hematol* 2020, **156**:103112.
401. Marrella A, Fedi A, Varani G, Vaccari I, Fato M, Firpo G, Guida P, Aceto N, Scaglione S: **High blood flow shear stress values are associated with circulating tumor cells cluster disaggregation in a multi-channel microfluidic device**. *PLoS One* 2021, **16**(1):e0245536.

402. Mardinian K, Okamura R, Kato S, Kurzrock R: **Temporal and spatial effects and survival outcomes associated with concordance between tissue and blood KRAS alterations in the pan-cancer setting**. *Int J Cancer* 2020, **146**(2):566-576.
403. Heidrich I, Abdalla TSA, Reeh M, Pantel K: **Clinical Applications of Circulating Tumor Cells and Circulating Tumor DNA as a Liquid Biopsy Marker in Colorectal Cancer**. *Cancers (Basel)* 2021, **13**(18).
404. Ossandon MR, Agrawal L, Bernhard EJ, Conley BA, Dey SM, Divi RL, Guan P, Lively TG, McKee TC, Sorg BS *et al*: **Circulating Tumor DNA Assays in Clinical Cancer Research**. *J Natl Cancer Inst* 2018, **110**(9):929-934.
405. Marsman G, Zeerleder S, Luken BM: **Extracellular histones, cell-free DNA, or nucleosomes: differences in immunostimulation**. *Cell Death & Disease* 2016, **7**(12):e2518-e2518.
406. García-Olmo DC, Domínguez C, García-Arranz M, Anker P, Stroun M, García-Verdugo JM, García-Olmo D: **Cell-free nucleic acids circulating in the plasma of colorectal cancer patients induce the oncogenic transformation of susceptible cultured cells**. *Cancer Res* 2010, **70**(2):560-567.
407. Korabecna M, Zinkova A, Brynychova I, Chylikova B, Prikryl P, Sedova L, Neuzil P, Seda O: **Cell-free DNA in plasma as an essential immune system regulator**. *Scientific Reports* 2020, **10**(1):17478.
408. Cresswell GD, Nichol D, Spiteri I, Tari H, Zapata L, Heide T, Maley CC, Magnani L, Schiavon G, Ashworth A *et al*: **Mapping the breast cancer metastatic cascade onto ctDNA using genetic and epigenetic clonal tracking**. *Nature Communications* 2020, **11**(1):1446.
409. Ferrier ST, Burnier JV: **Novel Methylation Patterns Predict Outcome in Uveal Melanoma**. *Life (Basel)* 2020, **10**(10).
410. Grunt M, Hillebrand T, Schwarzenbach H: **Clinical relevance of size selection of circulating DNA**. *Translational Cancer Research* 2017:S171-S184.
411. Liu Y: **At the dawn: cell-free DNA fragmentomics and gene regulation**. *British Journal of Cancer* 2021.
412. Breitbach S, Sterzing B, Magallanes C, Tug S, Simon P: **Direct measurement of cell-free DNA from serially collected capillary plasma during incremental exercise**. *J Appl Physiol (1985)* 2014, **117**(2):119-130.
413. Breitbach S, Tug S, Helmig S, Zahn D, Kubiak T, Michal M, Gori T, Ehlert T, Beiter T, Simon P: **Direct quantification of cell-free, circulating DNA from unpurified plasma**. *PLoS One* 2014, **9**(3):e87838.
414. Umetani N, Kim J, Hiramatsu S, Reber HA, Hines OJ, Bilchik AJ, Hoon DS: **Increased integrity of free circulating DNA in sera of patients with colorectal or periampullary cancer: direct quantitative PCR for ALU repeats**. *Clin Chem* 2006, **52**(6):1062-1069.
415. Neuberger EWI, Brahmer A, Ehlert T, Kluge K, Philippi KFA, Boedecker SC, Weinmann-Menke J, Simon P: **Validating quantitative PCR assays for cfDNA detection without DNA extraction in exercising SLE patients**. *Scientific Reports* 2021, **11**(1):13581.
416. Pollock PM, Harper UL, Hansen KS, Yudt LM, Stark M, Robbins CM, Moses TY, Hostetter G, Wagner U, Kakareka J *et al*: **High frequency of BRAF mutations in nevi**. *Nat Genet* 2003, **33**(1):19-20.
417. Nathan P, Hassel JC, Rutkowski P, Baurain J-F, Butler MO, Schlaak M, Sullivan RJ, Ochsenreither S, Dummer R, Kirkwood JM *et al*: **Overall Survival Benefit with**

Tebentafusp in Metastatic Uveal Melanoma. *New England Journal of Medicine* 2021, **385**(13):1196-1206.
418. Francis JH, Canestraro J, Brannon AR, Barker CA, Berger M, Shoushtari AN, Abramson DH: **Association of Plasma Circulating Tumor DNA With Diagnosis of Metastatic Uveal Melanoma**. *JAMA Ophthalmol* 2021, **139**(11):1244-1245.
419. Miller F, Zohar S, Stallard N, Madan J, Posch M, Hee SW, Pearce M, Vågerö M, Day S: **Approaches to sample size calculation for clinical trials in rare diseases**. *Pharm Stat* 2018, **17**(3):214-230.
420. Tsui DWY, Blumenthal GM, Philip R, Barrett JC, Montagut C, Bramlett K, Ladanyi M, Ghosh S: **Development, Validation, and Regulatory Considerations for a Liquid Biopsy Test**. *Clinical Chemistry* 2020, **66**(3):408-414.
421. Ko J, Baldassano SN, Loh PL, Kording K, Litt B, Issadore D: **Machine learning to detect signatures of disease in liquid biopsies - a user's guide**. *Lab Chip* 2018, **18**(3):395-405.
422. Liu L, Chen X, Petinrin OO, Zhang W, Rahaman S, Tang ZR, Wong KC: **Machine Learning Protocols in Early Cancer Detection Based on Liquid Biopsy: A Survey**. *Life (Basel)* 2021, **11**(7).
423. Liu MC, Oxnard GR, Klein EA, Swanton C, Seiden MV, Liu MC, Oxnard GR, Klein EA, Smith D, Richards D *et al*: **Sensitive and specific multi-cancer detection and localization using methylation signatures in cell-free DNA**. *Annals of Oncology* 2020.

Appendix

A.1 Supplementary Material -Chapter 2

A.1.1 Supplementary Figures

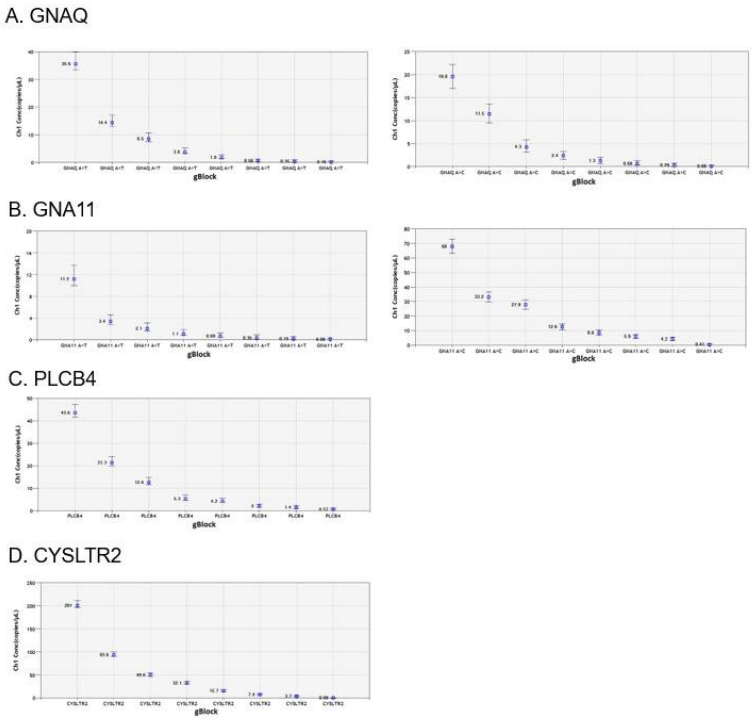

Supplementary Figure 1. ddPCR is feasible and valuable for sensitive sensing of specific UM mutated cfDNA. gBlocks that mimic A) *GNAQ*, B)*GNA11*, C)*PLCB4*, and D)*CYSLTR2* specific mutations were assayed by ddPCR assay on serial dilutions. Note that minimal levels of mutated copies were detected.

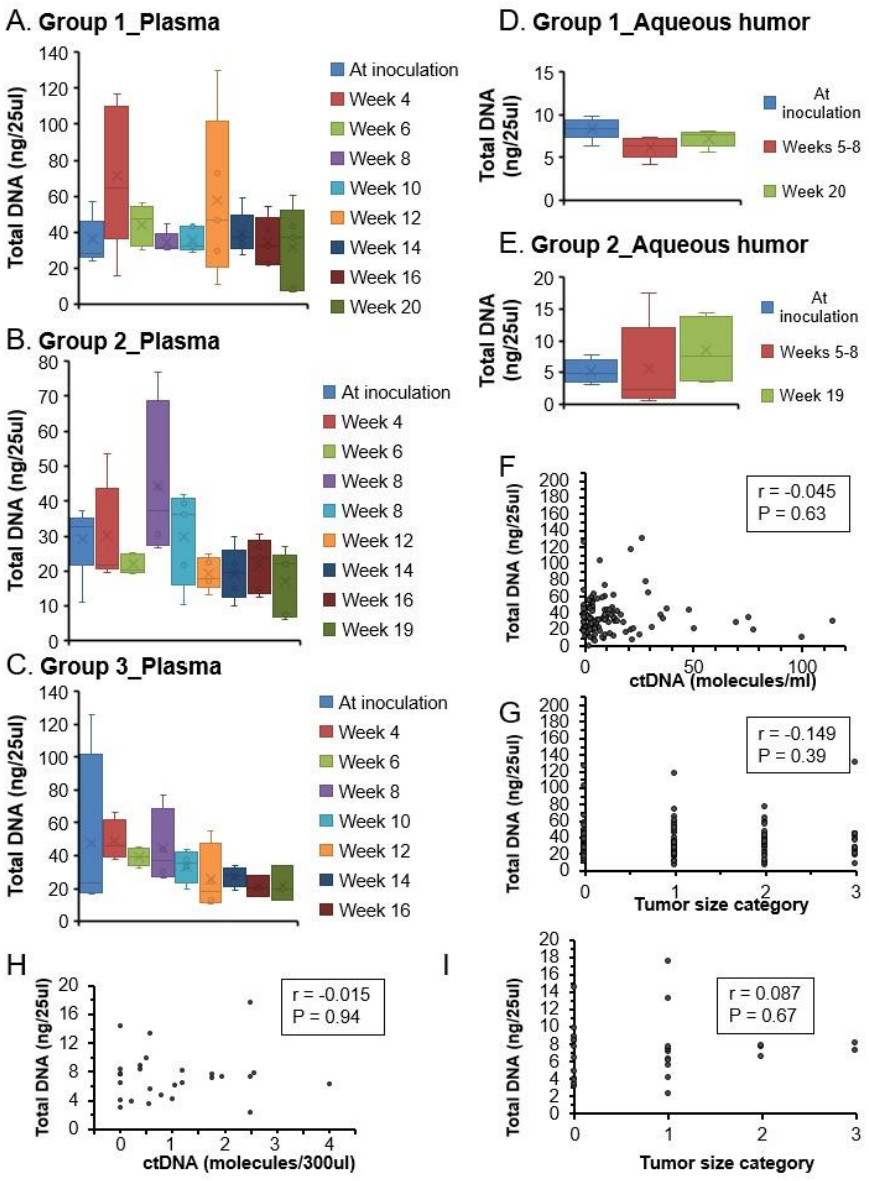

Supplementary Figure 2. Rabbit plasma total cfDNA levels did not correlate with either the levels of ctDNA nor tumor size category. A-C. Amounts of total cfDNA isolated from the plasma of rabbits from group 1 (**A**), group 2 (**B**), and group 3 (**C**). **D-E**. Amounts of total cfDNA isolated from the aqueous humor of rabbits from group 1 (**D**) and group 2 (**E**). **F-I**: Levels of total cfDNA isolated from the rabbit plasma (**F** and **G**) or the aqueous humor (**H** and **I**) of rabbits were plotted

against the amount of ctDNA (**F** and **H**) or tumor size categories (**G** and **I**). No correlation has been found.

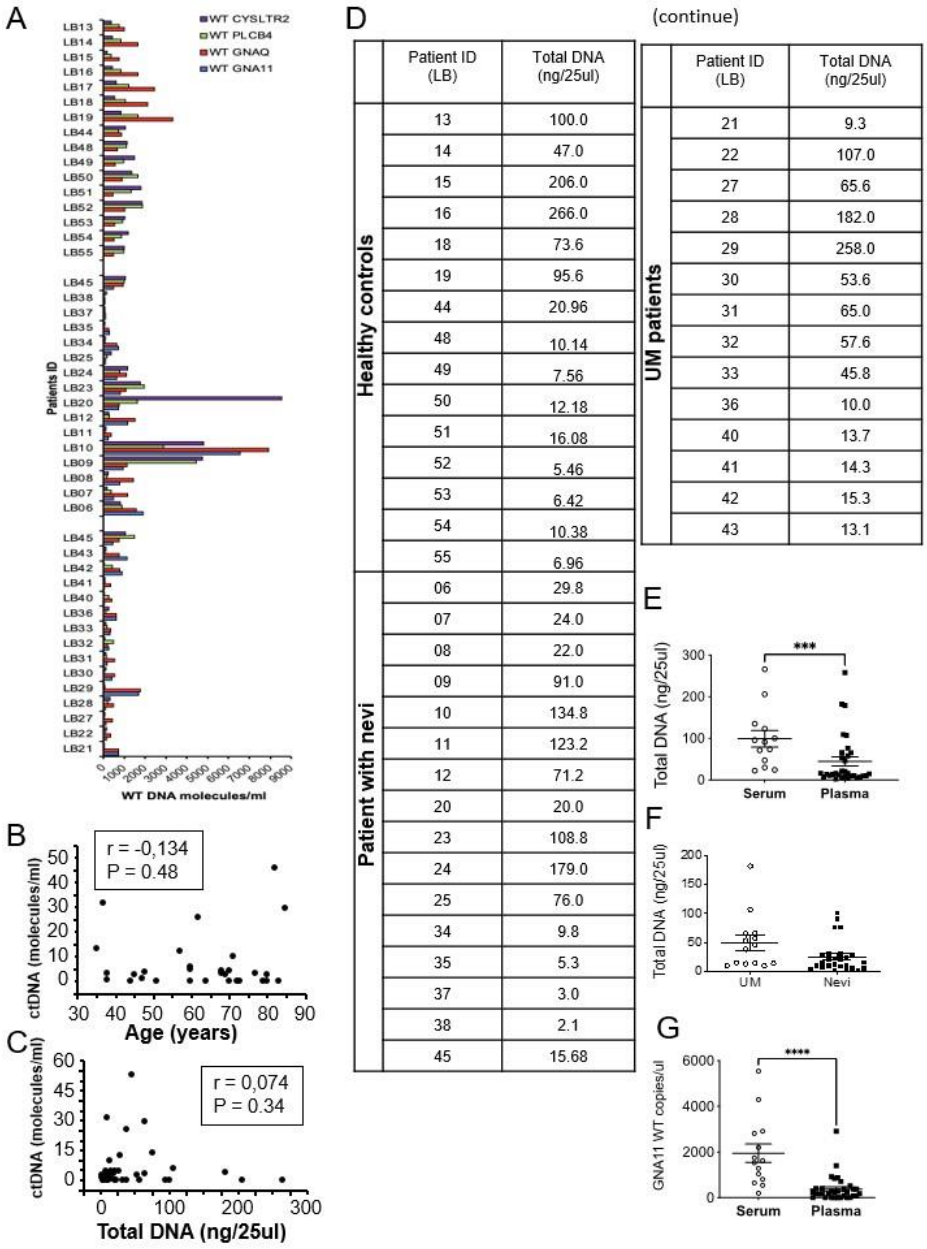

	Patient ID (LB)	Total DNA (ng/25ul)
Healthy controls	13	100.0
	14	47.0
	15	206.0
	16	266.0
	18	73.6
	19	95.6
	44	20.96
	48	10.14
	49	7.56
	50	12.18
	51	16.08
	52	5.46
	53	6.42
	54	10.38
	55	6.96
Patient with nevi	06	29.8
	07	24.0
	08	22.0
	09	91.0
	10	134.8
	11	123.2
	12	71.2
	20	20.0
	23	108.8
	24	179.0
	25	76.0
	34	9.8
	35	5.3
	37	3.0
	38	2.1
	45	15.68

	Patient ID (LB)	Total DNA (ng/25ul)
UM patients	21	9.3
	22	107.0
	27	65.6
	28	182.0
	29	258.0
	30	53.6
	31	65.0
	32	57.6
	33	45.8
	36	10.0
	40	13.7
	41	14.3
	42	15.3
	43	13.1

Supplementary Figure 3. UM patients blood ctDNA levels did not correlate with either the levels total cfDNA of nor the age of patients. A. Amounts of wild type cfDNA isolated from the plasma of enrolled patients. **B and C**. Levels of ctDNA isolated from the plasma of UM patients were plotted against the age (**B**) or the amount of total cfDNA (**C**). No correlation has been found.

D. Amounts of total DNA extracted from 2 ml of serum/plasma. **E**. Total DNA extracted from plasma and serum. **F**. Total DNA derived from all UM patients vs. all nevus patients. **G**. Wild-type copies per ml in plasma and serum. * P < 0.01, **** P < 0.001.

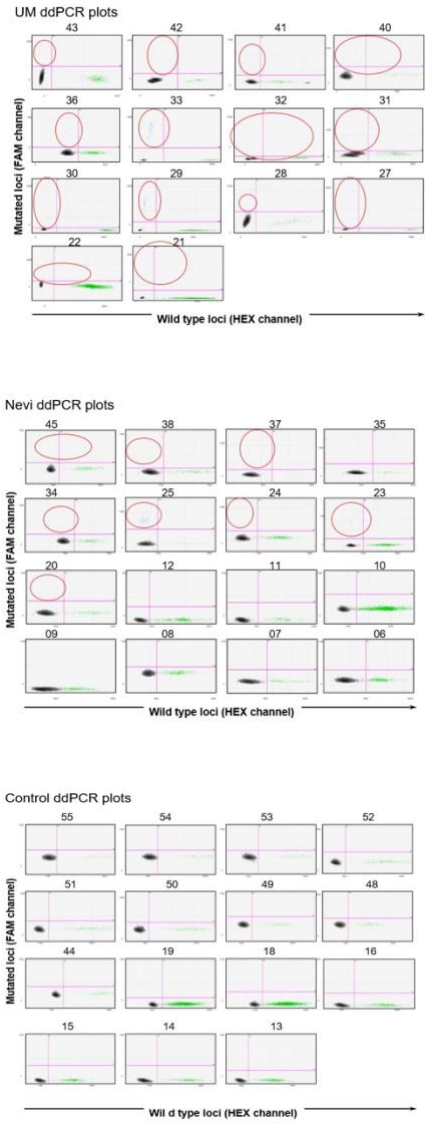

Supplementary Figure 4. 2D plots from ddPCR from: UM cohort (top), Nevus cohort (center). Control cohort (bottom).

A.1.2 Supplementary Tables

Supplementary Table 1. Description and mutational profile of used human UM cell lines.

Cell line	**Origin**	***GNAQ/11* mutational status**
92.1	PDX establish from primary tumor	*GNAQ* c.626 A>T
MP41	PDX establish from primary tumor	*GNA11* c.626 A>T
MP46	PDX establish from primary tumor	*GNAQ* c.626 A>T
MEL270	PDX establish from primary tumor *	*GNAQ* c.626 A>C
OMM2.5	PDX establish from metastatic lesion *	*GNAQ* c.626 A>C
OCM1	PDX establish from primary tumor	Wild type

* same patient

Supplementary Table 2. Summary of UM tumor formation in rabbits.

Rabbit ID	Cell line (mutation)	Time to tumor detection (weeks)	Tumor grade	Lifespan (weeks)
G1:1	92.1 (*GNAQ*)	5	3	20
G1:2	92.1 (*GNAQ*)	6	1	20
G1:3	92.1 (*GNAQ*)	5	2	20
G1:4	92.1 (*GNAQ*)	5	2	20
G1:5	92.1 (*GNAQ*)	5	3	20
G2:1	92.1 (*GNAQ*)	5	1	18
G2:2	92.1 (*GNAQ*)	6	0	18
G2:3	92.1 (*GNAQ*)	5	0	18
G2:4	92.1 (*GNAQ*)	4	0	18
G2:5	92.1 (*GNAQ*)	5	1	18
G3:1	MP41 (*GNA11*)	5	0	19
G3:2	MP41 (*GNA11*)	8	1	19
G3:3	MP41 (*GNA11*)	6	0	19
G3:4	MP41 (*GNA11*)	5	2	16
G3:5*	MP41 (*GNA11*)	-	-	3*

* excluded from the study due to cyclosporine toxicity

A.2 Supplementary Material -Chapter 3

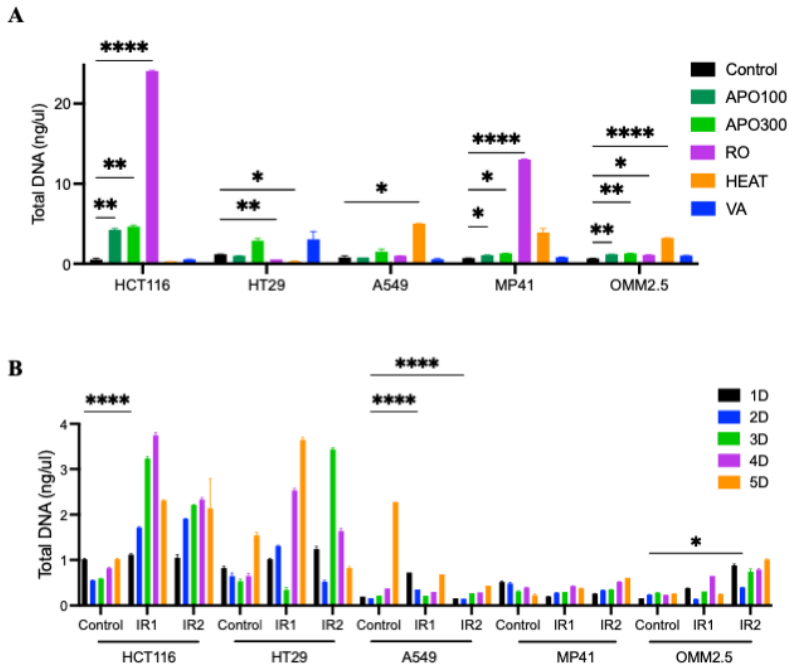

Supplementary Figure 5. (A) Graph shows total DNA (nontumor-specific fraction) in ng/µl after untreated (Control), 100 ng/ml (dark green) or 300 ng/ml (light green) APO2L (APO) for 48 hrs, 40 µM roscovitine (RO, in purpure) for 48 hrs, heat at 58ºC (in orange) for 30 min or exposed to 2 mM valproic acid (VA, in blue) for 48 hrs. **(B)** Graph shows total DNA every 24 hrs during the 5 consecutive days of doses of irradiation. HCT116, HT29, and A549 were exposed to 5 Gy (IR1) or 10 Gy (IR2) dose, whereas MP41 and OMM2.5 cells were exposed to 10 Gy (IR1) and 15 Gy (IR2) doses. Scored data are expressed as mean +/− SD (n = 3 independent experiments. * Indicates $p<0.05$, ** indicates $p<0.01$, whereas *** indicates $p<0.001$ compared against control.